THESIS FOR THE DEGREE OF LICENTIATE OF ENGINEERING IN GEOTECHNICAL ENGINEERING

In-situ testing of floating thermal piles in soft sensitive clay

ANDERS BERGSTRÖM

Department of Architchture and Civil Engineering
Division of Geology and Geotechnics
CHALMERS UNIVERSITY OF TECHNOLOGY

Göteborg, Sweden 2017

In-situ testing of floating thermal piles in soft sensitive clay
ANDERS BERGSTRÖM

ISSN -
Department of Architchture and Civil Engineering
Division of Geology and Geotechnics
Chalmers University of Technology
SE-412 96 Göteborg
Sweden
Telephone: +46 (0)31-772 2120

Cover:
The thermal test steel pile head, with load cell, heat exchange pipes and sensor cabling. Utby test site, Gothenburg.

Chalmers Reproservice
Göteborg, Sweden 2017

In-situ testing of floating thermal piles in soft sensitive clay
Thesis for the degree of Licentiate of Engineering in Geotechnical Engineering
ANDERS BERGSTRÖM
Department of Architchture and Civil Engineering
Division of Geology and Geotechnics
Chalmers University of Technology

Abstract

Thermal piles are structural piles with additional function of working as geothermal heat exchangers towards the soil volume. Heating and cooling process of soft soils is known to affect the stress state and soil structure, with potential consolidation settlements and creep as undesired consequences.

The aim of this thesis is to investigate the effects of static mechanical and cyclic thermal loading of floating piles in soft clay. A test site with soft sensitive clay is selected and the soil properties are characterised in an extensive field and laboratory test program. A full scale thermal pile and the surrounding soil volume is instrumented with a set of sensors.

A thermal loading rig, together with the thermal pile installed, has been successfully designed to absorb and extract energy to the ground. The thermal properties of the clay have been evaluated in the field using a Thermal Response Test (TRT). The field test setup is found to be capable of capturing changes in displacements, pore pressures and temperatures caused by the cyclic thermal loading. The change in pore pressures is strongly linked to the measured change in temperature in the clay. It has been shown that the thermal loading applied neither lead to significant pile head displacements, nor vertical deformations in the soil. The pile bearing capacity, recorded in a maintained loading test, has been found to be similar for both the thermal and the reference test piles. The test is adding novel data on the response from a driven floating thermal pile in soft sensitive clay.

Keywords: Thermal Piles, Energy piles, Field Test, Cyclic Thermal loading, Maintained loading test, Thermal Response Test, TRT, Thermo-mechanical behavior

Preface

My great gratitude is to my main funders SBUF (The Swedish construction industry's organisation for research and development), NCC and Hercules, Chalmers and Formas (The Swedish Research Council for Environment, Agricultural Sciences and Spatial Planning) for supporting this research project.

A dearly thank to Håkan Larsson for his cheerful work and generous support in the thermal installations at the lab and in the field, to Aaro Pirhonen for interesting discussions and sharing of the most beautiful and impressive craftmanship, and to Sebastian Almfeldt for enthusiastic help in programming and laboratory testing works.

Thanks to Hercules, in particular Mats Gustafsson, Mats Olsson and Peter Elmgren, for generous financial and practical assistance with concrete works, pile installation and equipment. Thanks to Sven Torstensson for shared enthusiasm and always available support with the pore pressure sensors, Ruukki represented by Antti Perälä and Jyrki Kesti for Finland study visit and providing of steel piles, Rune Hultquist for professional pile installation and nice collaboration in the field, and Hasse Alexandersson for a great amount of youthful curiosity and for positively reminding me of my growing up in the Småland entrepreneur area.

My appreciation to Chalmers and Chalmers Jordvärmegruppen seniors e.g. Björn Modin, Ingvar Rehn, Göran Sällfors and Kent Adolfsson for sharing interest and experiences from their research in energy storage in the ground initiated in the 1970 and 80's.

Many thanks to my examiner Minna Karstunen, and to my main supervisor Jelke Dijkstra for compellingly introducing me to different areas of Science from the history and today, for all kind of stimulating discussions and talks during the way and for bringing me to the completion of this work. Also a great thank to my co-supervisor Saqib Javed for thoughtfully encourage and friendly inviting me to the area of Building Services Engineering.

I also want to thank all my colleague PhD-students and staff members at the Division of Geology and Geotechnics at Chalmers. Futhermore, my colleagues and heads at NCC are my truly supporters, always full of friendly caring. Special thanks to my co-supervisor Tobias Larsson, my heads Christina Claeson-Jonsson, Lars Nilsson and Ayaz Nerway, and not least Lars-Olof Dahlström, Kristy Heng and Tara Wood for initiating this project.

The most enormous gratitude to my parents for your never ending love, respect and support in my life.

Finally thanks to my little family Lia, Måns and Anna for sharing my everyday.

Contents

1 Introduction

1.1 Background

In soft soils, as frequently encountered in Sweden, infrastructure and buildings often require deep foundations to ensure stability and limit settlement. The piles are primarily installed to transfer the construction loads to soil layers with sufficient stiffness and bearing capacity. In addition to providing bearing capacity, these deeper soil layers are also an attractive environment for potential geothermal heat exchange and heat storage. Thermal piles have been developed to exploit two functions, i.e. supporting structure and providing means to tap into shallow geothermal resources. Thermal piles, originally developed in the early 1970's (Brandl 2006), are structural piles with additional piping for circulating heat carrier fluid. This allows the heating system of the structure on top to use the heat capacity of the soil to extract or store energy from one period to another. The structural piles are then, in addition, used for geothermal heat exchange, potentially at a relatively small additional cost.

Energy foundations and thermo-active structures, such as thermal piles, can contribute to a more efficient handling of energy by using the thermal capacity of the soil. Surplus energy from one period of the day or over a year can be stored, to be used in a period of greater need. This need can be of heating or cooling, depending on the situation and the location. Most of the energy piles have been successfully employed in areas with competent (stiff) soils. In those settings the thermal response and the structural integrity of the piles, specially end-bearing piles, are of most concern rather than the bearing capacity of the soil.

On the other hand, soft soils, such as clay, will probably be more strongly affected by the additional thermal cycles resulting from energy foundations, i.e. the strength, the stiffness and the pre-consolidation pressure will change (Campanella and Mitchell 1968, Tidfors 1987, Leroueil and Marques 1996). For thin deposits of clay with end-bearing piles in a competent layer below, this will pose few additional complications. The down drag load from any additional settlement triggered by heating the soft soil layer is already incorporated in the design of the structural loads in the pile.

For thick deposits of soft clay considered in this thesis floating piles are used instead. Floating piles mobilise all resistance at the pile shaft. In the case of newly triggered or ongoing settlements in a soft clay deposit, additional down-drag loads can be mobilised at the pile shaft too. This complicated interaction between the pile and the surrounding soil is much more sensitive to effective stress changes and additional creep effects. Furthermore, some Swedish clays in their natural state show large natural water content above the liquid limit with a high sensitivity. It is unclear if any additional heating of floating piles in these sensitive clay deposits will compromise the stability of the piles or will lead to excessive pile head settlements.

This thesis presents the setup and results of a well instrumented field test performed to investigate the response of floating thermal piles in soft sensitive clay while injecting or extracting heat. The evolution of temperatures, stresses, pore pressures and deformations in the soil adjacent to the pile during monotonic and cyclic heating have been measured.

1.2 Aims and Objectives

The aim of this thesis is to investigate the effects of monotonic and cyclic thermal loading of floating thermal piles in soft sensitive clay on the interaction between the clay and the thermal pile. The focus is on capturing the soil behaviour in terms of pore pressures and deformations, as well as the change in temperature. The following main objectives are formulated:

1. Selection and extensive characterisation (in-situ & laboratory) of a test site with sensitive clay.
2. Design of the field test including loading rig, instrumentation and test protocol to study monotonic and cyclic thermal loading of floating piles under mechanical design load.
3. Test execution and data interpretation of results.

1.3 Limitations

- The concept of energy foundations, in practical installations, includes competence from a number of complementing expertises such as geotechnics, thermodynamics, building services, structural engineering, politics and regulations. This Thesis will focus on the effect of the thermal loading on the geotechnical response of the pile and the soil.
- The study will not include the behavior of a pile group, but focuses only on single piles. The studied piles are limited to driven pre-fabricated steel and concrete piles.
- The test piles will only be tested for low temperature storage, with temperature variations that are in the range of typical building heat pump systems, at 0–30°C.

2 Thermal piles in soft clay

2.1 Introduction

Thermal piles installed as pre-fabricated driven axially loaded floating piles in soft soils are not very common. The response of those piles is still subject of research, requiring knowledge on soil-structure interaction, piles and their installation effects, as well as an understanding on soft soils and their long-term response under thermal loading. This Chapter summarises only a selection of relevant prior research on the main concepts considered relevant for this study. After discussing the specifics of ordinary floating piles in soft soils and how their response is governed by the settlements in the soil, the effect of thermal loading on these soil settlements will be elaborated.

2.2 Pile foundations in clay

2.2.1 Pile types

In foundations, a pile is a construction element designed to transfer the loads from a superstructure into deep soil layers which due to its stress history normally has higher strength and stiffness compared to the shallow layers.
Piles can be separated based upon a number of different pile types, e.g. by:

- Material of the pile elements; concrete, steel or wood.
- Way of manufacturing the pile elements; in-situ in the ground or pre-cast before installation.
- Method used for installation; driven or bored piles.
- Effect of installation; displacement or non-displacement piles.
- Way of loading; axial (compression or tension) or lateral or combined loading.
- Way of transfering the load from the pile to the ground; shaft-bearing or end-bearing piles.

During the 20^{th} century steel and concrete have replaced wood as the most used material for piles. Depending on local conditions and actors, different pile systems are developed. In many countries, and in stiff soils, concrete piles produced in-situ are preferred. In Sweden, with common deposits of soft soil, pre-cast concrete piles and steel piles are used most (Pålkommissionen 2016), complemented by a small share of wooden piles. Furthermore, the bulk volume of piles installed in Sweden are relatively slender with L/D ratios over 150. As a consequence, the piles are most often designed for axial loading, as it is most structural and economically efficient. These pre-cast piles displace the soil during pile installation, strongly changing the stress history in the clay adjacent to the pile shaft. Originating from the local conditions and needs, the focus in this Thesis will be on driven precast displacement axially loaded floating piles in soft clay.

2.2.2 Pile bearing mechanisms

In a soil deposit with an assumed constant interface friction angle along the pile shaft, the shear strength capacity to transfer load between the pile and the soil will increase with depth as the vertical and the corresponding horizontal stresses are increasing with the accumulated weight from the soil layers above.

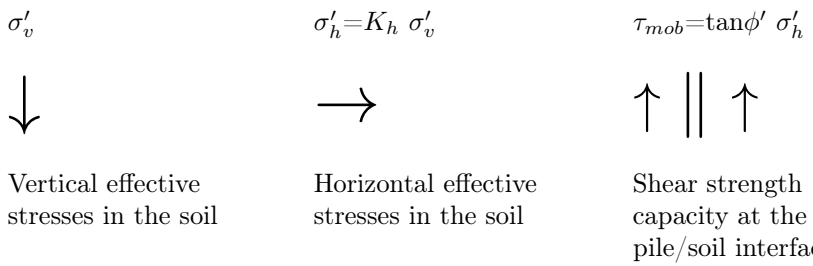

Figure 2.1: *Relation between the vertical (σ'_v) and the horizontal (σ'_h) effective stresses to the mobilisable shear strength (τ_{mob}) at the pile shaft. K_h is the coefficient of lateral earth pressure, and ϕ' is the (interface) friction angle.*

When a pile is loaded axially at the pile head, shear stresses are mobilised in the ground surrounding the pile. This mobilisation occurs in the zone of the soil around the pile base (end-bearing) and at the interface between the shaft and the surrounding soil (shaft-bearing), Figure 2.2. If the shear resistance is sufficient to carry the pile head load, then the axial stresses in the pile will gradually reduce to zero. If the shear resistance is insufficient, the pile will mobilise end-bearing resistance in the soil underlying the base, Figure 2.3. If the shear strength of the soil is exceeded a failure will occure in the ground. If instead the strength of the pile material is insufficient, there may be a structural failure in the pile.

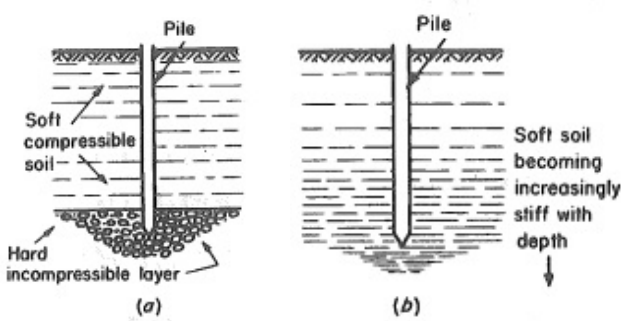

Figure 2.2: *Loadtransfer from pile to soil. a) End-bearing pile b)Shaft-bearing pile (Tomlinson 1994).*

.

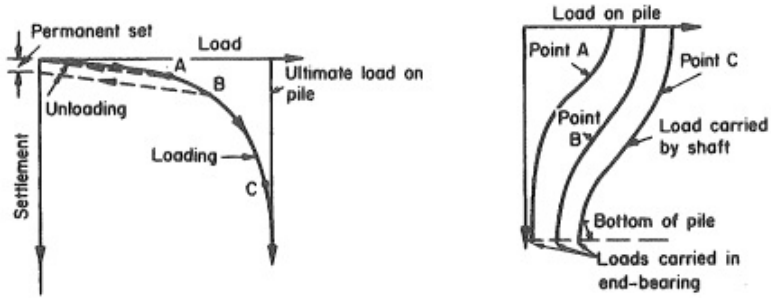

Figure 2.3: *Effects of mechanical loading a pile, in principle. Left: Load vs Settlement response. Right: pile shaft mobilization by depth. (Tomlinson 1994).*

The stiffness of a pile is generally considerably exceeding the stiffness of the soft soil. Consequently, when loading a pile and mobilizing the shear strength, distributed shear strains will appear in the soil surrounding the pile shaft. The level of shear strength mobilisation will evolve by time, as the load redistribution along the pile shaft and in the soil structure take place. For a floating friction pile this will generate an ongoing process of load redistribution, involving continuous changes of effective stresses and strains in the soil surrounding the pile. To mobilise full shear resistance, a slip between the shaft and the soil in the range of 2-5 mm is sufficient, while for the base a considerable larger deformation is required, typically 10% of the pile width (Alén 2012).

The (effective) stress levels in the clay close to the pile, however, are complicated due to the large distortions from the pile installation process. As opposed to less sensitive soils, in soft sensitive clay the pile installation disturbance generally results in a strength reduction and a lower stiffness of the clay. Some of this recovers in the subsequent pile set-up phase (e.g. Lehane and Jardine 1994, Fellenius 2014).

As the pile penetrates the soil during installation, the soil below the pile base is compressed and distorted, pushed downwards, and subsequently displaced laterally, Figure 2.4a. During this process any initial structure present in the clay will be destroyed. Consequently, the new soil conditions along the pile shaft will govern the future response of the pile. In soft clays with low permeability and restricted contraction, the soil distortion (i.e. shear) will typically be under constant volume (undrained conditions) where an increase of total stress will be accommodated by an equal increase in pore pressure and a decrease in effective stresses (e.g. Randolph 2003).

Excess pore pressures generated by the installed pile volume will gradually dissipate. The maximum excess pressure is generated close to the pile base during installation. During the equilisation of the excess pore pressures there is a regain in effective stresses in the soil, Figure 2.4b. At the same time aging and creep effects occur. It is not fully understood which mechanisms take place during this process. The time for the dissipation of excess pore pressures depends on the volume of piles installed and the actual hydraulic properties of the clay layer. Experiences from Gothenburg clay show equalisation times ranging from 3 to 6 month (Fellenius 1972).

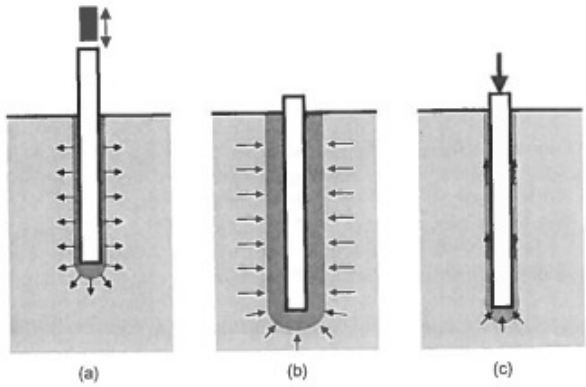

Figure 2.4: *Three main phases during history of a driven pile (adapted from Randolph 2003). The installation phase (a) includes severe distortion of the soil, changes to the fabric and a displacement of the soil to accommodate the volume of the pile. During equilibrium the soil undergo consolidation and aging, including both compression and tensile strains (b). The last phase (c) comprises the loading of the pile, resisted by the pile shaft friction (mobilised shear) and the end-bearing pressure at the pile base.*

The pile installation is resulting in a zone with large strains in the region of 1-2 time the pile diameter D (e.g. Olsson and Holm 1993, Hintze et al. 1997) up to $5D$ (Dijkstra 2015) depending on the material around the pile. Pore pressures are effected in a zone up to 10 - 15D (e.g. Olsson and Holm 1993). Measurements from a number of field tests performed directly after installation indicates about $\Delta u_i = 1$ to $2.5\sigma_{v0}{}'$ on excess pore water pressure close to the pile shaft (compiled by Yannie 2016).

When also using the piles for thermal transfer and storage, a zone around each pile will be affected by heating or cooling. Consequently the soil and pile will change in volume and likely generate changes in stress and strain in all directions. Clearly these changes will involve the same soil volume that is already remoulded and disturbed from the pile installation, and potentially the cycles also involves undisturbed soil at a further distance from the pile. The evolving soil behaviour adjacent to a pile during installation and thermo-mechanical loading are complex, and not yet fully resolved. In addition, it is unclear how the additional heating of a floating pile in a clay deposit will influence the short-term and long-term stability of the pile. Settlements of the superstructure on top of a piled foundation can principally be seen as the sum of the compression in the pile element, the slip between the pile and the ground, and the settlements in the ground.

Piles installed in soil layers with ongoing settlements may be affected by additional axial loads from negative friction also called down-drag. Negative friction occurs when the soil layers surrounding the pile vertically compress more than the pile elements resulting in additional mobilised shear stresses on the pile-soil interface. In areas with soil layers dominated by soft clay, negative friction will affect the pile. In deep deposits of subsiding soil layers these down-drag loads can be the dominating pile load.

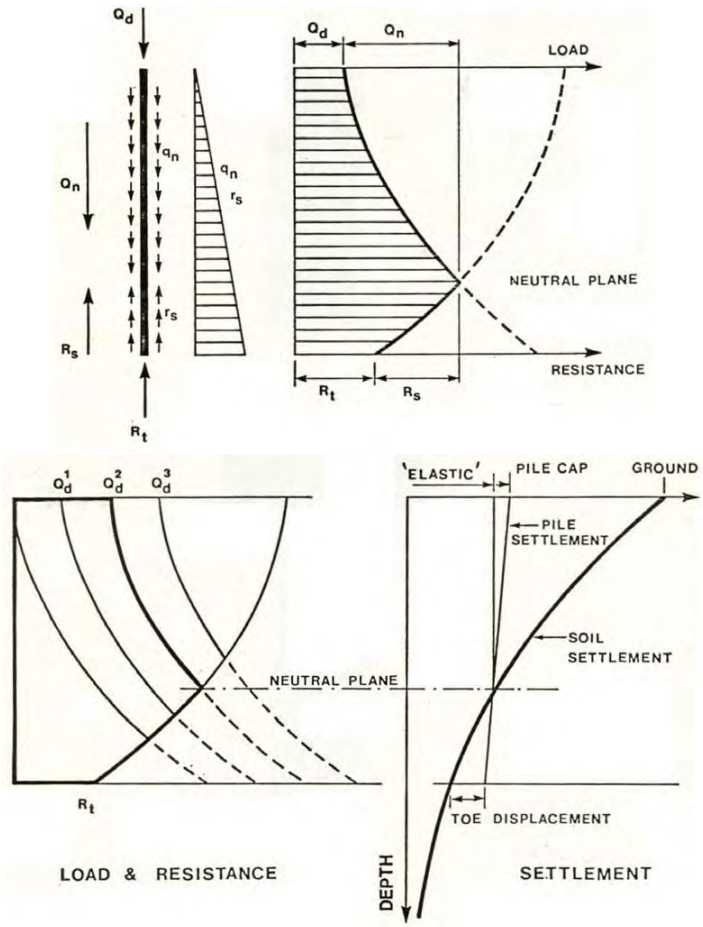

Figure 2.5: *The principle of the neutral plane method (Fellenius 1984). The neutral plane is located where the negative friction, down-drag, changes over to positive shaft resistance (the point of equilibrium). Its location is determined by the requirement that the sum of the applied dead load plus the down-drag load is in equilibrium with the sum of the positive shaft resistance and the base resistance of the pile. A change e.g. in loading at pile head or down drag will consequently make a change in location of the neutral plane, potentially generating settlements of the pile foundation.*

The neutral plane method is a way to visualize the expected load distribution and load transfer in piles that experience negative friction along the pile shaft (Fellenius 1984). The neutral plane defines the depth where the normal load changes sign, i.e. when it changes from a down drag load into shear stress that resists the pile, Figure 2.5. Important to know is that the negative friction originates from the difference in the compression strains between the soil and the pile. Therefore, for a floating pile, the load distribution evolves over time, as both the compression in the pile (which depends on the magnitude of the negative skin friction) and the soil (influenced by consolidation and the pile load) depends on the soil-structure interaction.

When heating or cooling a pile there will be a change in stress and strain due to (restrained) thermal expansion in the pile and in the soil, Figure 2.6. This is in addition to the mechanical loading at the pile head. Consequently, thermal cycles will result in a change of the load and resistance and changes in the position of the neutral plane. Furthermore, heating of the soil surrounding the pile might influence the soil response that governs the settlements in the deposit (thermal consolidation and creep).

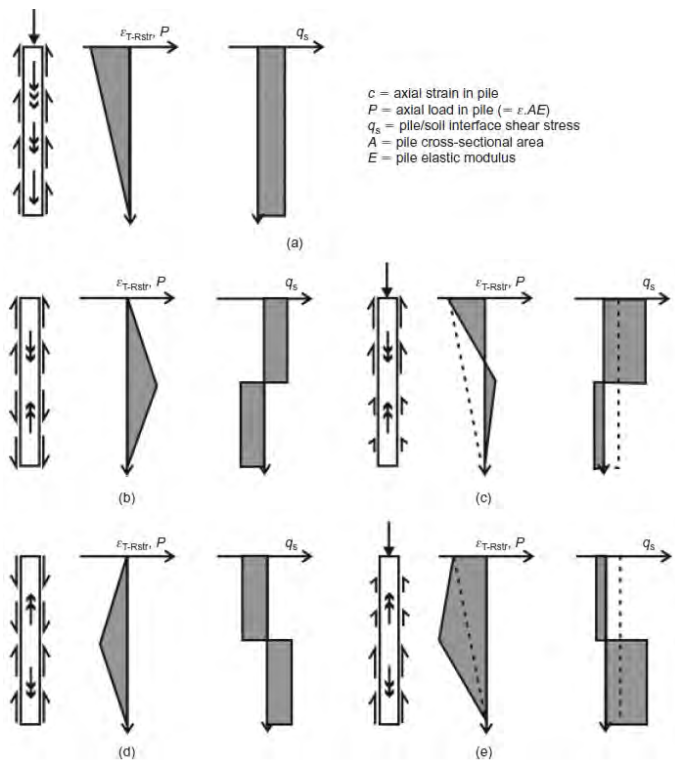

Figure 2.6: *Response mechanisms in principle for a pile undergoing different combinations of thermo-mechanical loading (after Bourne-Webb, Amatya, et al. 2009); a) mechanical load only; b) cooling only; c) combined loading and cooling; d)heating only; e) combined load and heating.*

2.2.3 Cyclic pile loading

Perhaps the most relevant work on the effects of cyclic loading on piles in soft soils is by Karlsrud et al. (1993) who tested the axial cyclic response of open and closed ended piles in soft clays that are somewhat comparable to those in Sweden. A general observation, presented in Figure 2.7, shows that the undrained response drops off quickly in the first 100 loading cycles, and it depends on the mean (average) stress level. Furthermore, two-way loading (full load reversal towards extension) has a much more pronounced effect. In order to better understand this pile response a closer look in the soft soil behaviour under cyclic loads is required.

Depending on the loading amplitude, frequency, mean stress level and the number of cycles cyclic loads will effect the bearing capacity and the pile head settlements. More pronounced effects are expected in case of a full reversal of load where the unloading loop extends to tension loads. In soft clays the long-term ultimate limit state bearing capacity under cyclic loading is lower than the capacity under monotonic loading. In undrained loading the main mechanism links to the build up of excess pore pressures resulting from irrecoverable volumetric and shear strains in the soil. The effective stress in the soil gradually reduces up to the point the next loading cycle cannot be sustained. This mechanism is graphically elaborated in Figure 2.8. This softening mechanism is further accelerated when the clay is prone to collapse of pore space as a result of degradation of micro-structure. The latter is of concern in sensitive clays, such as those found in the Western part of Sweden.

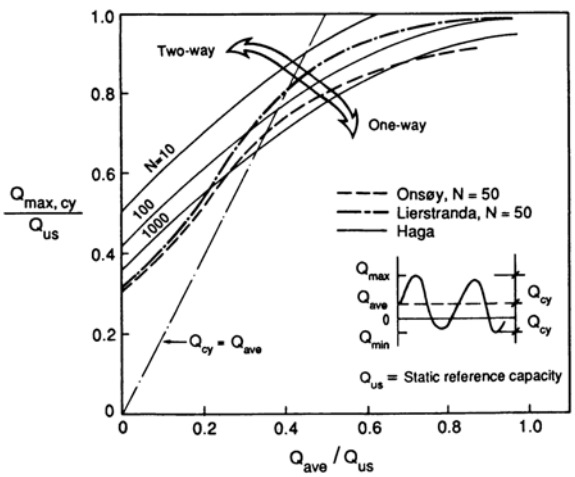

Figure 2.7: *Cyclic capacity (failure) diagram (adapted from Karlsrud et al. 1993) giving a picture of the influence of cyclic loading on the pile capacity in undrained conditions. It relates the peak cyclic failure load amplitude, $Q_{max,cy}$, to the average load, Q_{ave}, and the number of load cycles, N, the piles could sustain before failure was reached. Both axis are normalised with respect to the ultimate static capacity Q_{us}. The cyclic capacity drops rapidly when $Q_{cy} > Q_{ave}$ and thus get a two-way loading (including tension).*

In partially drained conditions the magnitude of pore pressure accumulation depends on the characteristic time period of loading, and the characteristic time period for dissipation of excess pore water pressures. Additional excess pore pressures will accumulate, when the loading period is smaller than the time required for dissipation of excess pore pressures. When the loading period is much larger than the period for dissipation, drained conditions are obtained where for most clays the response from cyclic loading will be a gradually hardening, corresponding to an accumulation of strains with decreasing rate by time, as seen in Figure 2.17.

The above discussion is further corroborated by an extensive laboratory campaign (Wichtmann et al. 2013), who presented a series of anisotropically consolidated undrained cyclic triaxial tests in compression and extension on high quality block samples on soft marine Onsøy clay. The results indicate that, similar to the cyclic pile tests, for a given average shear stress the number of cycles to failure decreased with an increasing shear stress amplitude. Furthermore the undrained cyclic strength was proportional to the loading frequency (rate), i.e. the number of cycles until failure decreased with lower loading rates and increased with increasing loading rate. Although in the laboratory tests the frequencies were rather high (0.1–0.001 Hz), and the conditions undrained the mechanisms still agree well with the field tests presented in Karlsrud et al. (1993) where the loading period still was reasonably short (10 s period representing North Sea wave loading). In case of thermal piles the loading period will be substantially longer, hence partially drained to drained conditions can be expected.

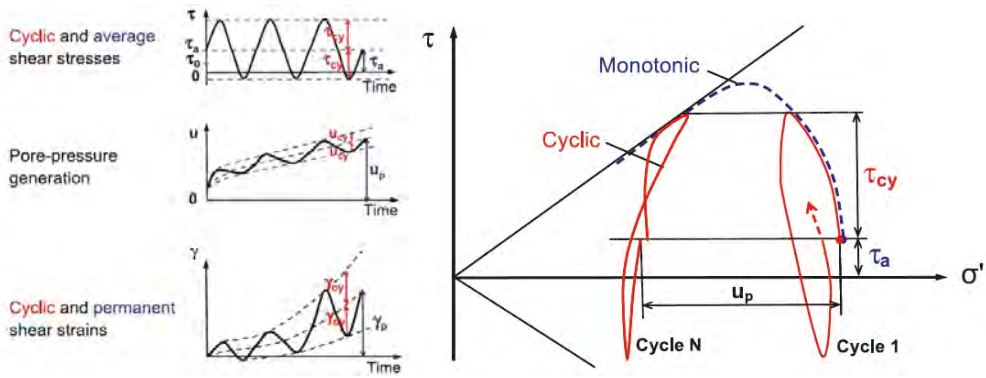

Figure 2.8: *The development of pore pressure, u, and shear strain, γ, with time for a soil element subjected to undrained cyclic loading (from Andersen 2009). τ_0 is the initial consolidation shear stress. The cyclic loading amplitude, τ_{cy}, around a constant shear stress, τ_a. Left: The cyclic loading generates a permanent, u_p, and a cyclic pore pressure component, u_{cy}. The increased pore pressure reduces the effective stresses in the soil, resulting in increased shear strains, γ_p and γ_{cy} with time. Right: The effective stress path for undrained tests to show the difference between a monotonic and cyclic loading.*

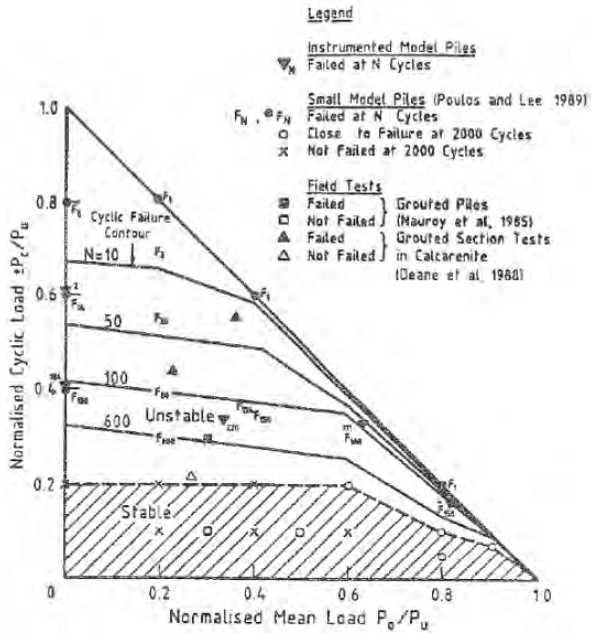

Figure 2.9: *Cyclic load interaction diagram (Poulos 1989) for assessing the significance of cyclic loading, from the proportion of cyclic loading in relation to the static structural load, and the number of cycles repeated. P_c is the cyclic load, P_0 is the mean load and P_u is the static load capacity*

.

For design purposes, the cyclic pile response can be generalised in a design chart, as shown in Figure 2.9. In most situations the bearing capacity reduces, especially if the loading amplitude is large compared to the mean load level. Unfortunately, rate effects are lumped in the chart, and most data is based on undrained loading situations. In case of thermal piles only a low number of load cycles will mobilise a larger soil volume, i.e. as low as 1–2 cycles per year. Following the design chart in Figure 2.9 50–100 cycles (or years for a thermal foundation) the cyclic loading amplitude may be as large as 0.5 before problems are expected. This is a conservative estimate, as in drained conditions this probably will improve (no pore pressure accumulation).

2.3 Soil behaviour under thermal loading

It becomes apparent from the discussion on the pile behaviour in soft soils that the ongoing deformations (settlements) in the soil govern, to a large extend, the pile head displacements and the bearing capacity for floating piles. Additional heating, such as resulting from thermal piles, might negatively impact these deformations, depending on condicitions. This Section will elaborate some of the processes triggered by thermal loading in soft soils on the element level and in the field scale.

2.3.1 Element level response

Temperature has two major impacts on soil: (i) the thermal expansion of the pore water and solid particles, and (ii) a thermally induced modification of the strength of contacts between particles or aggregates (Leroueil and Marques 1996).

When heating or cooling, most material will change in volume. In the case of free expansion the material will expand following:

$$\varepsilon_{T,free} = \alpha_{exp}\Delta T \tag{2.1}$$

where $\varepsilon_{T,free}$ is the strain at free expansion, α_{exp} is the coefficient of volumetric expansion and ΔT is the change in temperature. Heat exchanger piles, therefore, will have thermally triggered volume changes (Figure 2.10) that can lead to additional stresses when restrained, as well as stresses in the soil. This is in addition to the hydro-mechanical stresses after installation and application of working loads at the pile head. If the material expansion response is fully restrained, Figure 2.10b, the thermally generated stresses in the pile, σ_T, will follow:

$$\Delta\sigma_T = E(\alpha_{exp}\Delta T) \tag{2.2}$$

where α_{exp} is the coefficient of expansion and ΔT is the change in temperature. E is the Young's modulus of the pile material.

The volumetric expansion coefficient for water is non-linear temperature dependent. Water is most dense at 4°C, and when heated to about 30°C the volumetric expansion is about 0.5 percent. When water freezes it expands about 9 percent of it original volume at room temperature, 20°C. In contrast, the clay minerals from Swedish clay deposits have a coefficient of volume expansion, α_{exp}, of about 0.025 10^{-3} K^{-1}(Tidfors 1987). Thus, during heating, the expansion of water ($\alpha_{exp,water}$=0.18 10^{-3} K^{-1}) will dominate the soil expansion, as the water expands significantly more than the clay minerals.

In case of heating, depending on the rate and magnitude, this thermal consolidation mechanism will generate excess pore pressures that subsequently dissipate. In turn these changes in effective stress can trigger additional deformations in the soft clays considered here.

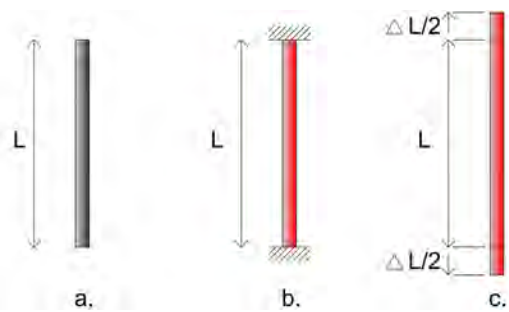

Figure 2.10: *Effects of thermal volume change on a pile. a.) Initial state. b.) Heating of a restrained pile (ε_T=0) will generate stresses in the pile. c.) Free boundary conditions will allow the pile expand when heated.*

In *drained* conditions, where the temperature increase is sufficiently slow, water drains out of the pore system without generation of significant excess pore pressures, an intrinsic weakening effect of higher temperature is compensated by a strengthening effect from a lower void ratio. The latter strengthening is, however, not as significant in sensitive clays that are common in Scandinavia (e.g. Rankka et al. 2004). A decrease in void ratio and a more dense soil structure will not naturally mean a strengthening in a sensitive clay, as the micro-structure of the clay may collapse when loaded before re-bonding in a new stucture. In *undrained* conditions, where the heating rate is large in relation to the characteristic time for consolidation, heating generates excess pore water pressures and, consequently, a decrease in effective stresses. The process is more or less reversible, due to the constant volume conditions, and no significant particle arrangements occur in the soil (Mitchell and Soga 2005). However, in sensitive clays the micro-stucture will be damaged. Repeated undrained loading may still lead to problems as discussed in Section 2.2.3.

The apparent preconsolidation pressure, as evaluated from element level 1D compression tests (vertical loading and restrained lateral deformation) in the laboratory, decreases with rising temperature (e.g. Tidfors 1987, Eriksson 1989). These laboratory tests were performed at different temperatures in oedometer and CRS cells where the fluid surrounding the test samples was controlled in the interval $5 - 50°C$.

This observation on measured preconsolidation pressure was also presented in Leroueil and Marques (1996) and inked with the impact of strain rate in the compression test, Figures 2.11 and 2.12. An increase in temperature entails a decrease of the hydraulic conductivity (Section 2.3.2), likely facilitating consolidation during the compression test. This could indicate an important influence of dynamic viscosity on the change in preconsolidation pressure with temperature (Marques et al. 2004).

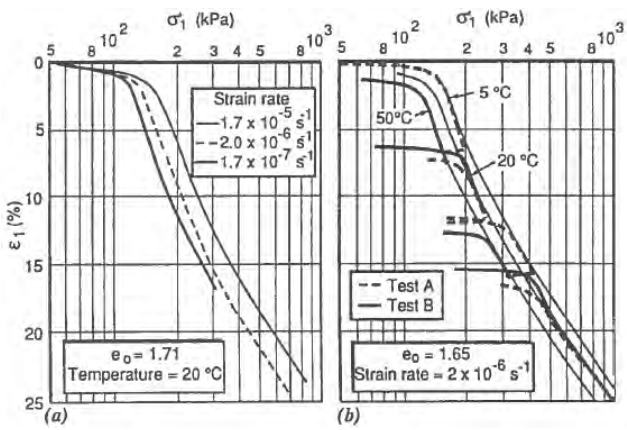

Figure 2.11: *Temperature and strain rate effects on one-dimensional compression tests (Leroueil and Marques 1996). For each step of temperature change, the press was stopped and the sample was heated or cooled under drained conditions. The press was resumed after 24 h at constant temperature. The test results indicate that the preconsolidation pressure will decrease with raising temperature, in the same way as a decrease in strain rate gives decreasing measured preconsolidation stresses.*

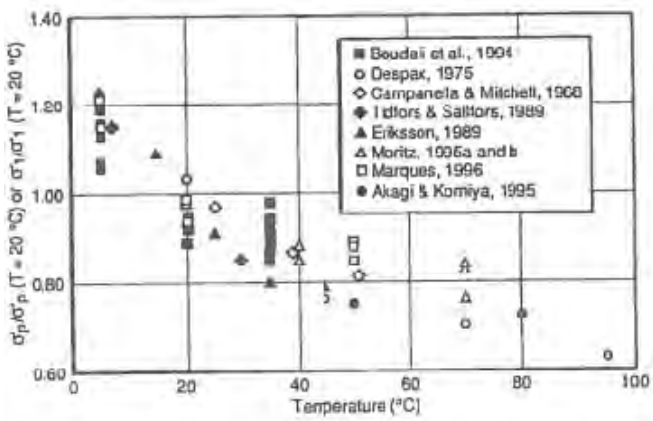

Figure 2.12: *The preconsolidation pressure, σ'_p, normalised with respect to the preconsolidation pressure measured at 20 °C (Leroueil and Marques 1996). The decrease in preconsolidation pressure with temperature is almost 1 % per °C in the temperature interval up to 40° C, as of interest for thermal piles.*

Figure 2.11 presents the result from two test series when altering the temperature during a CRS test. The change in temperature makes the effective stress-strain curves jumping from one constant temperature curve to another, confirming there is a thermal influence on the measured behavior.

In the other end of the spectrum, during freezing the difference in the expansion of the pore water and the soil constituents drives the generation of ice lenses and a complex mobility of pore water. These processes irreversibly change the original clay structure, and the result after thawing is a completely different material with inferior stiffness and strength. Thus, the operation of thermal piles should not reduce the soil temperature below the freezing point.

The volumetric thermal expansion coefficient of steel and concrete is in the range of 0.012 10^{-3} K^{-1}. This means that a thermal change of 20°C in a pile of 10 m length will induce a potential total lengthening of the pile of about 2.4 mm. This will generate substantial stresses in a pile in the case elongation is constrained by the soil (Amatya et al. 2012, McCartney and Murphy 2012). Additionally, the thermal expansion of the pile may generate lateral internal stresses in a solid concrete pile. Finally, the cyclic expansion and contraction of the pile might lead to softening of the pile–soil contact strength and an accumulation of plastic displacements, typically in the first 10-20 cycles (Pasten and Santamarina 2014) . This is, however, more of concern in stiff soils where the shear mechanisms is expected on the pile–soil interface and not in the soil (as is the case in soft soils).

2.3.2 Flow in soft soils

For a saturated soil the hydraulic conductivity (also called permeability) k (m/s) depends on properties of the fluid (dynamic viscosity and density) and the arrangement of soil particles (specific permeability). For soil materials with fixed shapes and sizes of the particles the specific permeability, K (m^2), mainly depends on the porosity and pore connectivity.

The relation between the hydraulic conductivity k and specific permeability K can be expressed as (e.g. Muir Wood 2009):

$$k = K\frac{\rho_w g}{\mu_w} \tag{2.3}$$

where ρ_w is the density of the water, μ_w is the dynamic viscosity and g the gravitational acceleration. Typical values of k used in engineering practice in Swedish clays are k=10^{-10} – 10^{-8} m/s. Both the dynamic viscosity of water and water density are temperature dependent, see Figure 2.13. Consequently a change in temperature also affects the hydraulic conductivity (e.g. Chen et al. 2017). The relative difference in viscosity when the temperature varies from 5°C to 20°C is a decrease of about 50%. Groundwater modelling is an active research area for the conditions considered here, however, the generalised Darcy equations (e.g. Bear and Verruijt 2012) are adequate for soft clays with low hydraulic conductivity (Mitchell and Soga 2005).

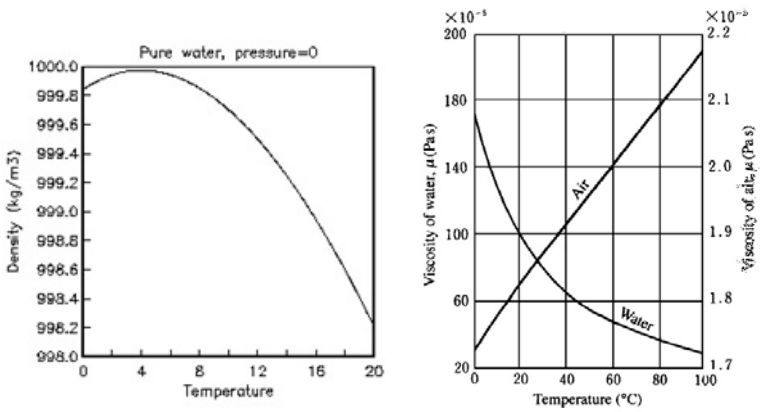

Figure 2.13: *The density and viscosity of water are non-linear temperature dependent (sam.ucsd.edu).*

2.3.3 Energy conduction in soils and piles

Thermal conductivity, thermal resistance and heat capacity are the three key parameters when designing a thermal pile system. Heat transfer in soil occurs mainly by conduction and secondly by convection (e.g. Mitchell and Soga 2005, Brandl 2006). In heat conduction energy is passed from one region to another by molecular transfer. In heat convection energy is transfered when thermo-dynamic systems move relative to each other, e.g. flow of water or gas. In saturated fine grained soils, convection is limited because of the low hydraulic conductivity of the soil. In soils exposed to temperatures below 0°C freezing and thawing process can effect the heat transfer.

Heat flow is modelled by an equation similar to that of groundwater flow. However heat flow is driven by the temperature gradient instead of the pore pressure gradient. The conductive heat flow is also governed by the proportions and the structure of the soil constituents. The solid phase of the soil mass is the most conductive, followed by water and air, respectivally. Consequently, saturated soils have higher thermal conductivity than dry soils. Typically, the thermal conductivity of different types of soils and rocks vary from around 0.2 W/mK to 5 W/mK, depending on the mineral and water content. Saturated clays are in the middle of this range, and have thermal conductivities between 0.9-2.3 W/mK (GSHPA et al. 2012, Sundberg 1991). The thermal conductivity of the plain water is approximately 0.6 W/mK at atmospheric pressure.

The thermal conductivity of concrete piles follows the same order as the soil, as concrete also consists of minerals and water. The conductivity of saturated concrete is typically between 1.4-3.6 W/mK (Loveridge et al. 2014). The thermal conductivity of steel is, however, of higher order, and is between 30-60 W/mK depending on the steel quality.

Heat capacity is the energy needed to raise the temperature of the system by one Kelvin. It is a meassure of the potential of the material to store heat. Volumetric heat capacity for most soil minerals is around 2.3 MJ/K/m^3 (GSHPA et al. 2012). Water has a volumetric heat capacity almost twice as high, 4.2 MJ/K/m^3, whereas the volumetric heat capacity of air is only around 1 kJ/K/m^3. This means the phase proportions of the soils, if not fully saturated, are important in determining the overall heat capacity.

Thermal design approaches for vertical ground energy systems are typically based on the thermal resistance, R, (mK/W) of the heat exchanger, in this case the pile (e.g. Loveridge 2012, Javed and Spitler 2017). The thermal resistance of a pile is the relation between the temperature difference of the fluid in the pipes to the pile-soil interface, and the heat transfer rate per meter (W/m). The thermal resistance depends on the thermal conductivity and the geometry of the pile. Consequently, a large-diameter concrete pile has a considerably higher thermal resistance than a small-diameter steel pile.

Measuring the thermal properties of individual soil layers in a clay deposit is difficult. Therefore it is more common to analyse the overall soil profile. The method most often used for determining thermal properties of the subsurface and thermal foundation systems is a Thermal Response Test, TRT (e.g. Javed 2012, Murphy et al. 2015, Bourne-Webb, Burlon, et al. 2016). In its most typical application, a TRT involves measuring the thermal response when circulating a fluid through the ground heat exchanger while supplying a constant amount of power to the fluid. In the evaluation, a constant Δ T$_{fluid}$ between

ingoing and outgoing fluid reflects a uniform heat input into the surrounding soil. A standard TRT rarely exceeds 60 h. However, with increasing pile diameters, there is a need for increasing the test time. This, generally, is for piles with diameters exceeding 300 mm (Loveridge 2012).

Thermal response tests are subject to errors caused by e.g. uncertainties in measurements, in design parameters or in analysis methods. Uncertainties in the methods of analyses are consequences of limitations in the mathematcial method used to determine the ground conductivity and pile resistance. There are also uncertainties caused by the duration of the TRT and the correspondence between the measurements taken and the boundary conditions required in the evaluation method used. The overall uncertainty is found to be 5-10% for the ground thermal conductivity and as much as 20% on the thermal resistance (Javed 2013). A longer test duration increases the accuracy of the TRT, as it takes the test closer to a thermal steady state with a constant thermal flow rate. At the same time, a longer duration test reduces the impact of errors from thermal fluctuations e.g. caused by daily air temperature changes, possibly effecting surface pipe installations.

There are a number of different methods to calculate the ground thermal response, including analytical solutions, transient models and numerical simulations. The most simplified method is to consider the pile to be an infinitely long line heat source within an infinite medium. The exact line source analytical solution is an integral of the pile or soil radius of interest. Most often an approximation is used to get a simpler algebraic expression (summarized in e.g. Javed 2010). For interpretation, the soil thermal conductivity, λ_s, is then calculated as:

$$\lambda_s = \frac{q}{4\pi k} \tag{2.4}$$

where q is the heat flux (W/m) supplied and k is the slope of the straight line fitted to the measured fluid temperature, when temperature (T) is plotted against logarithmic time, $\ln(t)$.

The pile resistance, R_p, is then determined by equation 2.5 where t is the time, T_f (K) is the mean fluid temperature at time t, T_0 is the undisturbed ground temperature, α is the soil thermal diffusivity, γ is a constant and r_p is the radius of the pile. The soil thermal diffusivity is equal to λ_s/ρ_s and C_s where, ρ_s is the soil density (kg/m^3) and C_s is the specific heat capacity of the soil (J/kgK). By analysing the response curve the thermal response of the soil can be separated from the response of the pile.

$$R_b = \frac{1}{4\pi\lambda_s}\left[\frac{T_f - T_0}{k} - ln\left(\frac{4\alpha t}{\gamma r_p^2}\right)\right] \tag{2.5}$$

The soil thermal conductivity from a number of international TRTs on pile heat exchangers (summarized by e.g. Murphy et al. 2015 and Vieira et al. 2017) are found to be in the range of about 1 to 6 W/mK, with a mean value of 2.5-3.5 W/mK. This range is higher than the thermal conductivity of most geological and structural materials. This indicates potential issues with the duration of the TRT (primarily measuring the pile and not the soil response). Most of the summarised tests are on piles with a relatively small

aspect ratio, $L/D \leq 75$, and none is installed in saturated soft clay deposits. The thermal resistances from the summary above are in the range of 0.06 to 0.37 m/WK.

2.3.4 Temperature effects on consolidation and creep in soft soils

Consolidation is the physical process underpinning time delayed deformations due to mechanical loading in a soil with low hydraulic conductivity. The external total stress increment is first fully transferred to the pore water. In systems with draining boundaries these excess pore water pressures subsequently dissipate due to the flow that is driven by the pressure gradient.
Thermal consolidation refers to the generation of excess pore pressures due to an increase in temperature resulting from the dissimilar expansion coefficients of the pore fluid and the soil constituents. As discussed in previous Section additional changes in the flow behaviour can be expected due to the effects of the temperature on the fluid viscosity and density.

Creep behaviour in soils is defined as ongoing deformations under constant effective stress. An example schematic creep curve from a laboratory test is shown in Figure 2.14. The coefficient of secondary compression, α_s or $C_{\alpha\varepsilon}$, is the rate of deformation under constant effective stresses, i.e. although the creep starts at $t = 0$ it can only be determined from the data after consolidation has finished (excess pore pressures from the load increment are dissipated).

Thermal creep in soils is somewhat more difficult to define as it refers to all processes that lead to a change of creep rate at constant effective stress under a change of temperature. This unsatisfactory definition results from a still unknown driving mechanism of creep in fine-grained particulate media, such as clays.

In general, the creep parameter is dependent on the deformation and the stress history of the soil. The maximum value of C_α is found around the preconsolidation pressure of the clay (e.g. Yin et al. 2011, Olsson 2013), see Figure 2.15. Claesson (2003) generalised this behaviour in a 1D phenomological model, though nowadays comprehensive effective stress based models are available (Sivasithamparam et al. 2015). Results from systematic thermal tests performed in laboratory also confirm the consistent behaviour with largest creep rates near the apparent preconsolidation pressure.

Experimental evidence indicates that an increase in temperature results in an increase in the creep rate, (e.g. Akrouch et al. 2014) though in stiff clays.

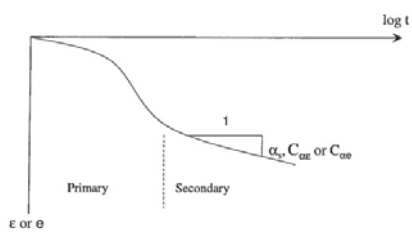

Figure 2.14: *Creep under constant effective stresses during time, describing the creep parameter C_α (Olsson 2010).*

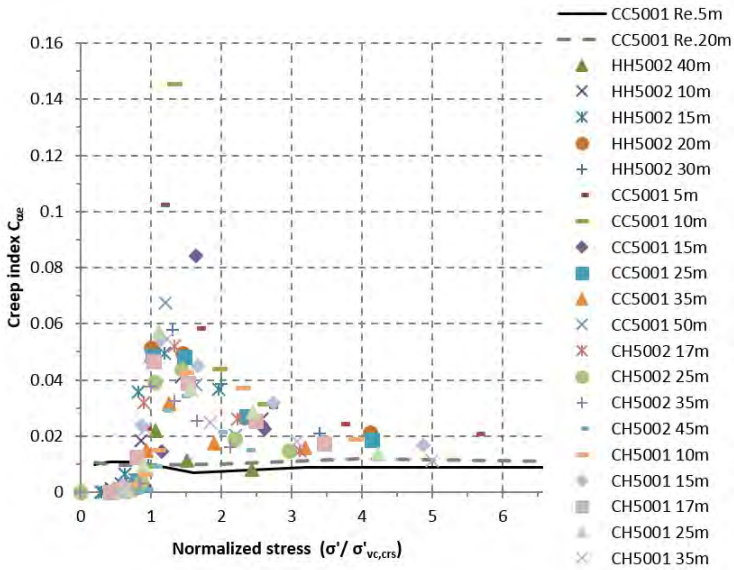

Figure 2.15: *Evaluated values of the creep index C_α from clay samples from the Gothenburg area (Olsson 2013). The maximum values of C_α are found around the preconsolidation pressure, $\sigma'_{vc,crs}$. Note that the two remoulded clay samples behave different, as their soil history is deteriorated.*

Campanella and Mitchell (1968) performed a series of undrained triaxial compression tests on samples consolidated to the same initial effective stress level but at different laboratory temperatures. The results indicated that consolidation at different temperatures resulted in a decrease in void ratio after consolidation is finished. During repeated cycles of heating and cooling the decrease in void ratio was smaller, but still there was an additional decrease from each cycle. Campanella and Mitchell (1968) also stated that the effect of a cycle of heating followed by cooling, as in Figure 2.11, mimics the change in the apparent pre-consolidation due to aging and creep under a constant external load, as in Figure 2.16.

For piles installed in soft clay the long-term static bearing capacity is sometimes discussed as the *creep load*. The creep load is the limiting load for creep failure to appear from long-term static loading. The creep load is often found to be about 0.7 to 0.8 Q_{ult} from mainly undrained quickly maintained static load load tests (Bengtsson and Sällfors 1983, Eriksson et al. 2004). For a full discussion on the underlying mechanisms is referred to Yannie (2016).

Following the above, depending on the stress history, the load increment, and the heating conditions, an increase in the temperature of a normally consolidated or slightly overconsolidated clay potentially leads to additional creep deformations, which in turn affect the pile head settlements.

The creep rate of a pile is proportional to the magnitude of the mobilised shear along the pile shaft. The remoulded zone from pile installation adjacent to the pile will

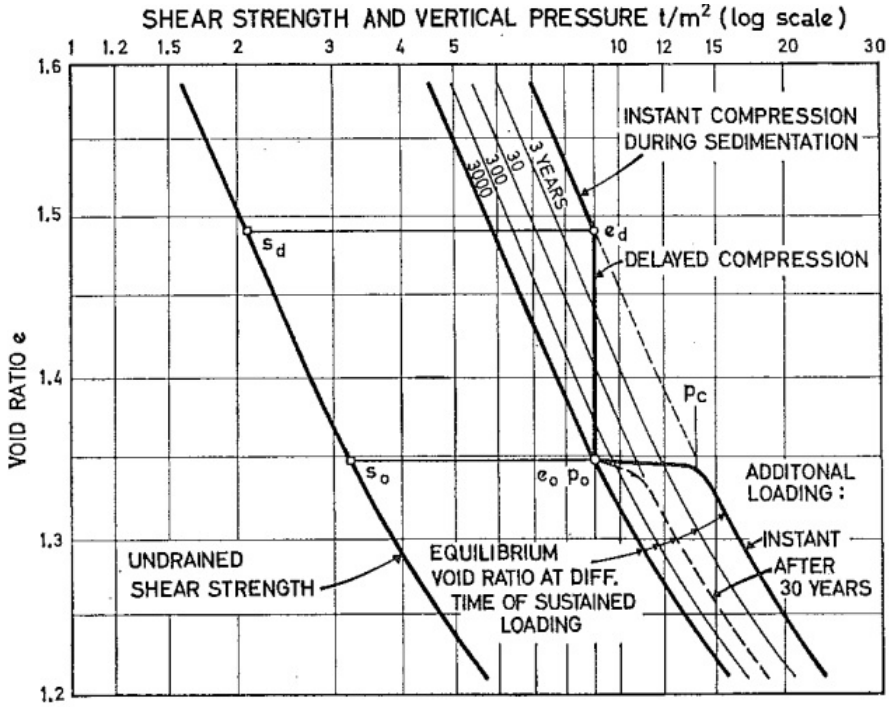

Figure 2.16: *A diagram describing the conceptual model of consolidation according to Bjerrum (1967). The different curves represents the equilibrium void ratio for different values of effective overburden pressure at a specific time of sustained loading. The "delayed compression" represents a reduction in volume at unchanged effective stresses. The model was intended to explain the overconsolidation of soft virgin clays resulting from geological aging.*

likely behave with different creep rate for a given load compared to clay at a larger distance. In remoulded clay the creep rate is systematically lower in relation to the intact clay, independently of mobilisation (Olsson 2013). At further distance, with less thermal influence from the pile, a smaller effect of additional temperature induced creep is expected, though the initial creep rate will be higher as the clay is less disturbed. As long as the heating effects do not lead to a dramatic softening on the pile-soil interface the far field on-going deformations will drive the long-term settlements of a pile. The thermal pile response, therefore, depends on the relative magnitude of the disturbed zone around the pile (with low creep rate) and the total soil volume affected by the thermal heating.

2.4 Pile design and Limit states

Pile design is often based on empirical design methods calibrated against pile load tests (e.g. Randolph 2003). In engineering practice it is attractive to find a relation between a measurable quantity in the soil, such as the undrained shear strength, and the experienced loading capacity of a pile from a pile load test. In Sweden pile design is normally performed using the α- or β- methods. The main difference is that the first is a total stress method often used for fine grained soils, whilst the β-method is an effective stress based method.

As opposed to international developments on pile design (e.g. Lehane, Chow, et al. 2000, Lunne et al. 2009), in Sweden the total stress method is primarily used for the prediction of Ultimate Limit State (ULS) bearing capacity of piles in fine grained soils, such as clays. In this method, α is used as a by experiences calibrated proportional correlation factor between the undrained shear strength of the clay (usually measured in-situ using a vane-test) and the measured bearing capacity of a single pile axially loaded in compression. In coarse grained materials the friction between the pile and the soil is formulated as function of the the horizontal effective stresses, σ'_h, and the interface friction coefficient, $\tan\phi'$, along the pile shaft. The horizontal stress, σ'_h, is linearly proportional to the effective overburden stress, σ'_v, represented by earth pressure coefficient, K_h. The earth pressure coefficient is often collapsed with the friction coefficient $\tan phi'$ in a β factor due to difficulties in determining the horizontal effective stress component and the friction coefficient.

In the design of end-bearing piles the main focus is on loading capacity of the pile to ensure the strength of the pile in ULS. An end-bearing pile may likely be fully exposed for negative skin friction as the pile tip is relatively fixed. To prevent detrimental effects from negative skin friction in locations with deep deposits of soft clay, piles may instead be designed as floating friction piles. The latter is a Serviceability Limit State design (SLS) where the pile head settlements under the working load are compatible with the building. The floating energy piles considered in this Thesis, therefore, focus on the SLS performance that is governed by the soil deformations which most likely are more significant than the deformations of the pile element itself.

In Swedish practice negative friction is taken into account in pile design when the relative movement pile-soil exceeds 5 mm (Eriksson et al. 2004). In international literature (Fellenius 1972, Torstensson 1973 among others) a relative movement of $D/20$ to $D/100$, in relation to the pile diameter D, is found sufficient to mobilise considerable negative skin friction. In this case where the main mechanism is at the pile shaft the 5 mm criterion is more reliable as strain in the failure plane adjacent to the pile does not scale with pile diameter, as it is a property of the soil.

For a floating pile, as shown in Figure 2.5, the pile dimensioning above the neutral plane is governed by the pile segment strains and below the neutral plane by the (long-term) soil deformations. In Swedish conditions the practical experience is that, for the design loads used, floating piles installed in soft soil layers rarely fail (creep rupture), but may considerably settle in SLS. This e.g. when the piles are too short leading to a neutral plane location in a soil layer that still experiences significant ongoing deformations from historic fills, or new surface loads, groundwater draw down etc. (e.g. Claesson, Holmberg, et al. 2007).

2.5 Field scale thermal loading response

Systematic data on the performance of thermal piles in soft soils is ideally gathered in well controlled physical model tests at elevated stress level in the geotechnical centrifuge as these have favourable time scaling of the diffusion processes (consolidation and heat conduction): $t_m = t_{in-situ}/N^2$ where N is the geometrical scaling factor, the proportion of the centrifuge model in relation to the in-situ dimensions (Taylor 2003). As opposed to the soils considered in this study, the few publications that report physical model tests on thermal model piles (e.g. Stewart and McCartney 2013, Ng et al. 2014 and Nguyen et al. 2017) mainly studied laboratory soils (sand and kaolin clay). Although it is not impossible to re-create a sensitive soil in the laboratory (Meijer and Dijkstra 2013) still the long-term creep effects of interest here will not be properly scaled. As a result, field scale testing of thermal piles need to be considered. Results from the centrifuge tests performed by Ng et al. 2014 is presented in figure 2.17, indicating a hardening effect on the clay from the cyclic loading.

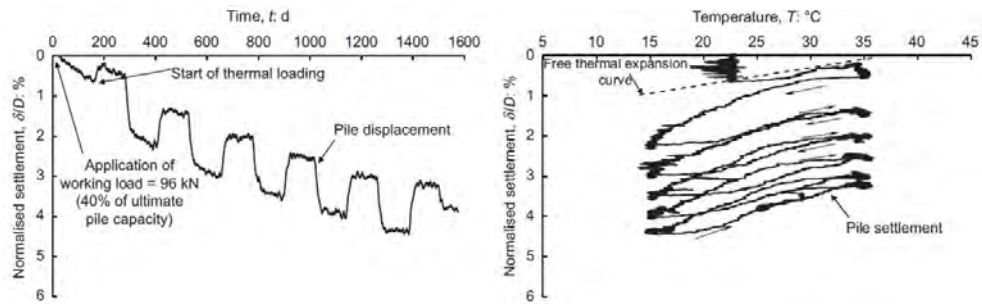

Figure 2.17: *Results from centrifuge tests on a floating pile in slightly overconsolidated kaolin clays, OCR=1.7 (Ng et al. 2014). Accumulation of mechanical and thermal strains (pile head displacements), with decreasing rate by the number of cycles (hardening). The thermal loading cycles are varying between 13 and 36° C, with each cycle lasting for 216 minutes in the centrifuge, corresponding to 8 month in prototype scale (scaling factor 40g). The dimensions of the model pile is D=22 mm and L=420 mm (L/D=19).*

So far no field tests on thermal floating piles in soft soils are found in the literature. Full scale thermal pile tests are with only a few exceptions performed on bored or auger piles (Brandl 2006, Laloui et al. 2006, Bourne-Webb, Amatya, et al. 2009, McCartney and Murphy 2012, Hemmingway and Long 2013, Abdelaziz 2013, Loveridge et al. 2014, Hu et al. 2014, Murphy et al. 2015, Sutman et al. 2015, Singh et al. 2015, Yu et al. 2015, You et al. 2016 and Zarrella et al. 2017). In most cases the test piles are also in large diameters D >400 mm. Driven precast piles are used only in a few presented tests (Lennon et al. 2008, Park et al. 2013, Carlsson 2015, Kesti 2015 and Alberdi-Pagola et al. 2016). In case of small diameter piles the slenderness ratio is still relatively small, i.e. L/D <70, compared to Swedish piles (Lennon et al. 2008, Akrouch et al. 2014, Sutman et al. 2015, Carlsson 2015, Alberdi-Pagola et al. 2016, Ronchi et al. 2016 and You et al. 2016). Piles with a larger L/D, >70, have been tested too, but all in stiff clay, loess or

sand, not in soft clays (Abdelaziz 2013, Loveridge et al. 2014 and Hu et al. 2014). A limitation of the tests reported so far is that all these tests focused on piles installed in stiff soils, varying from saturated silty clay to unsaturated sand or gravel. In those cases the additional stress in the pile from restrained expansion were of most concern (see Fig. 2.6), in addition to the thermal response of the soil. Most provide some site investigation data and sometimes results from field instrumentation is presented in addition to the pile response. The main focus has been on the thermo-mechanical pile response and not so much on the soil behaviour of the soil surrounding the pile.

From the results of the field tests above, simplified descriptive load transfer mechanisms have been developed for a pile subjected to thermal thermal loading only and in combination with mechanical loading (e.g. Amatya et al. 2012). Most recently, Bourne-Webb, Burlon, et al. 2016 have presented a comprehensive review of analysis and design methods for thermal piles. Although there is an absence of research on (floating) thermal piles in soft soils there is a substantial body on (shallow) thermal storage in soft clays. In Sweden the Council for Building Research initiated an ambitious research program to meet the clearly expressed governmental ambition of limiting the use of energy and the national dependency on oil. The research projects included a few full scale installations of vertical thermal collectors (hoses) in different soils, and laboratory testing of thermal behaviour of clay, among others and resulted in several publications on ground heat exchangers and ground thermal response (e.g. Jordvärmegruppen/CTH 1979, Claesson, Eftring, et al. 1985, Adolfsson and Sällfors 1987 and Tidfors 1987).

Results from one of the fields tests, performed in soft clay in Kungälv in 1981–1984 comprising a soil volume of 12x12x12 m^3, reported excess pore water pressures in the order of 5 kPa in the middle of the soil volume when increasing the soil mean temperature from 15-30 °C (Adolfsson and Sällfors 1987, Adolfsson and Sällfors 1990). In the end of heating, the excess pore pressures started to dissipate, though relatively slow, i.e. a year for full dissipation. A 25 mm heave of the soil surface was measured during the first heating cycle, while during the following cycles a accumulated total settlement of about 45 mm after 3 years was measured. The deformation in the soil were primarily measured in the top soil layers (which have low mean effective stress level). Another thermal heat storage extending 38x65x35 m^3 was installed in soft clay in Kungsbacka 1981 for permanent use (Rhen 1988). Cycles of heating and cooling the storage mean temperature in the range of 7-15 °C generated an excess pore water pressure in the middle of the storage of about 5-10 kPa. Settlements were measured in the area between 1981-1984, in total about 25 mm at the ground surface of the facility. These were not solely from the heating cycles, as an additional surface loading from a fill was reported. During periods of heating the storage the ground surface was heaving about 15 mm. This was explained corresponding to the volumetric expansion of water during heating.

More recently, the Swedish Geotechnical Institute (SGI) performed laboratory and field tests at elevated temperatures (e.g. Sundberg 1991, Moritz 1995 and Gabrielsson et al. 1997). The tests looked primarily at heating soft clays to high temperatures, up to 80 °C at a test field in soft clay in Linköping with dimension 10x10x10 m^3. Additional excess pore pressures of ±40 kPa were measured during the heating and cooling cycles. The cyclic thermal loading generated large settlements, in excess of 80 mm after 2.5 year of testing. The first cycle generated settlement of 30-35 mm, Figure 2.18. However, these

temperatures are above those used for thermal piles.

Floating piles installed for thermal storage in soft sensitive soils may trigger settlements in the clay, and consequently this poses a risk of excessive settlements of the pile foundation itself. Therefore, this research will perform novel field tests on mechanically loaded slender floating thermal piles in soft sensitive clay under monotonic and cyclic thermal loading.

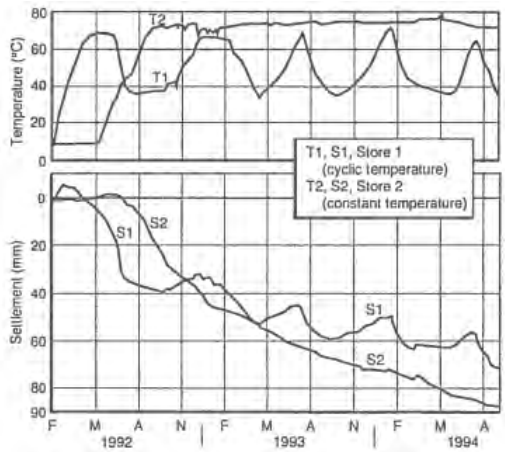

Figure 2.18: *Temperature change register and accumulated settlement and cyclic heave from heating of the ground surface from thermal tests in Linköping, presented by Moritz (1995).*

3 Test site; conditions and soil properties

3.1 Introduction

Instrumented test piles are installed at two locations in the Gothenburg area; Utby and Chalmers Johanneber Campus, see Figure 3.1. The test piles are full scale in-situ floating piles installed in deposits of soft clay. In this Chapter the evaluated soil condition and properties from the field and laboratory investigations are presented for the Utby test site, which is the main test site.

3.2 Utby test site

The test site is located in Utby in eastern Gothenburg city, in an area in the middle of the river Säveån valley. Position of the test site in reference system SWEREF99/WGS84 is 57.7367, 12.0692. The area surrounding the test site is relatively flat with ground surface level varying between +9.0 and +10.0 according to the Swedish National reference level system RH2000. The test site is located at a distance of approximately 150 m from the small river Säveån. The mean water level (MW) of the river in the section perpendicular to the test site is close to +0.7 (RH2000). The fluctuation between extremes high water level (HHW) and low water level (LLW) in Säveån is in the range of 2.5 m.

Figure 3.1: *Location of the test sites on the Gothenburg map. Utby test site (long array) and Chalmers Johanneberg Campus test pile (short array).*

3.2.1 History

The postglacial soft soil layers at the test site in Utby were deposited about 14.000 years ago, when the glacial inland ice melted off. In the Säveån river valley the post glacial clay is rarely more than 10 m deep. Post glacial clay was deposited in sea water with less salt content than during the clacial clay sedimentation. Glacial clay is typically a homogenous grey coloured clay, with decreasing clay content and increasing common silt/sand layers towards the depth. The post glacial clay in the area is typically dark grey due to organic content, sometimes mudclay. Visually it is hard to distinguish between glacial and post glacial clay. The most reliable way is by analysing shell species, which characterise different environments of sedimentation. This however has not been done for this test site. The geological history of sedimentation in the Säveån river valley is presented in more details by Engdahl and Påsse (2014).

Today's river valley is partly industrial and partly domestic, with some natural parts, see Figure 3.2) In 2014 a strip area in the outskirt of the industrial area was exploited and the ground was improved. The organic topsoil, approximately 0.5 m, was removed and replaced with gravel of the same layer thickness. A small part of the exploited area, approximately 10 m x 30 m, was used as the test site for the thermal piles.

Figure 3.2: *Test site location, marked with a circle in the middle of the figure. The test site is located adjacent to the natural valley area of Säveån river. (www.powerfoto.nu)*

3.3 Soil properties, Utby test site

The Utby test site is investigated by a combination of in-situ tests as well as element level laboratory tests. The natural stratigraphy at the test site is characterized as homogenous soft clay. The top clay layer has developed into a crust, not exceeding 1 m in thickness. At the bottom of the soft clay deposits, there is a 1-3 m thick till deposit. A distinct sulphide smell was occasionally experienced from instrumentation pipes at site. Index properties of the soft clay are summarised in Table 3.1.

Table 3.1: Soil properties determined from routine laboratory tests. The bulk density, ρ, is in tons or Mg per kubik meter of the material. The natural water ratio, ω_N, the liquid limit, ω_L, the sensitivity, S_t, and the shear strength, τ_{fu}, are all evaluated from fall cone test results in the laboratory (SGF 1993). The sampling in the filed is performed using the standard piston sampler, STII, or the Mini Block Sampler, both seen in Figure 3.5.

Depth (m)	*Sampler* $(-)$	ρ $(tons/m^3)$	ω_N (%)	ω_L (%)	S_t $(-)$	τ_{fu} (kPa)
5	STII	1.55	81	63	30	10
6	STII	1.59	71	55	26	9
6	Block		69	52	27	12
7	STII	1.58	72	55	27	10
7	Block		71	53	32	14
8	STII	1.54	71	60	28	14
8	Block		78	60	36	16
9	STII	1.58	75	61	29	17
9	Block		77	57	32	14
10	STII	1.58	70	60	(5)	(3)
15	STII	1.58	57	-	-	-
20	STII	1.65	67	62	32	31
25	STII	1.73	49	43	25	24

3.3.1 In-situ tests

In-situ tests are performed using field vane tests and cone penetration tests (CPT). Field vane tests are performed to assess the in-situ undrained shear strength every meters between 2-28 m depth, Figure 3.3. The vane tests are performed following the Swedish guidelines in SGF Report 2:93E (SGF 1993). The dimension of the vane is ⌀65 mm and the height is 130 mm. The CPT tests are performed in 3 separate investigation points, located close to the positions of the thermal piles at the site. The CPT tests are performed in Sounding Class CPT3 according to the Swedish guidelines in SGI Information No 15 (Larsson 2015). The diameter of the CPT probe used is ⌀ 35.7 mm, with a cone tip angle of 60°. The friction sleeve has an area of 15000 mm^2. The evaluation of undrained shear stress originating from the CPT is performed following the Swedish guidelines, in the software Conrad. Input to the software calculation is 1.0 m fill and crust material as top soil layers, pore water pressure table at 1 m depth, and the clay defined as high sensitive between the depth of 5 to 10 m according to results from the piston sampling. The software evaluates the undrained strength from the registered net cone tip pressure $q_{net} = q_c - \sigma_{v0}$. The raw sounding data is presented in Appendix A.1.

The thermal response test, TRT, (Section 2.3.3) performed in the piles is in itself an in-situ field test to empirically determine the thermal properties of the soil profile. In this presentation the TRT results are presented in Section 5.5 as it is an end result of the field test.

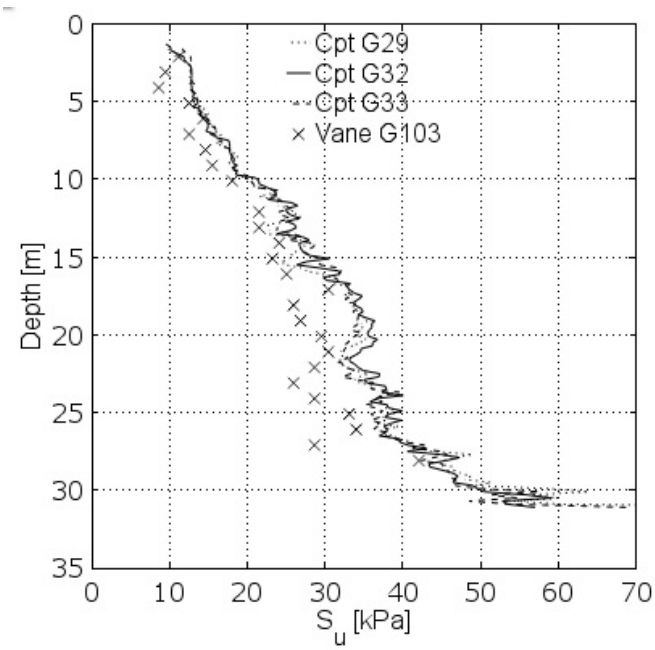

Figure 3.3: *Undrained shear strength from field in-situ tests. The CPT-sounding is evaluated according to Swedish guidelines in Larsson (2015). Location in plan and raw data is presented in Chapter 4.*

3.3.2 Sampling for laboratory tests.

Specimens on soil at the test site are collected by sampling from different depth. For sampling the Standard 50 mm Swedish Piston Sampler STII is used, supplemented with a Mini Block Sampler developed by Norwegian University of Science and Technology (NTNU) in Trondheim, see Figure 3.5. A comparison on the performance and results from SPII-samples and blocksamples at the Utby test site is presented by Karlsson et al. (2016), focusing on the effects on sample disturbance.

The handling of the samples, from the test field to the climatized laboratory environment (8 °C), are performed swift and carefully to minimize the sample disturbance. The laboratory tests scheme is designed to enable laboratory tests performed in a few days after sampling at the test site.

3.3.3 Laboratory tests

The soil properties i.e. density and water content, are determined using laboratory standard analyses on the collected samples. The soil properties determined are presented in Tables 3.1 and 3.2.

The thermal conductivity and heat capacity are determined in laboratory environment using a thermal properties analyzer, KD2 pro. The results from a measurement sequence of 24 h are presented in Figures 3.4. The measurements are performed at two different temperatures, 5 °C and 22 °C. The results indicate similar properties independent of the actual temperature of the sample. The thermal conductivity is measured to be 1.17-1.18 W/mK and the heat capacity 3.2-3.4 MJ/Km^3.

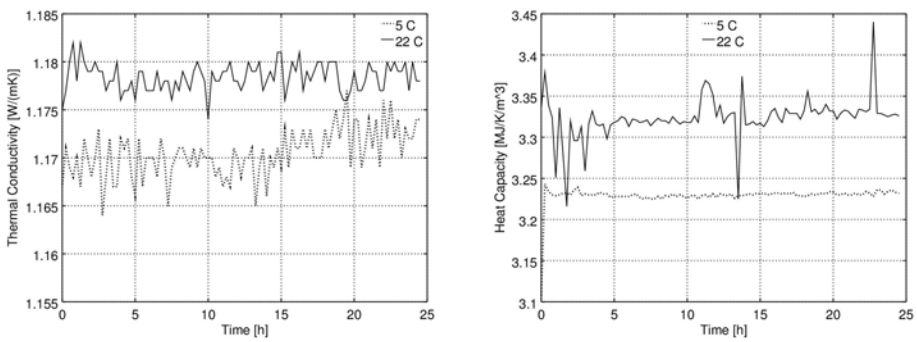

Figure 3.4: *The thermal conductivity and heat capacity determined from tests at 5 °C and 22 °C ambient temperature.*

Figure 3.5: *Piston Sampling STII, 50 mm diameter, and Mini Block Sampler, with a diameter of 165 mm and height of approximately 300 mm. The soft clay at the test site is easily observed in the photo.*

Constant Rate of Strain tests (CRS) are used to initially determine the compression properties, summarised in Table 3.2. The evaluation is made based on the $\sigma - \epsilon$-plot. Incremental Loading oedometer tests (IL) are also performed on similar samples from the same depths as for the CRS tests. In Figure 3.6 and 3.7 the results for CRS and IL oedometer tests are plotted with respect to normalised stress (vertical effective stress in the sample divided by evaluated in-situ vertical effective stress) and the axial strains for different depths. When comparing the CRS and IL response the CRS curves indicate somewhat higher values on the preconsolidation pressure than is the case for the corresponding IL oedometer test.

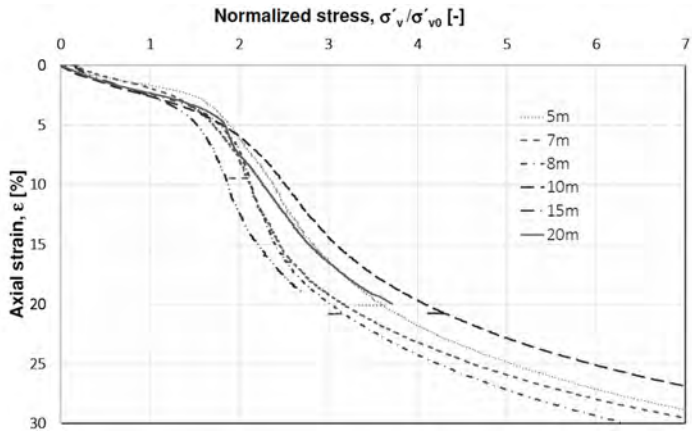

Figure 3.6: *Load - compression response from CRS tests.*

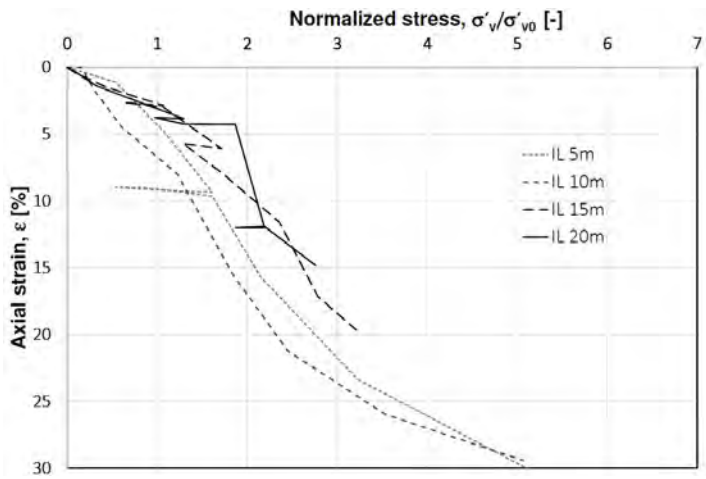

Figure 3.7: *Load - compression behavior from IL tests.*

Table 3.2: Properties of Utby clay. The stiffness properties are evaluated from the CRS tests performed on samples from each depth presented. The effective vertical stresses in-situ, σ'_0, are calculated from the bulk densities and the pore pressures measured at the site. From the CRS test results the preconsolidation pressure, σ'_c, M_0 and M_L are evaluated according to Swedish practice (e.g. presented in Larsson 2008). M_0 is the oedometer modulus in the elastic range and M_L is the oedometer modulus immediately after yielding.

Depth (m)	*Sampler* ($-$)	σ'_0 (kPa)	σ'_c (kPa)	M_0 (kPa)	M_L (kPa)
5	STII	37.2	55	3050	310
6	STII	43.0	75	2520	445
6	Block		62	3200	395
7	STII	48.7	63	2560	325
7	Block		63	4080	580
8	STII	54.0	84	2780	260
8	Block		92	4440	350
9	STII	59.7			
9	Block		105	4480	385
10	STII	65.3	107	3090	700
15	STII	93.3	120	3700	515
20	STII	123.1	180	7140	1290

Further a series of triaxial tests are performed. The size of the samples are 50 mm in diameter and the height is 100 mm. In the test the sample is first anisotropically consolidated to an estimated in-situ effective stress level and subsequently sheared in undrained conditions with a displacement rate of 0.01 mm/min. Results from these anisotropically consolidated undrained compression tests (CAUC) are presented in Figures 3.8-3.10. The critical state friction angle is in the range of 30-31 degrees. The peak strength is reached at an axial strain level of 1 to 2.5 percent.

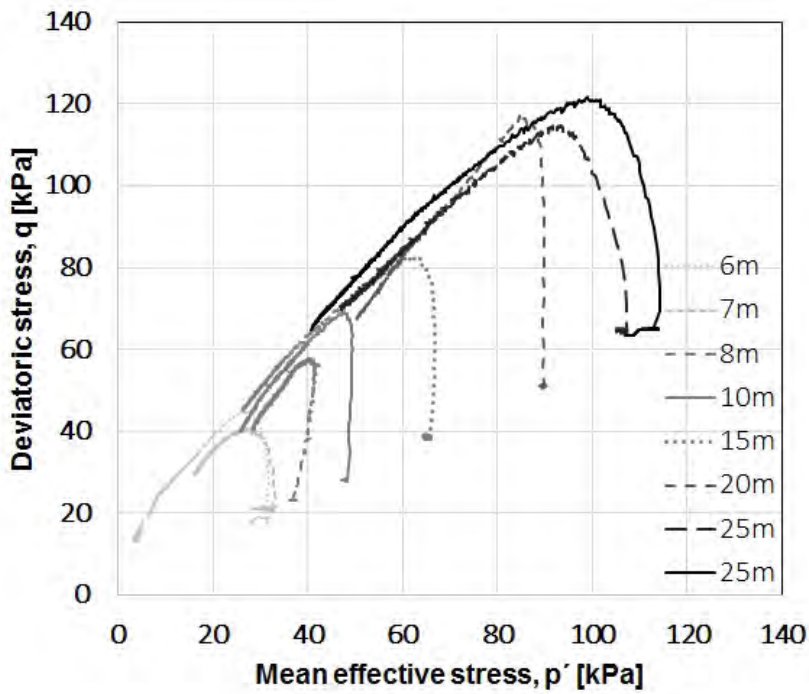

Figure 3.8: *Undrained triaxial test results from samples from a number of depth, presented as mean effective stress vs the deviator stress.*

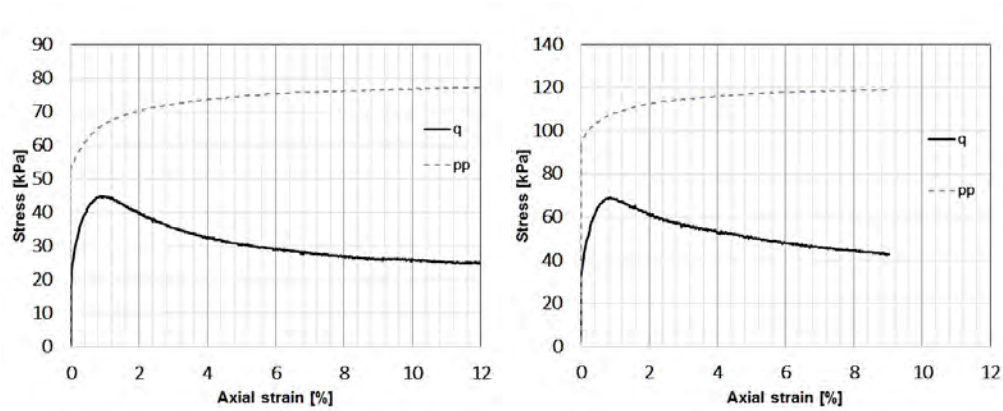

Figure 3.9: *Vertical (σ'_v) and horizontal (σ'_h) effective stresses, deviatoric stresses (q) and generated pore pressure (pp) vs axial strain, from triaxial tests on samples from 6 m and 10 m depth.*

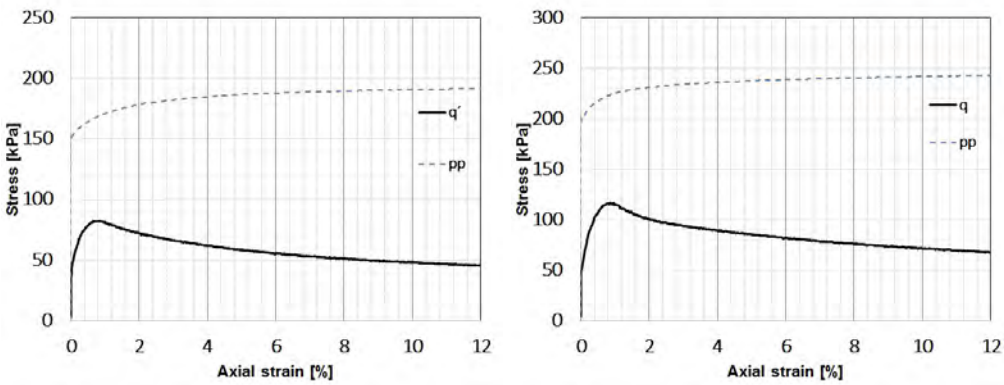

Figure 3.10: *Stress-strain response from triaxial tests on samples from 15 m and 20 m depth.*

3.4 Preparatory test site

For preparatory tests on pile and thermal exchange pipes installation, a test site is established at the Chalmers Johanneberg Campus area, see Figure 3.11. The soil properties at this test pile site are characterised as 1 m of gravel on top of 5 m peat and 12 m of soft silty clay. This is determined from CPT-sounding and from piston sampling performed. The total depth of the deposit is close to 18 m. At bottom of the stratigraphy there is a thin layer of till. The ground water level is located 0.1-0.2 m below the ground surface. There are no measurements performed on the pore water pressure distribution by depth. Further there are no measurements performed on soil sample level of the thermal properties of the soil. The density of the clay at 10 m depth is 1.5 tons/m^3. Natural water content w_N is about 80%.

Figure 3.11: *Preparation works at the test site at Chalmers Johanneberg Campus area. The exchanger pipes and fiber sensors are prepared, fixed together and rolled up before installation in the field.*

4 In-situ thermal test pile setup

4.1 Introduction

The thermal test piles at Utby test site are slender floating steel and concrete piles, installed in a very soft sensitive clay. The mechanical load is applied on the steel piles as a static dead weight load. The thermal loading is applied on one of the steel piles as heating and cooling cycles of 5-20 days length. At the Utby test site the piles and the soil are instrumented with a wide array of sensors in order to capture thermal and soil response during operation of the thermal pile. In this Chapter the loading rig for static loading, test pile design and instrumentation is elaborated.

4.2 Design considerations

The field test steel piles are arranged in pairs, one thermal pile for testing and one reference pile in similar specifications and instrumentation as the thermal pile. Additionally, an instrumented concrete pile with the same length as the steel pile is installed to compare differences in thermal response of steel and concrete piles. The test piles include a slender steel pile and a reinforced pre-cast concrete pile. The slenderness, length/pile diameter ratio, L/D, for the steel pile is 240 and for the concrete pile is 105. A steel pile with full instrumentation was used as the main test pile. The use of the steel pile minimises the time required to change the temperature and forms a well defined thermal boundary that responds fast in relation to the soil.

The static load is chosen to be a dead weight load since it will stay constant without need of regulation. Load interference effects are also avoided as no anchorage piles or rods are used to mobilise the load.

Instrumentation of pile and loading rig, see Figure 4.2, is done so that the differences between test pile heating and cooling operations can be compared for the thermal and the reference pile. The sensors in the clay have been installed using plastic rods. This is to minimise thermal disturbance of the soil from the instrumentation. The sensors in the steel piles are installed in pile segments to enable proper calibration of the pile instrumentation. All sensors are systematically cross-calibrated before use.

The location of the test site is in an area with thoroughly investigated homogenous soft sensitive clay deposit. The test site is in a fence protected area with access to a reliable electricity supply and a road superstructure to e.g. facilitate safe transportation of materials and equipment.

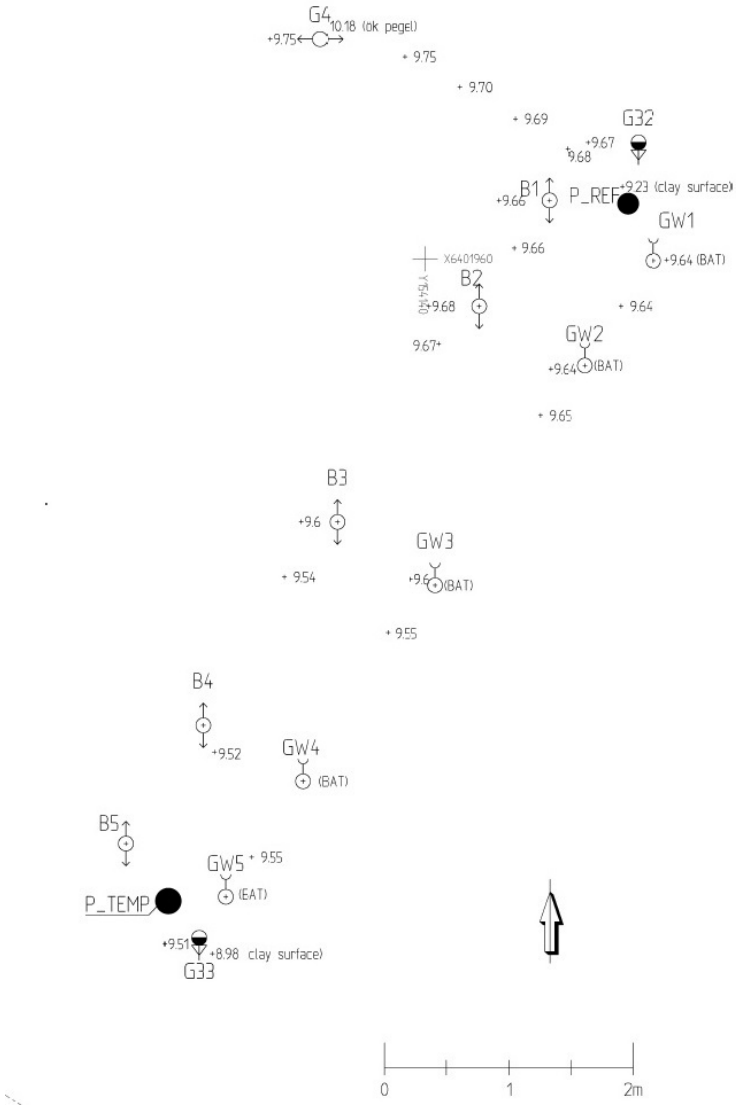

Figure 4.1: *Plan Utby test site. The thermal steel test pile is notated P-TEMP and the paired reference pile is notated P-REF. Bellow-hoses for measuring settlements are notated B1-B5 and sensors to capture pore water pressure is notated GW1-GW5. G4 is a settlement plate. Out of figure, 20 m to the west, an independent reference point is established consisting of a settlement plate, bellowhose and a pipe for ground water table monitoring. The concrete test piles are installed in a parallel position 10 m to the south-east.*

4.3 Thermal test piles and field loading rig

4.3.1 Test piles and pile installation

The main test site in Utby include four floating test piles. Two test piles are made of steel and the two others are made of concrete. The steel piles are SSAB/Ruukki ∅115 mm x 6.3 mm thickness with a total length of 28.8 m each. The precast concrete piles have a square section, 270 mm x 270 mm, with a hollow pipe in the center for the installation of the collector pipes. The length of the concrete piles is 28.0 m each. In positions between the steel and concrete test piles additional end bearing piles are driven to bedrock to serve as vertical reference level, and for partly bearing the loading rig used for static loading of the test piles.

The steel piles are installed using a hydraulic hammer Furukawa HB8G carried from a mobile lorry rig. The concrete piles are installed using a piling rig (Liebherr LB20). The concrete pile is jacked using the weight of the pile hammer. Because of the soft clay there was no need for vibration/hammering.

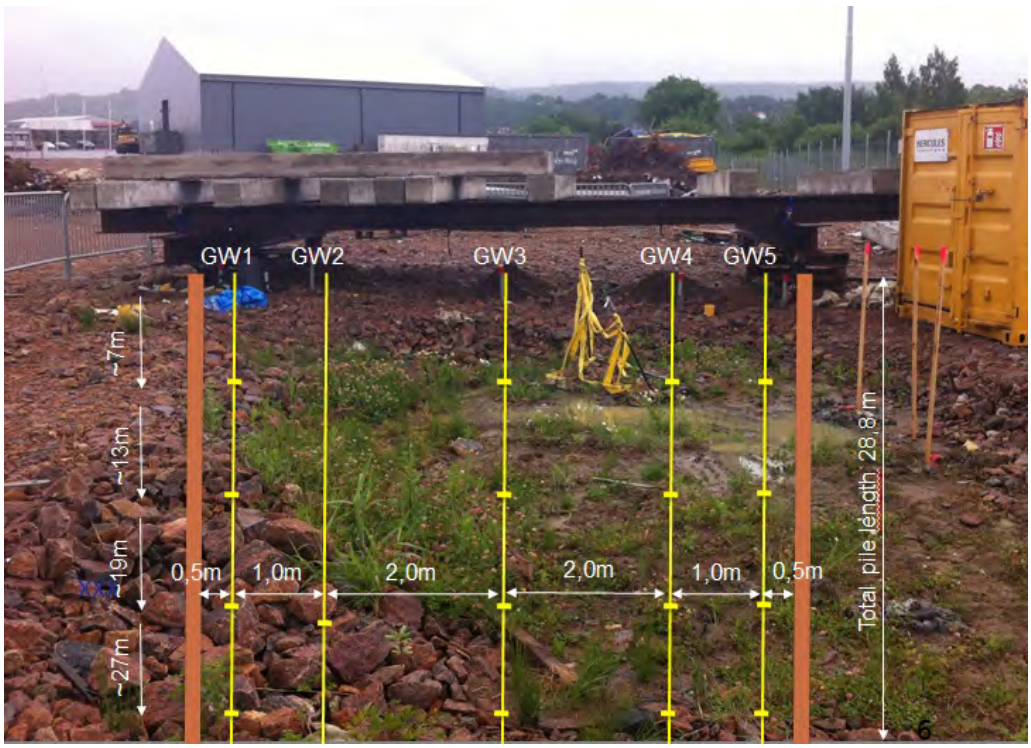

Figure 4.2: *Instrumentation for capturing pore pressure and temperature data in the soil profile at different distances from the test piles and at different depth from ground surface. The thermal pile used for heating cycles is the one at the right in the figure. The paired reference pile is to the left.*

The SSAB/Ruukki piles are made in steel quality S440J2H. The Hercules precast piles are made in concrete strength quality C50/60 following the standard SS-EN 197-1. The reinforcement steel in the piles is of quality B500B following the standard in SS-EN 212540. Main reinforcement bars are 2∅12 mm in each pile section corner. Shearing reinforcement bars are ∅5 mm.

The 28.8 m steel test piles are composed of sections of 6.0 m length separated in between by shorter sections of 1.2 m length. Strain gauges and temperature probes are glued on the inside surface of these 1.2 m pile sections. Cables for connecting the sensors to a logger are taken inside the pile and brought out through an opening in the pile head. The logger equipment is housed in a steel 10 foot insulated container standing close to the rig.

Figure 4.3: *Loading rig under construction and loading. At the left part of the rig the foundation piles are endbearing, at the right side the piles are floating and are used in the thermal tests. The container behind is for housing computer, logger etc. The concrete test pile is installed out of the figure, to the left.*

4.3.2 Static loading

For static loading of the floating steel test piles a dead weight loading rig was placed on the pile heads, see Figure 4.3. The main structure of the rig is made from steel HEB 300 beams. The main structure is further reinforced with diagonal beams to prevent horizontal torsion in the rig, which can be seen in Figure 4.3. Concrete elements of 5 m length, each with a weight of approxiamtely 900 kg, provide the load required for mobilising the pile serviceability load, see Section 4.6. The static load is maintained for 6 months before and during the thermal testing period.

4.3.3 Thermal sensors in the pile

Temperature in the piles is measured using Resistance Thermal Detectors, RTDs, and Optic Fiber Sensors, OFSs.

Table 4.1: Summary of sensors installed to capture temperature at Utby test site.

Position	*Type*	*Quantity*	*Comment*
Ground surface	Resistance thermal detector, RTD	1	
Thermal pile	Resistance thermal detectors, RTDs	2	
	Optical fiber sensors, OFS	6	
Reference pile	Resistance thermal detectors, RTDs	2	
	Optical fiber sensors, OFS	6	
Concrete pile	Resistance thermal detectors, RTDs	1	
	Optical fiber sensors, OFS	3	
Soil	Solid-state sensors	17	

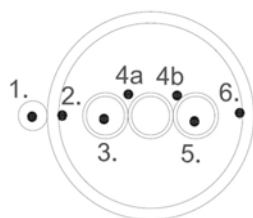

Figure 4.4: *Section of steel pile, ∅ 115 mm, with fiber optic sensors positions together with ∅ 25 mm fluid pipes. In the middle there is one single extra ∅ 25 mm pipe to facilitate optional injection of concrete. The fiber sensors are numbered 1 to 6. Sensor 4a/4b is one single fiber following the fluid pipe in a full loop.*

Figure 4.5: *Pile head designed to let collectors, cables and fibre sensors pass in and out of the pile. Inside the piles a U-tube heat exchanger, made of high density polyethylene (HDPE) pipe, with 25 mm outer diameter was installed for exchanging heat with the ground. A load cell to measure data on applied static load is placed between the loading rig beams and the pile head.*

The installed RTDs in the piles are 4-wire Pt100 sensors (Pentronic 21-20101) covered in a vulcanized thermoplastic elastomer coating to meet protection class IP68. The sensors in the steel pile are installed at 7 m and 14 m depth, fixed with silicon to the inside of the piles. One sensor is cast in the concrete pile during production in the pile factory. The sensor is located close to the pile interface at the middle of one side in the pile section. The sensor is positioned in the pile at 13.0 m depth from the pile head.

Furthermore the optic fibers for temperature measurements are installed at different positions in the pile cross section, see Figure 4.4. The fibers are installed inside the collector pipes to measure the temperature in the fluid along the continuous pipe loop. In addition, fibers are fixed on the outside of collector pipes and also inside and outside of the steel pile wall. The fiber measurement in the pile is complemented with RTDs at pile head level, for measuring temperature of in- and outgoing fluid.

The optic fiber fixed at the outside of the pile, at the interface between the pile pipe surface and soil, is a reinforced fiber Ultra-Fox-Plus 2G50/125 OM2, a multi-mode fiber with the core diameter 50 μm and the cladding 125 μm, following the ISO standard for optical multi-mode cables OM2. The connector to the fiber sensor logger is E2000/APC. The fibers fixed inside the pile and together with the collectors are 50/125 OM2 Simplex 3mm green LSZH, with E2000/APC fiber optic connectors.

Figure 4.6: *Inclinometer sensor fixed at the main beam of the loading rig. The sensor was later covered with an adhesive climate protection mat.*

4.3.4 Displacement instrumentation in piles and loading rig

The static loading rig, Figures 4.2 and 4.3, has welded measure points for levelling in four positions around the structure. As the test site is located at large distance from outcrops of rock there is a lack of proper levelling reference. Therefore two piles at the test site are driven to bedrock, to be used as fixation. These piles are also used to carry the static loading rig in two of its four corners. The two remaining loading rig corners load the floating test piles.

The loading rig has two horizontal inclinometers logging regularly together with the other sensors at the site, see Figure 4.6. The inclinometers at the pileheads capture the inclination of the two main steel beams on top of the loadcells. This setup ensures determination of pile head settlements with time. The inclinometers are the SCA121T from muRata. The inclinometers have a voltage to angle conversion error of $<0.002°$ for inclination angles $<5°$ of the beam toward the horizontal line. The sensor itself is manufactured in protection class IP66. Additionally the sensors are covered by a climate protection mat at the test field.

4.3.5 Instrumentation to capture stain and stress in the piles

The strains in the piles result from mechanical as well as thermal loading stresses. Strain gauges are installed inside the steel piles to capture strains in the steel with depth. The strain gauges are installed at four depths below the ground surface; 1 m, 7 m, 14 m and 21 m.

Four strain gauges at each level are mounted together in a full bridge configuration. Each full bridge is internally connected and mounted in a position to eliminate thermal response in the bridge and exclusively register vertical strain. The strain gauges are HBM YX31. The gauge factor is 2.01 and gauge resistance 120 Ω. Each full bridge configuration is connected with a PVC coated 6-wire cable, HBM Caba 1, to the logger. Length of the cables varies from 9 to 34 m. The wire losses are compensated in the data logger.

A load cell is mounted at each pile head, between the loading rig main beams and the test pile, see Figure 4.5. The load cells are sourced from Vetec 363YH-30t, with a capacity of 30 tons.

4.4 Field instrumentation in the clay

From an instrumentation point of view, the pile length and soil volume involved is huge and impossible to fully populate with sensors. Therefore, a limited number of sensors need to be properly located to assess the performance and impact of heat exchange between the pile and the soil. As the clay is deposited in close to horizontal layers over a wide area, the assumption is made that the clay properties at the test site area are horizontally homogenous. Consequently, the heating and hydraulic impact of the clay has been assumed to be radial symmetric around the pile. Therefore, representation of the soil volume is covered by sensors in only one vertical section perpendicular to the pile. Bellow-hoses for measuring distributed settlements manually, and sensors to capture temperature and pore pressure data are located at four levels and at different distances from the pile, see Figures 4.1 and 4.2. Sensors installed for temperature measuring are summarised in Table 4.1.

4.4.1 Temperature at ground surface

The air temperature at ground surface is logged continuously during the test period. The sensor used is a Pt100 resistance thermal detector (RTD). The sensor is located close to ground level in a 24 h shaded position at the test site.

4.4.2 Thermal sensors in the soft soil

The temperature in the soil is captured at different levels and different radial distances from the piles in 17 measuring points in total, see Figure 4.2. The sensors are typically installed at four levels, but as a consequences of unexpected tip resistance during installation one was left at a smaller depth than originally planned (position GW2).

The temperature sensors used are manufactured together with a sensor for pore pressure, designed and marked as BAT-sensors, presented in the Section below. The pipes for installing the BAT-sensors are in plastic instead of the traditionally used 1 inch galvanized steel pipes. The temperature sensor in BAT Mk III Std used, is a solid-state sensor using the properties of a semiconductor.

4.4.3 Pore pressure sensors

The instrumentation used for pore pressure measurments is the BAT-sensor system (BAT 2015). The physical main components of the BAT-system consists of a filter tip and a sensor body connected via a rubber coated wire to a logger unit. The filter tip is a plastic body containing a filter, a cell filled with de-aired water (air evacuated under vacuum before installation) and a rubber membrane, Figure 4.7. The membrane is punctured with an injection needle mounted in an adaptor on the sensor body so that the cell pressure is registered by a piezo resistive sensor. These are absolute pressure readings that need further correction for barometric pressure. The temperature sensor positioned together with the pore pressure sensor is used for temperature compensation of the measured pore pressure data.

The pore water pressures in the soil at the test site are captured at different levels and different radial distances from the piles in 17 measuring points (Figures 4.1 and 4.2). Further, the pressure head of the groundwater in the bottom permeable soil layer is measured in an open piezometer pipe.

Figure 4.7: *Pore pressure and temperature sensor (BAT). Filter tip, plastic pipe and a specially designed installation rod.*

4.4.4 Instrumentation for capturing depth differentiated settlements

Potential settlements caused by the thermal piles in soft sensitive clay is one of the main unknowns of interest in this project. Therefore different methods to capture settlement, as summarized in Table 4.2, have been used at the test site. Positions of instrumentation for capturing differentiated settlements are shown in Figure 4.1.

Table 4.2: Instrumentation to capture settlements at the test field, see Figure 4.1 for positions.

Sensor	*Position*	*Comment*
Settlement plates	G4, G6	G6 ref. at 20 m dist. from test piles.
Bellow hoses	B1 - B5, B6	B6 ref. at 20 m dist. from test piles.
Levelling points	P_{temp} , P_{ref}	At the loading rig.
Inclinometers on rig	P_{temp} , P_{ref}	Horizontal positioned on the loading rig.

Bellow-hoses have been used for manual measurements. The corrugated bellow-hoses, Figure 4.8, have an outside diameter of 30 mm with metal rings at one meter interval. During installation the hoses are extended to avoid the natural compression of a weight of the hose itself. The hoses have been measured by the same person at every instance. This minimises effects from operator bias. With this configuration, potential settlements in the specific soil layer can be detected with an estimated accuracy of ≤ 5 mm for each 1 m interval.

Figure 4.8: *Part of a bellowhose used for capturing depth differentiated settlements. The hose in the figure is cut lengthwise to illustrate the position of the ring, in the black socket, responding to the sensor device.*

The settlement plates comprise of horizontal plates 250x250x10 mm^3, with a welded vertical steel bar inside a plastic tube. The plates are installed at 0.5 m depth. The top of the steel bar reaches to ground level for levelling. The levelling is made from two different position set-ups to eliminate potential misreadings. The loading rig on top of the floating test piles is levelled at the same time. The rig on top of the end bearing piles is used as reference level. The levelling instrument used is a Wild NA20.

4.5 Calibration of sensors

Before installation all sensors are calibrated under controlled conditions in the laboratory at Chalmers. The thermal sensors are calibrated against the thermometers Dostman 650 and Ebro TTX100, both with an accuracy of 0.1 °C. The sensor calibration procedure used crushed ice water to get 0°C. Thereafter the sensors are also calibrated in water against the laboratory calibration thermometer at 7-8 °C, 18-19 °C and in one case at 43 °C. The accuracy of the Pt100 is 0.15 °C, and of the BAT thermal sensors 0.3 °C (Appendix A.2).

The pile segments including the strain gages, and the load cells, are calibrated at Chalmers concrete experimental hall before installation at test site (Appendix A.4). In the calibration procedure the pile segments are subjected to loading loops with a max 200-300 kN in compression, corresponding to the designed geotechnical ultimate state load capacity in the field. Half of the pile segments are also calibrated in extension, max 100 kN, to mitigate bending effects during the calibration.

The BAT pore water pressure sensors are calibrated in a pressure cell at Chalmers geotechnical laboratory (Appendix A.3). During calibration the cell pressure is increased in controlled 50 kPa increments in a cycle from 0 to 250 kPa and back to 0 kPa. The calibration procedure is performed at two different temperatures, 8°C (climate room) and 18°C (room temperature). The accuracy of the pore pressure sensors is <0.3 kPa.

The optical fibers used for thermal measures are calibrated at site by running a section of the fiber through a package of known temperature, an icebox. The inclinometer sensors used to register the occurance of vertical displacement of the loading rig on top of the test piles are calibrated using a rotatable rig (Appendix A.5).

4.6 Data acquisition

Data acquisition (DAQ) is the process of sampling analog and digital signals from sensors that convert the physical response. The analog signals are first converted to the digital domain before further processing and storage. At the Utby test site the sensors in the pile and on the loading rig are connected to a National Instruments (NI) data aquisition system CDAQ-9172. The CDAQ is supplied with module NI 9237 to directly convert the signals from the load cells and strain gauges. A NI 9219 module samples the Pt100 temperature sensors and a NI 9205 converts the analog signals from the inclinometer sensors.

BAT-sensors are connected to a separate module, Profound ISB.0033. This DAQ is synchronized together with the central system. As the air pressure is varying with

weather conditions and the pore pressure sensors are absolute, the Profound-module has an internal absolute air pressure sensor for compensating the pore pressure readings.
In the computer at the test site a program designed in LabView merges data from all DAQ systems at the test site together in one single comma separated (csv) text file. The text file is hosted on a commercial cloud and as such available also at a distance from the test site. The data is logged in intervals between 15-60 minutes. For background conditions at the test site the intervals are 60 minutes. The low frequency keeps the logging file in practical small size. During the thermal tests the logging frequency is increased to every 15 minutes.

For sampling of data from the optic fiber sensors another logger is used, physically built in the mobile heating rig. The fiber logger is a Sensornet 4 channel Halo DTS (Distributed Temperature Sensing Equipment).

4.7 Mechanical loading

The mechanical load is applied as a static dead weight load. A load cell is used to arrive at the intended load and to capture data on the working load, Figure 4.5. The calculated expected design load R_d, Eq.4.2, is 90 kN for a 28 m long circular 115 mm (θ) floating pile with given conditions of the test site (see Section 3.3). The calculation is made using a traditional total stress approach (α-method). The method uses the evaluated undrained shear strength, without the traditional rate correction factor connected to w_L, as documented in Eriksson et al. (2004). The undrained shear strength used in the calculations is τ_{fu}=14 kPa 0-6 m depth, from there increasing linearly with 1.4 kPa, to 45 kPa at 28 m depth. Design coefficients used in the calculations to predict the long term load capacity are presented in Table 4.3. The ultimate state pile bearing capacity is calculated to be 270 kN, with no applied partial safety coefficients (γ,κ=1.0).

$$R_k = \int \alpha\theta \frac{\tau_{fu}\kappa_t}{\gamma_M} dz \tag{4.1}$$

$$R_d = \frac{1}{\gamma_{Rd}} \frac{R_k}{\gamma_R} \tag{4.2}$$

Table 4.3: Coefficients used in the test pile design calculation to predict static test load.

	Coefficient	*Comment*	*Reference*
γ_M	1.5	Soil material	(Boverket 2015, Tab. I6)
γ_R	1.2	Pile bearing capacity	(Boverket 2015, Tab. I7)
γ_{Rd}	1.1	Model factor, cohesion piles	(Boverket 2015, Tab. I4)
κ_t	0.7	Time permanence factor	(Eriksson et al. 2004)

4.8 Thermal loading

Inside the piles a U-tube heat exchanger is installed for exchanging heat and cooling with the ground, Figures 4.4 and 4.5. The remaining volume inside the pile is filled with water contained in a thin plastic capsule lining. The thermal loading is applied to the soil by circulating a fluid in the pile. The fluid is heated or cooled at a constant heat flux. The mobile rig, Figure 4.9, is constructed in 3 circuits, Figure 4.10, to enable a controlled transmission of energy produced in the rig and delivered to the thermal pile U-tube. The circuits connect a heatpump, a fluid buffer tank and a heat exchanger for transmission of energy to the pile heat exchanger. Heating can be supplied from electrical heaters or from the heat pump. For cooling, chilled fluid is delivered from the reversible heat pump.

For the thermal loading, an electrical heater is used to deliver a constant heat flux of 1.3 kW. This is equivalent to 50 W/m, as recommended in ASHRAE (2007). Experiences from tests in practice indicates that effects should be 20-50 W/m for collectors in soil (Bourne-Webb 2013). For cooling, the TRT rig deliveres fluid to the pile entering collector hose in the temperature of range of 4-5°C.

In comparison to an ordinary Thermal Response Test, TRT, the mobile rig has the capacity of delivering both heating and cooling. In addition, it is equipped for monitoring not only the ingoing and outgoing fluid temperatures, but also the temperature at different depths in the ground, using distributed temperature sensing.

Figure 4.9: *The mobile heating rig positioned close to the mechanical loading rig in Utby.*

.

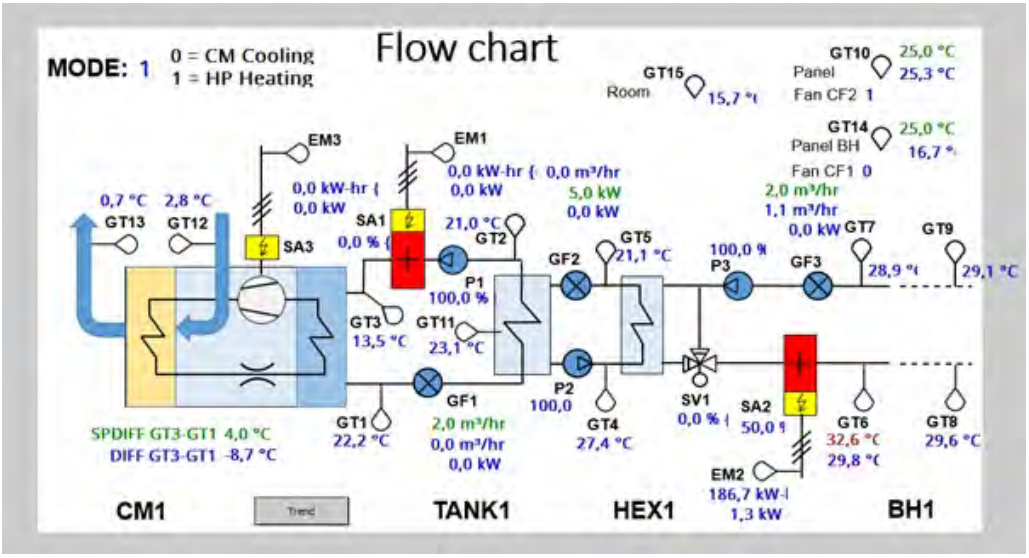

Figure 4.10: *The TRT rig flow chart. The rig consists of 3 circuits connecting a heat pump (CM1 in the figure), a buffer (TANK1) and a heat exchanger (HEX1). In- and outgoing pile collector fluid (BH1) temperatures can be seen to the right. (Plot from 161228, after about 6 days of heating). The electrical heater (EM2) is used for heating the test pile fluid, and the reversible heat pump delivers the cooling.*

4.8.1 Test plan

Heating and cooling in the tests is limited to temperatures above 4-5 °C and up to 25-30 °C in the pile heat exchanger. The natural temperature in the ground is measured starting 6 month before the thermal tests. Measurements presented starts at t_0=01/12/2016. The first heating cycle starts 22/12 2016.

The test plan for cyclic heating and cooling was designed to exchange heating or cooling respectively for at least 4-5 days per cycle. This is for the heat to spread a distance in the clay of at least five times the pile diameter, >5D. This distance is to involve also the intact clay outside the zone of heavily distorted clay effected from the pile installation. The number of cycles were designed to be more than five. This is to induce potential thermal displacements that typically appear after the first few cycles.

Table 4.4: Applied heating and cooling cycles on the steel thermal test pile in Utby.

Start	*End*	*Duration*	*Heatflux/ cooling fluid temperature*
22/12 2016	12/01/2017	21 days	1.3 kW
12/01/2017	25/01	13 days	4-5°C
25/01	30/01	5 days	1.3 kW
30/01	03/02	4 days	4-5°C
03/02	08/02	5 days	1.3 kW
08/02	13/02	5 days	4-5°C
13/02	17/02	4 days	1.3 kW
17/02	23/02	6 days	4-5°C
23/02	28/02	5 days	1.3 kW
28/02	06/03	6 days	4-5°C
06/03	10/03	4 days	1.3 kW
10/03	15/03	5 days	4-5°C
15/03	21/03	6 days	1.3 kW

4.9 Preparatory thermal test pile

The pilot thermal pile at Chalmers Johanneberg Campus was installed in December 2015. This initial installation was primarily aimed to investigate various aspects of thermal response testing. This pile is a 18-m-deep floating steel SSAB/Ruukki pile with 115 mm diameter and 6.3 mm wall thickness. It has the same diameter as the piles later installed at Utby test site. However, the pilot pile has a shorter length due to the limited depth to bedrock. The pilot thermal pile in this phase is used as a trial run of the TRT rig before performing the tests at the Utby test site.

Table 4.5: Applied heating and cooling cycle on the thermal test pile at Chalmers.

Start	*End*	*Duration*	*Heat flux/ cooling fluid temperature*
21/11 2016	22/11/2016	1 day	1.3 kW
22/11/2016	22/01/2016	0.5 day	7-8°C
22/11 2016	25/11/2016	3 days	1.3 kW
25/11/2016	27/01/2016	2 days	4-5°C

5 In-situ tests on a thermal pile in soft clay

5.1 Introduction

This Chapter presents measurements from the Utby test site on temperature in pile and soil, excess pore water pressures, pile head loads and displacements in soils and in pile head. Results on the measured relation between thermal and static loading mechanisms are analysed and presented.

5.2 Loading of piles at Utby test site

5.2.1 Mechanical loading

Mechanical load on the steel test piles is applied as a static load. The load is measured using a load cell at each pile head. The load measured is presented in Figure 5.1. The load is applied in one increment and kept constant over the full test period. Although the static load is a dead weight gravity load, a fluctuation of about 0.5 kN is observed in the measurements. The fluctuation (noise) is not coinciding with the thermal heating and cooling cycles in the pile, as they are also observed before and after the thermal loading.

After ending the thermal tests, a final maintained load test (ML) is performed, with stepwise loading in equal sized loading increments, see Figure 5.3. The loading starts from the SLS level applied during the thermal tests, i.e. 85-87 kN/pile.

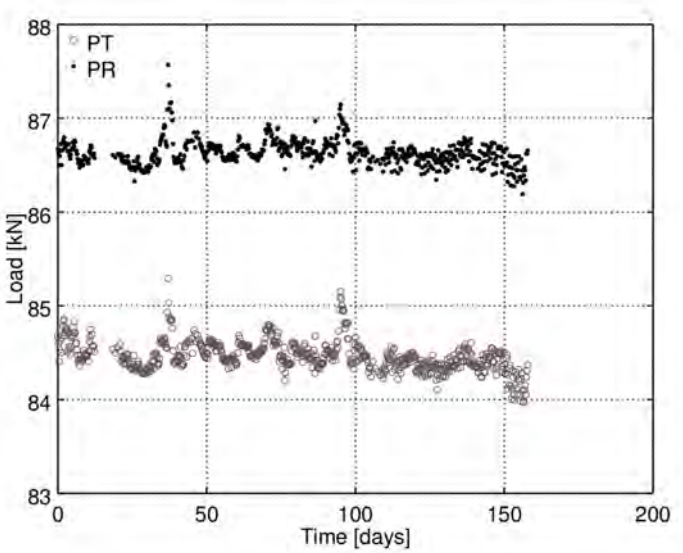

Figure 5.1: *Pile load at steel test piles at the Utby test site. PT is the thermal test pile and PR the reference pile. Plot time started 1/12 2016.*

When interpreting a loading test there are a number of reasonable definitions of the failure load of a pile, e.g. the load for which rapid settlement occurs under sustained or slightly increasing applied load (e.g. Sandegren et al. 1980 or Tomlinson 1994). Eurocode (ISO 2016) and Swedish Commission of Pile Research (Alheid et al. 2014) recommends that the interpreted failure load correspond to settlements equal to $0.1D_{pile}$, where D_{pile} is the pile diameter. Such definition, however, does not consider the elastic shortening of the pile, which can be substantial for long and slender piles. Moreover, large pile dimensions will give unreasonably large displacements for the super structure (Wrana 2015). The performance of the static loading test of the slender piles at the Utby test site follows the recommendations of Olsson and Holm (1993), giving that the total displacement of the pile head during loading should be at least 60 mm before unloading. The loading steps are recommended to be 5% of the evaluated ultimate limit state capacity (ULS), i.e. 15 kN/step, applied in timesteps of 15 min.

Figure 5.2: *The loading rig beam on top of the thermal test pile after static loading test to failure. After failure, the pile head is displaced about 0.5 m downwards, ending at ground surface. Compare Figure 4.5 (before failure).*

The ultimate state bearing capacity, with no applied partial safety coefficients, is calculated to be 270 kN. The test piles reached failure load at 172-178 kN, corresponding to an α_{ML}-factor of 65% of the undrained shear strength s_u in the clay. The failure is rapid and brittle, 4 mm of vertical pile head displacement is measured when levelling shortly before the failure appeared. Both test piles behaved similar, the thermal test pile, however, failed about 2 minutes before the reference pile.

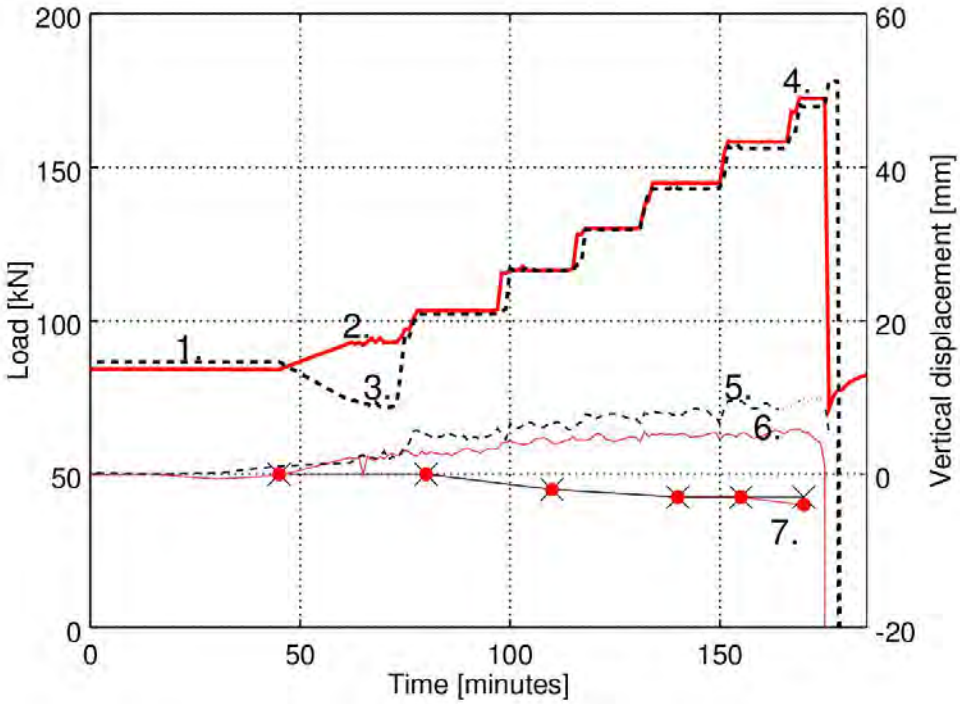

Figure 5.3: *Maintained static loading test (ML) to ULS performed 170626. The initial SLS loading of 84-87 kN (1.) was applied before the thermal tests, in spring of 2016. Before starting the loading test the concrete elements on the loading rig was re-arranged, seen as a difference between the thermal pile loading (2.) and the reference pile loading (3.). The loading is applied in steps of 15 kN in timesteps of 15 min until failure occurs at 165 kN (4.). Manual levelling of the pile displacement shows settlement of 3-4 mm (7.) before failure. The inclination of the loading rig is registered and transfered to vertical displacement for the thermal pile (6.) and the reference pile (5.). The loading rig main steel been is bent down from the loading, seen as a positive displacement ending with a rapid downward motion.*

5.2.2 Thermal loading of the pile

The thermal loading of the test pile comprises a constant heat flux during heating and constant temperature in the outgoing fluid during cooling. The temperature measured on the pile wall at 14 m depth during the complete test period is shown in Figure 5.4. The latter indicates successful application of the test protocol, Table 4.2.

In conditions where the pile is restrained from vertical expansion, a change in temperature will generate axial stresses in the pile. For example, in the steel pile of ∅115 mm used at the test field, the thermally generated stresses from an increase in temperature of dT=20°C will be 50 MPa, or 105 kN if evenly distributed over the pile cross section. This corresponds to 40% of the calculated ULS load capacity.

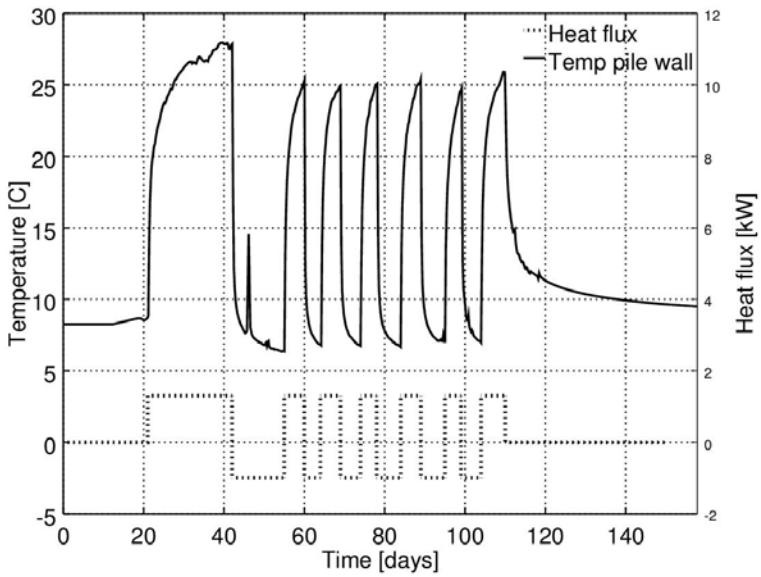

Figure 5.4: *Thermal loading cycles measured at 14 m depth on the pile wall. Zero time represents 1st December 2016. The heat flux is presented schematically. In reality, the flux during the cooling cycles is not entirely constant.*

5.3 Soil response during thermal response test

5.3.1 Temperature and excess pore pressure development

Water expands more than clay minerals due to temperature increase. As a result, the excess pore water pressures generated in case the heating rate is larger than the pore pressure dissipation rate. The initial pore water pressures with depth at Utby, before the thermal test, are plotted in Figure 5.5. The hydraulic gradient profile corresponds to hydrostatic pressure with pressure head at a depth of about 1 m. In the permeable soil layer at the bottom, the value of the measured pressure head in the piezometer pipe has been artesian in periods during the test, up to 5 kPa above ground surface.

The temperature in the soil before starting the thermal tests is relatively constant through the soil profile, varying from 8.2 °C to 8.8 °C.

The temperature at the ground surface level gives one of the heat storage system boundary conditions, potentially affecting the soil in near surface soil layers. The recorded data on local air temperature at the Utby test site is plotted in Figure 5.6. The winter period January-March 2017 was exceptionally warm and without snow compared to average local conditions. The average daytime air temperature was with a few exceptions below 0°C. The air temperature at ground surface level may effect the temperature in the top soil layers. From Figure 5.6 and 5.9 can be seen that the fluctuation in air temperature over a day is not sensed at 7 m depth.

During the first heating cycle, in this section called the Thermal Response Test, the heat propagation in the clay is captured in terms of change in temperature over time. Simultaneously, the excess pore water pressures are measured at the same time intervals and positions in the soil. The logging interval is every 15 minutes. Figures 5.7 and 5.8 show the propagation of increasing and decreasing temperatures and excess pore pressures during the Thermal Response Test.

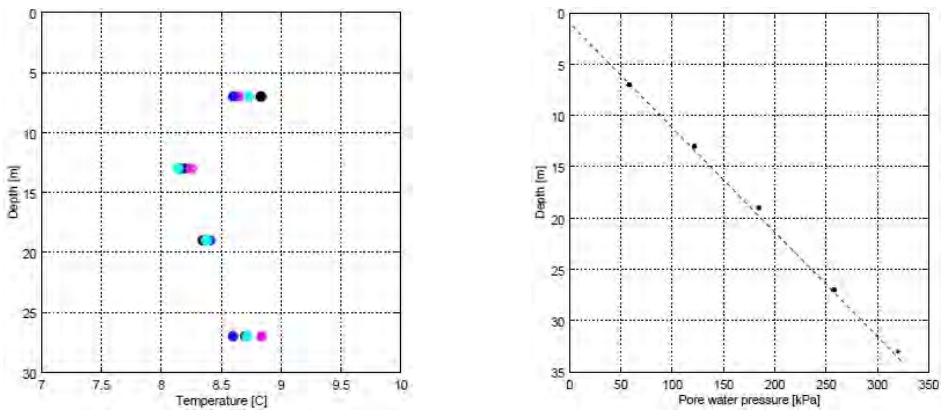

Figure 5.5: *Initial temperature and pore water pressure in the soil profile, date 1/12 2016. The dotted line in the left figure represents a hydrostatic pressure with pressure head at 1 m depth. The temperatures in the first figure has been measured at different distances from the test pile.*

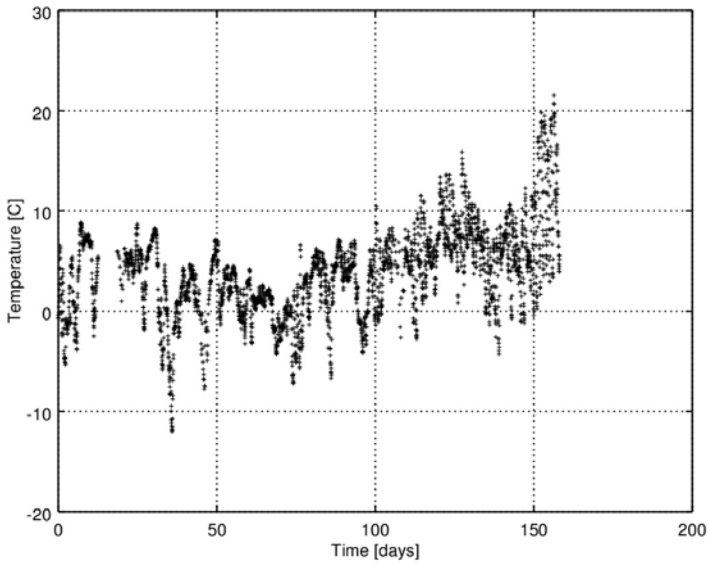

Figure 5.6: *Temperature data at ground surface level at the test site in Utby. The sensor is located in a 24 h shaded position. Plot time started 1st December 2016.*

Initially the temperature gradient between pile and soil temperature is significant and therefore the thermal propagation rate is large close to the pile. The heat flow brings the front of heating further away from the pile meanwhile the thermal gradient per distance unit gradually reduces. After a long time with constant thermal conditions there will eventually be a steady state between in- and outgoing heat flow to the soil section, forming a log-shaped curve. This stationary state is a situation far from most practical applications, where the heat flux most likely will vary over time. For Utby thermal tests, as seen in Figure 5.9, the soil temperature is still increasing even after 21 days of heating with a constant heat flux of 50 W/m.

Increased heating clearly generates an increase of the pore pressures, which is shown in Figures 5.7 and 5.8. However, as the clay is low permeable, the convective flow of pore water is a very slow process. In the test period of 21 days the mean convective flow is calculated to transport less than a few centimeters given the hydraulic conductivity is less than 10^{-8} m/s. Consequently, thermal heat flow in the clay for the temperature interval used in the tests is mainly transfered by conduction rather than by convection. The excess pore pressure propagation, however, will distribute fast in the saturated clay, as shown in Figure 5.9 where the temperature and pore pressure response are plotted against time for sensors at 0.5 m and 1.5 m distance from the thermal pile. The pore pressure readings detect a change before a temperature change is measured.

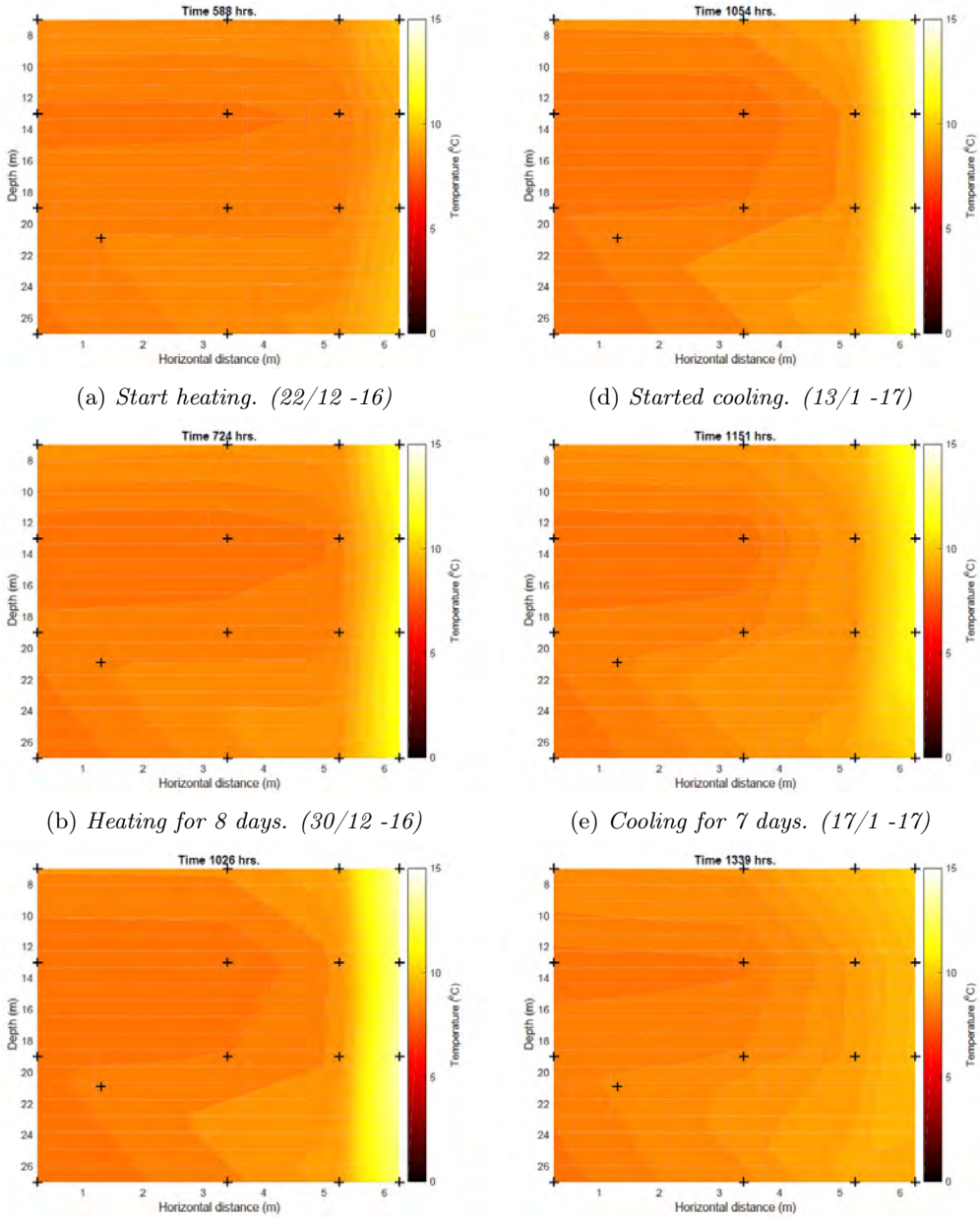

(a) *Start heating. (22/12 -16)*

(d) *Started cooling. (13/1 -17)*

(b) *Heating for 8 days. (30/12 -16)*

(e) *Cooling for 7 days. (17/1 -17)*

(c) *Heating for 21 days. (12/1 -17)*

(f) *End of cooling. 25/1 -17*

Figure 5.7: *Thermal propagation during initial the Thermal Response Test. The sensor positions are indicated in black crosses.*

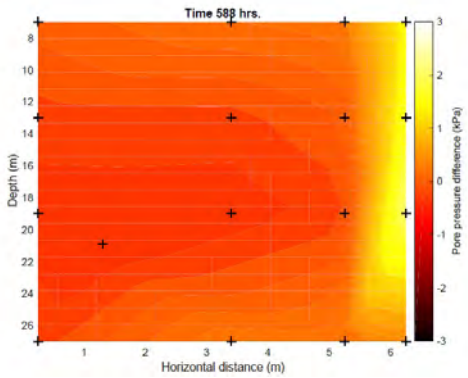

(a) *At start of heating. (22/12 -16)*

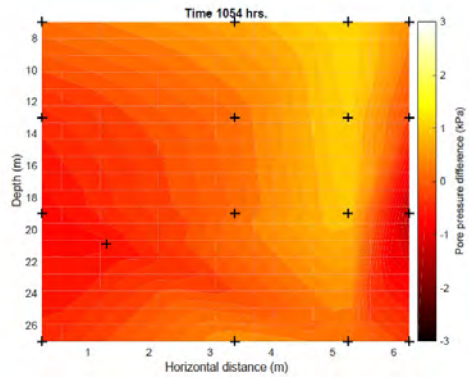

(d) *Started cooling. (13/1 -17)*

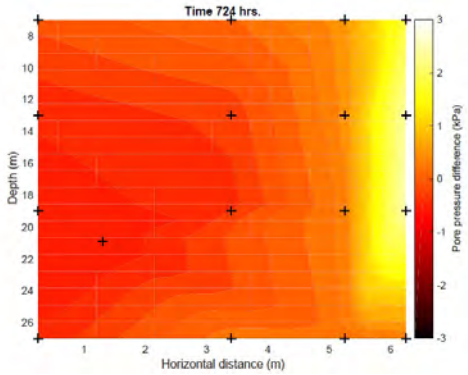

(b) *Heating for 8 days. (30/12 -16)*

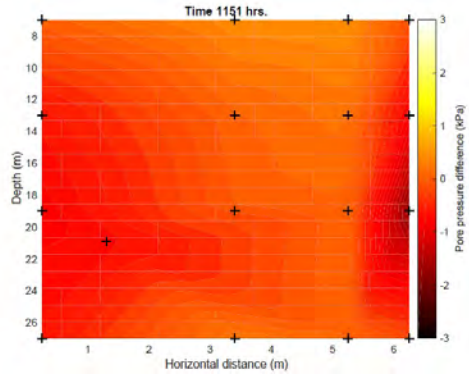

(e) *Cooling for 7 days. (17/1 -17)*

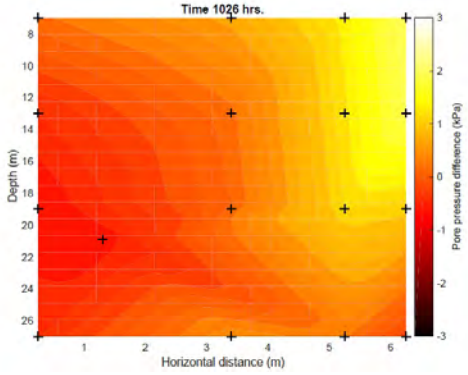

(c) *Heating for 21 days. (12/1 -17)*

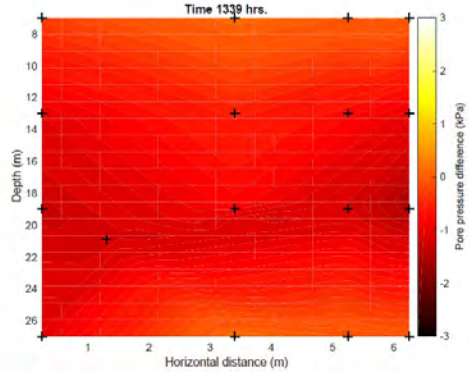

(f) *At the end of cooling. 25/1 -17*

Figure 5.8: *Change in pore pressure [kPa] during the Thermal Response Test. The sensor positions are indicated in black crosses.*

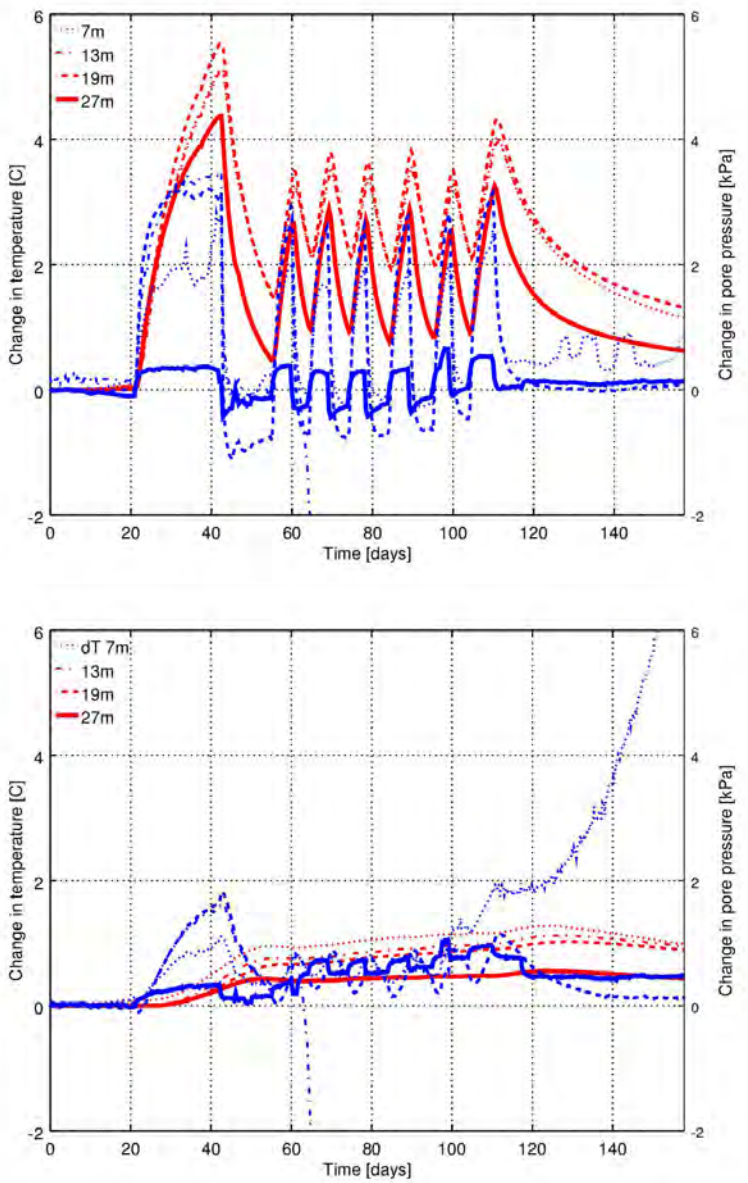

Figure 5.9: *Measured change in temperature (red) and excess pore pressure (blue) in the clay, at 0.5 m and 1.5 m distance from the thermal test pile. The pore pressure sensor at 7 m depth seems to malfunction after about 100 days.*

5.3.2 Strains in the test piles

Displacements of the pile heads have been monitored continuously during the test period via two inclinometers at the loading rig. The measured data is presented as a vertical displacement in Figure 5.10. In addition manual levelling of the pile head and rig is logged. At the inside of the pile shafts, strain gauges were installed at 4 different levels. Unfortunately most of the these sensors started to malfunction before the start of the thermal tests.

5.3.3 Strains in soil

If the excess pore water pressure is unable to drain then the clay may expand or heave. Also the effective stresses in the soil will decrease, resulting in consolidation and/or creep deformations in the clay. Hence, there is the need for strain measurement in the soil.

The soil section between the two test piles is instrumented with five bellow-hoses, at 0.5, 1.5, 3.5, 5.5 and 6.5 m distance from the thermal pile. Measuring of the bellow-hoses have been performed manually, as described in Section 4.4. The measured vertical strain data is presented from individual bellow-hoses in Figure 5.11. The strain is calculated as the measured displacement in relation to the corresponding length of the bellow-hose segments from the measurement in November 2016 i.e. prior to the thermal tests. There are fluctuations in the measured data, most often below the accuracy of the manual measurements. There is a trend that the main captured bellow-hose displacement seems to appear at the upper part, within a few meters depth, though this is not observed in all individual bellow-hose measurements. As there are no obvious measured displacements observed from levelling at ground surface settlement plates, Figure 5.10, the bellow-hose deformations may be the effect of tension creep in the hoses themselves. During installation the hoses are extended to compensate for the hose weight and from experiences the bellow-hose top levels sometimes show unrealistic measured settlements.

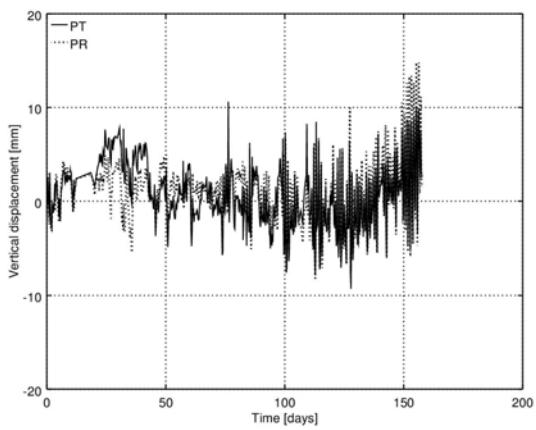

Figure 5.10: *Vertical displacement calculated from the automated measured change in inclination on the loading rig beam structure.* T_0*=1/12/2016.*

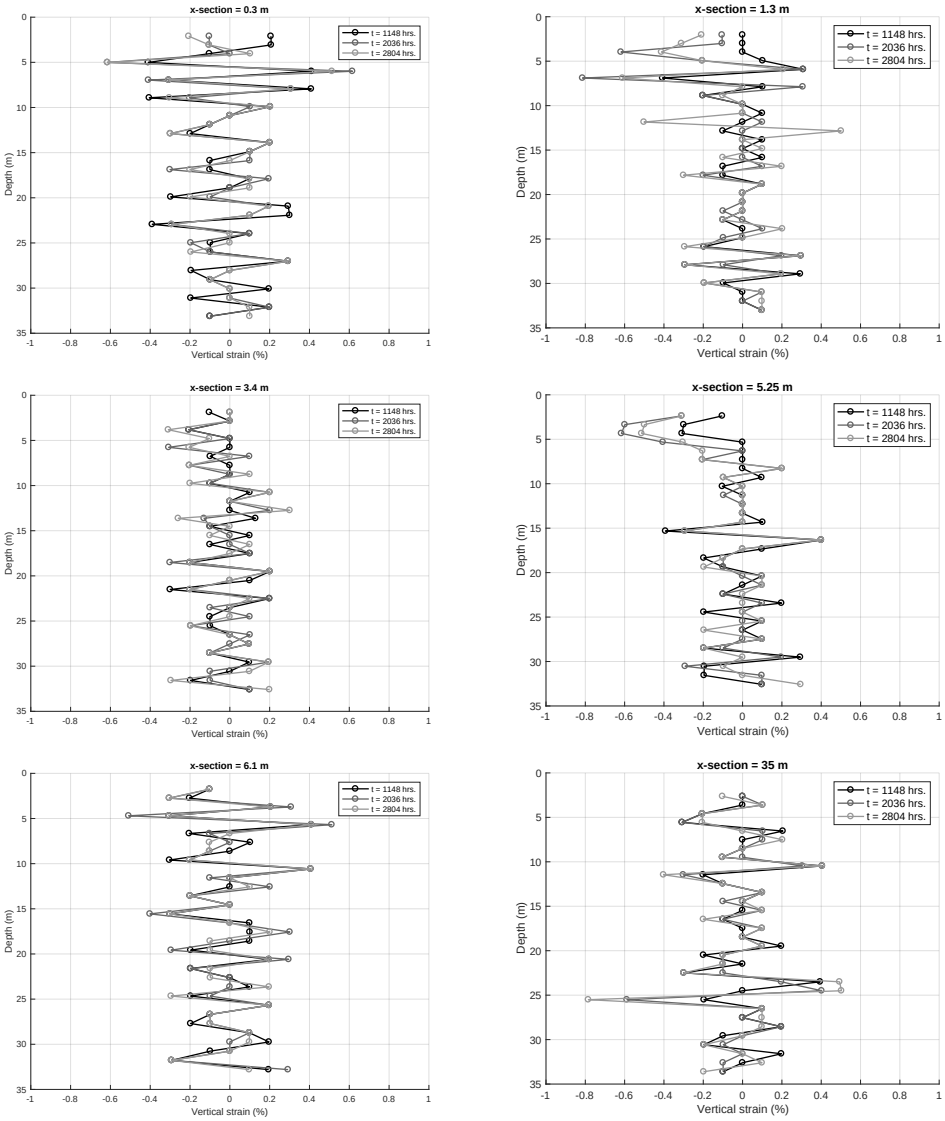

Figure 5.11: *The bellow-hoses are manually measured at every 1 m length. The settlement plates levelling indicates that soil settlements at ground surface, the total strains, during the test period are very small. Therefore, with an assumed sum of limited total strain, increasing strains captured at one level in the bellow-hoses is followed by decreasing strains in adjacent measuring level.*

5.4 Soil response from thermal cyclic loading

5.4.1 Temperature and excess pore pressure development during cyclic heating

The cyclic test includes 6 heating cycles of between 4-5 days each, see Figure 5.4. These tests are performed in addition to the initial Thermal Response Test. The cycles are not identical in duration, with a few hours difference in period. The thermal flux during heating is constant though. During cooling a target constant temperature of outgoing fluid of 4°C is aimed for.

The temperature distribution in the clay around the thermal pile is presented for selected times during the cyclic loading in Figure 5.12 to 5.14. The times presented are selected after completed periods of heating periods and cooling respectively. The corresponding temperatures evaluated from the distributed fiber optic sensors inside the fluid pipe and at the inside of the steel pile are presented in Figure 5.15. There is a satisfactory agreement between the measurements from the optic fibers and from the other thermal sensors in the test pile.

Similar to the Thermal Response Test, the cyclic thermal loading also generates a cyclic response in the excess pore pressures, as shown in Figure 5.9. As the frequency of cycling was high, neither the thermal flow nor the convective pore water flow reaches beyond the closest sensor sections at 0.5 m and 1.5 m distance. All cycles can be considered transient cycles. The cyclic response in excess pore pressure is observed at both 0.5 and 1.5 m distance from the test pile. On the other hand, the response in the cyclic temperature changes is clear at 0.5 m distance, but only perceptible at 1.5 m distance. The detected temperature at 1.5 m distance before and after the performed Thermal Response Test period indicates a small increase in temperature, Figure 5.9. This is assessed to be the consequence of the asymmetry in time between heating and cooling during the Response Test, with a net heating delivered to the soil.

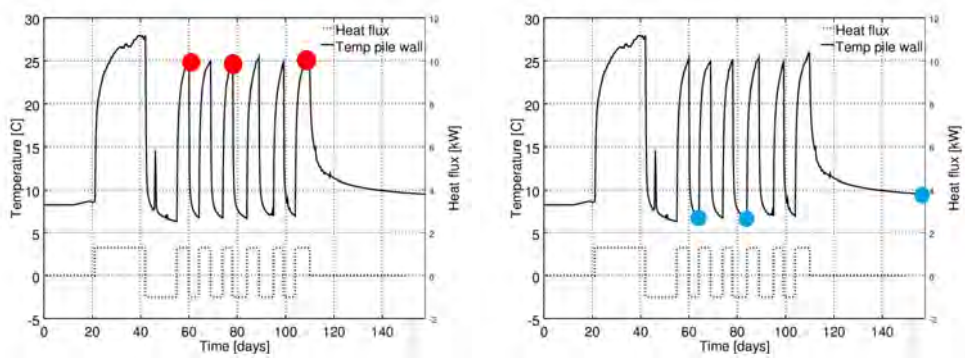

Figure 5.12: *Cyclic thermal loading, markers to recognize times plotted in Figure 5.13 (temperature peaks after periods of heating) and Figure 5.14 (after periods of cooling).*

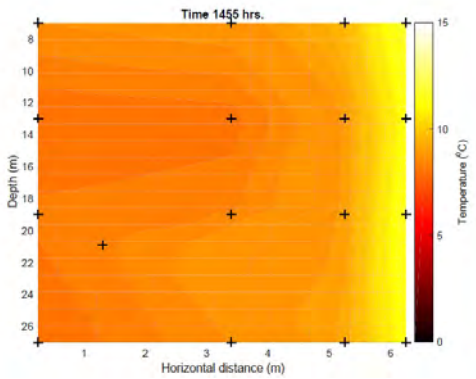

(a) *Temperature after heating in cycle No 2, the first short heating cycle (30/1 -17).*

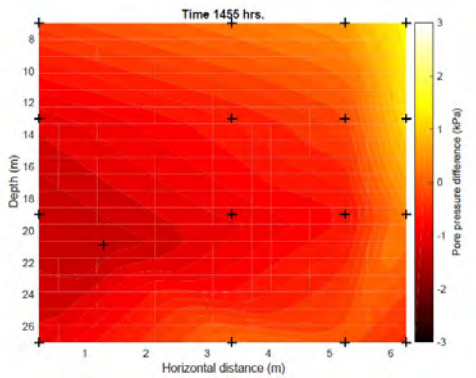

(d) *Excess pore pressure after heating in cycle No 2 (30/1 -17).*

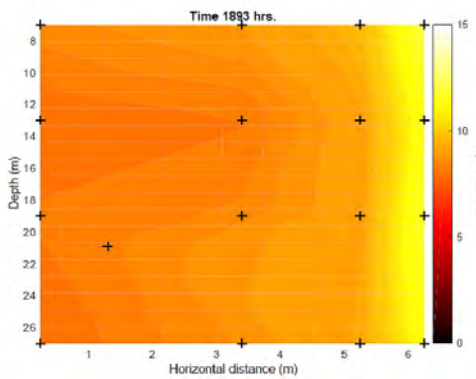

(b) *Temp. after heating in cycle No 4 (17/2 -17).*

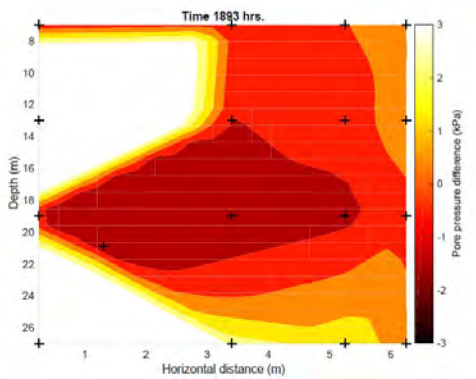

(e) *Excess pore pressure (17/2 -17).*

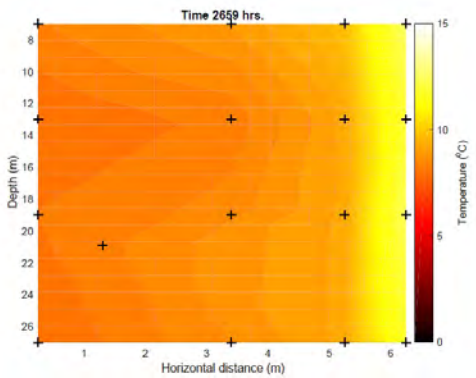

(c) *Temp. after heating in cycle No 7 (21/3 -17).*

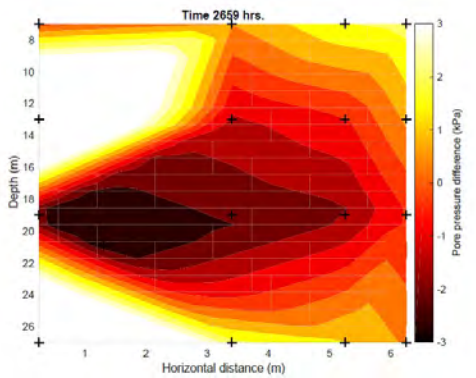

(f) *Excess pore pressure (21/3 -17).*

Figure 5.13: *Temperature and pore pressure change after periods of heating during the cyclic tests. Time presented follows from Figure 5.12. Sensor positions are indicated in black crosses. The dominating thermal flow response is measured from the sensors at 0.5 m and 1.5 m distance from the test pile. The response in the pore water sensors indicates the by time a few of the sensors might malfunction, generating white fields in the figures to the right.*

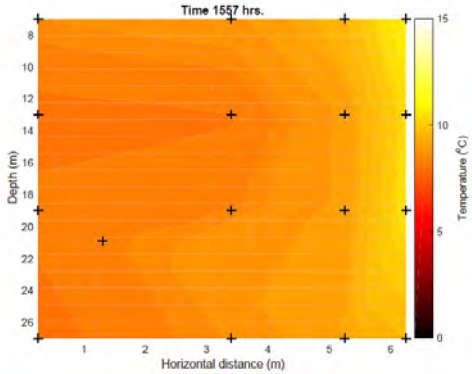

(a) *Temp. after cooling in cycle No 2 (3/2 -17).*

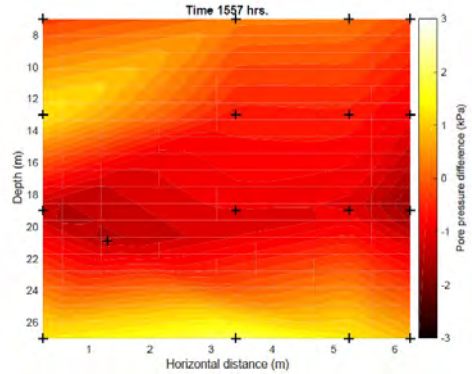

(d) *Excess pore pressure (3/2 -17).*

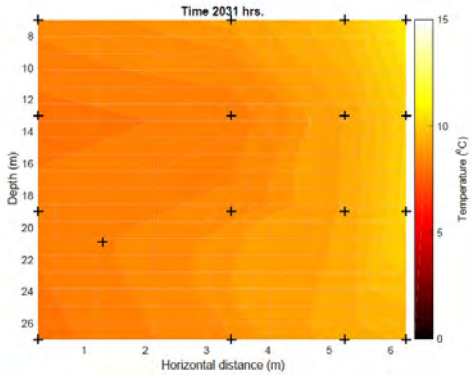

(b) *Temp. after cooling in cycle (23/2 -17).*

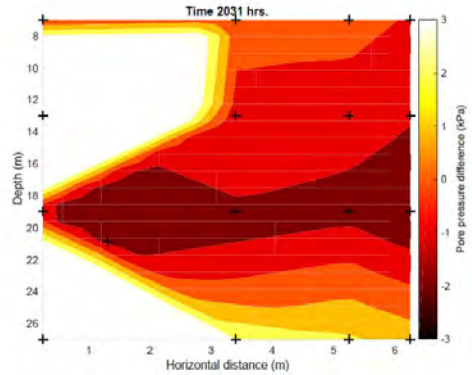

(e) *Excess pore pressure (23/2 -17).*

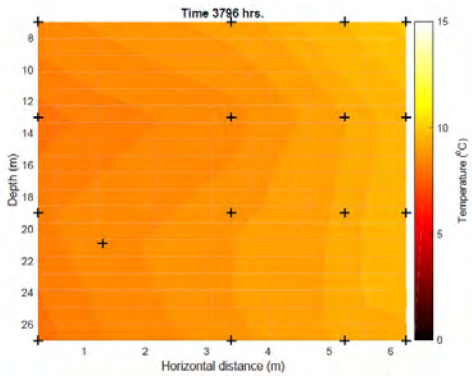

(c) *Temp. after cooling in cycle (6/5 -17).*

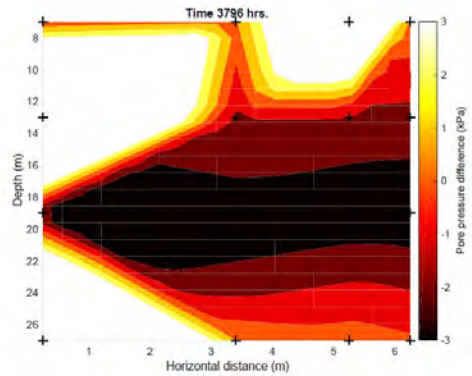

(f) *Excess pore pressure (6/5 -17).*

Figure 5.14: *Temperature and pore pressure change after periods of cooling during the cyclic tests. Times presented follows from Figure 5.12. Sensor positions are indicated with black crosses. The response in the pore water sensors indicates that over time a few of the sensors might malfunction, generating white fields in the figures to the right. In addition to 5.13 the sensor at 1.5 m distance and depth 7 m also starts to malfunction.*

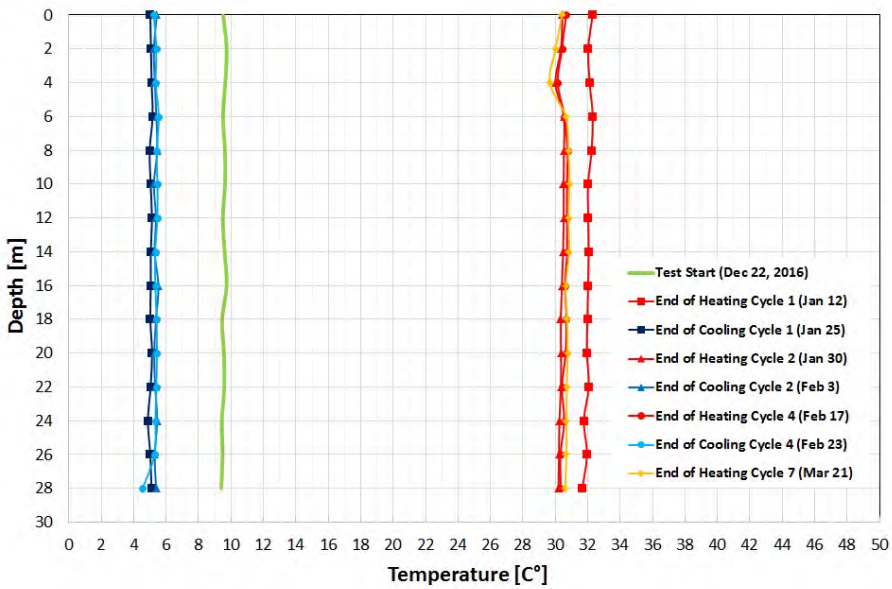

(a) *Temperatures from the distributed fiber optic sensors inside the down-going fluid pipe in the pile. (Sensor position 3. in the pile section in Figure 4.4).*

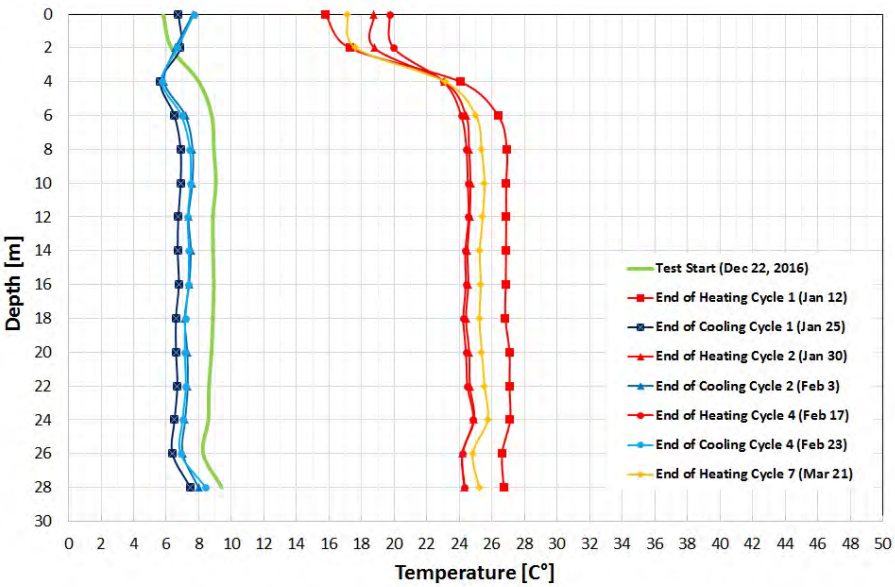

(b) *Temperatures from the fiber optic sensors at the inner boundary of the steel pile shaft. (Sensor position 2. in the pile section in Figure 4.4).*

Figure 5.15: *Temperatures evaluated from the distributed fiber optic sensors in the steel thermal test pile after periods of heating and cooling during the cyclic tests. Times presented follows from Figure 5.12.*

5.4.2 Strains in the test piles

At the Utby tests both the live load and the number of cycles are relatively small. As a result, the manual levelling of the pile heads did not show any vertical displacements larger than the measurement accuracy.
The continuous inclinometer measurements, Figure 5.10, show a frequent distortion in captured data. When compared to air temperature at ground surface level, Figure 5.6, it is found that this distortion occurs uniform with the variation of captured temperature. The steel structure on which the inclinometer sensors are mounted seems thermally sensitive, as the manual levelling of the pile heads gives no displacements. The sensors, however, make it possible to trustworthy detect when there is a rapid position change, as was the case during the Maintained Loading Test.

5.4.3 Strains in the soil

The instrumentation to capture data on vertical displacements in the soil during cyclic thermal loading are bellow-hoses and settlement plates, the same arrangement as for the thermal response test discussed in more detail in Section 5.3.3.

The bellow-hoses are measured on a monthly period during the tests. The measured displacement per meter depth in the bellow-hoses is transfered into strain. The changes in strain, in relation to the conditions before the Thermal Response Test 1/12 -2016, are presented in Figure 5.11. There is a fluctuation in the measured strain, mainly within 0.2 to 0.3%, at most within 0.6%. As the measured strain frequently oscillate with depth, it indicates that the fluctuations are related to measurement accuracy. There is no clear trend in increasing or decreasing strain with time in the captured data from the bellow-hoses. The monthly performed measurements from the settlement plates indicate no settlement at ground surface level during this test period, neither close to the piles and the bellow-hoses nor outside the impact area of the pile tests.

5.5 Thermal properties from Thermal Response Test

For evaluation of the mean thermal properties in the soil profile Thermal response tests (TRT) are performed (Section 2.3.4). Compared to the standard TRT practice (less than a week), the initial TRT performed at Utby is extended (21 days). The thermal conductivity of the clay in Utby is evaluated as 1.3 W/mK by using the line source approximation and analysing the thermal response in quasi steady state. Corresponding evaluation of the thermal conductivity of the clay from the tests performed on the concrete pile gives a higher value, 1.5 W/mK. From the laboratory tests on samples, presented in Figure 3.4, the thermal conductivity in the clay is evaluated to be approximately 1.2 W/mK. The TRT results tend to overestimate the thermal conductivity in relation to the laboratory measurements. The difference between TRT results and laboratory measurements on thermal conductivity is 10% for the steel pile and roughly 25% for the concrete pile. This is well or even exceeding what is reported in the literature.

The thermal resistance of the piles are also evaluated from the TRTs. The concrete pile is naturally found to have higher thermal resistance than the steel pile. The TRT

evaluations give the thermal resistance, R_p, of 0.27 mK/W for the concrete pile, and 0.15 mK/W for the steel pile .

The concrete piles larger thermal resistance seems to make the TRT evaluation more sensitive to test duration. This affects the results despite having a long test duration of 15 days for the concrete pile. In the evaluation of the TRTs performed in Utby also more advanced methods have been used for evaluation of the thermal conductivity and resistance, including parameter estimation and numerical modelling. The results indicate that for the steel piles there is just a marginal difference in the evaluated thermal conductivity between the different methods (<5%), but for the concrete pile the difference is in the range of 20-25%. The more advanced methods gives less diverged results from the measurements in the laboratory.

5.6 Implications for using thermal piles in soft clay

When installing a precast pile, there is a large distortion in stress and strain for the soil. In the soil, there is an extensive disturbance in the zone close to the pile. The radius of the disturbed zone is often linked to the pile diameter installed and within $5D_{pile}$ (Dijkstra 2015). In the performed thermal tests, the response in change of temperature and pore water pressure is observed in a radius of 1-2 m distance from the pile, i.e. $<20D_{pile}$, involving clay that is heavily disturbed and remoulded, as well as intact natural clay. A prediction of the soil response on mechanical and thermal pile loading is made on clay sampled before pile installation, only disturbed by the piston sample procedure itself. An implication is the uncertainties on the actual properties of the clay involved in carrying the pile load. Furthermore the pore pressure is changed because of the pile installation, changing the effective stresses over time during the reconsolidation following the pile installation. There is a great complexity as the properties of the clay surrounding a pile are not continuous neither over distance nor over time. On top of that, the installation of instrumentation to extensively capture these differences, itself disturbs the soil and affects the results.

During reconsolidation and re-bonding of the clay structure following the pile installation and thermal loading, the disturbed clay close to the pile will recover some strength and stiffness. Though, it is unlikely that the stiffness will reach the level of the original intact natural material. This is depending on time past since installation, but also on e.g. the original sensitivity and level of overconsolidation of the clay involved. There is no general conclusion, as all sites have their unique history and properties that need to be incorborated.

The tests performed and presented from Utby are for single piles only. In practical building installations, the thermal piles will be installed in a matrix and the thermal response from one thermal pile will potentially interact with the neighbouring piles. The distance between the thermal piles will follow on a number of presumably more dominating design considerations involving e.g. construction and installation needs. Potentially the thermal effects from a group of piles will exceed the response from a single pile because of accelerated generation of excess pore water pressures.

The use of thermal piles in building practice is assumed to be most frequent for seasonal storage i.e. relatively long periods of heating or cooling. The cyclic thermal test performed on the Utby piles is made in shorter cycles, 5-20 days. The temperature response in the clay decays exponentially with the distance from the pile. Furthermore, the disturbance in the clay is also a function of the imposed heat flux (W/m). The response of longer periods of constant heating will affect soil at larger distances from the pile. Consequently, the change in soil thermal response takes longer time for larger soil volumes.

Thermal Response Tests are used in evaluation of the thermal characteristics of the thermal piles and the soil. However, there is still a need for development of evaluation methods and practice to more accurately determine the thermal conductivity of the soil and the thermal resistance of the pile, specially for piles with large thermal resistance. Fortunately this is an already identified and active area of research.

The thermal tests are performed on piles made of steel and of concrete. The thermal conductivity of steel clearly exceeds the conductivity of concrete. Furthermore a massive concrete pile has a larger mass and in this test case also a larger dimension. Generally the inertia of heat change is larger for a concrete pile than for a corresponding steel pile. Though, from the soil perspective this difference may be nothing more than a retardation of thermal response to the soil. Still both steel (>30 W/mK) and concrete (1.7 W/mK) have superior thermal conduction than the clay at the test site (1.17 W/mK). However, from a pile perspective the material and dimension gives different conditions for generating internal stresses inside the piles following from thermal change, potentially increasing the risk of appearing cracks and decreasing the design load capacity.

6 Conclusions & recommendations

The thermal and geotechnical studies on the response of thermal piles is an active research field. This thesis focused on experimentally studying the geotechnical response of a single floating thermal displacement pile in soft sensitive clay by means of a well instrumented field test. The main findings and recommendations for future research are summarised as follows:

6.1 Conclusions and discussion

Test design

This is the first field test that reports the results for floating thermal piles in soft sensitive clay. A comparative study between a thermal and an ordinary pile is performed to isolate mechanisms in the sensitive clay that can be attributed to the thermal loading of the pile.

In order to minimize the time required to change the temperature in the pile and maximize the excitation in the clay, small diameter (D_{pile} = 115 mm) tubular steel piles are used. Furthermore, the pile length is substantial (28 m), thereby minimizing boundary effects from the surface, and a working load of 84 ± 0.5 kN has been applied during the thermal loading program that lasted 3 months with an additional monitoring period of one month.

The Thermal Response Test (TRT) rig has been successfully designed to inject/extract power corresponding to 50 W per meter pile length for extensive periods of times (weeks). The thermal testing has been extended to five additional 4-5 day cyclic heating and cooling cycles. The duration of the cycles is chosen such that a pore pressure and temperature change in the soil is recorded at a distance of 5 pile diameters ($5D$). This distance is considered to cover sufficient soil volume to incorporate disturbed (from pile installation) and intact clay.

Optical fibre based distributed temperature measurements are performed in the pile and on the pile interface in addition to local temperature measurements and strain gauges. Although great care was taken in assembly, sealing and calibration of the strain gauges in the pile, they proved to be unreliable for the majority of the test period. The instrumentation in the soil comprised a large number of embedded sensors to measure (excess) pore pressures, temperature (at the same location) and vertical displacements using bellow hoses.

After cross-calibration, existing BAT pore pressure instruments are suitable for simultaneous monitoring of pore pressure and temperature variations in the subsoil with an accuracy of respectively 0.3 kPa & 0.3 °C for moderate test durations. The in-situ installation of the BAT probes in soft soils enabled the novel use of plastic tubes and filter tips, instead of the customary metal, to minimize the impact on the temperature readings. The pore pressure readings of some of the instruments, located furthest from the thermal pile started to malfunction after 65 days.

This research demonstrates that the measurement of vertical displacements using bellow hoses remains challenging for vertical displacements < 5 mm.

Test results

The average temperature in the soil at the relevant depths before thermal loading was 8°C. Monotonic thermal loading of the soil during the extended thermal response test that lasted 21 days showed a maximum excess pore pressure at the nearest instruments at 0.5 m of 3 kPa which was uniform with depth, this reduced to 1.5 kPa at the next instrument level, 1.5 m distance. The monotonic cooling showed comparable behaviour leading to maximum negative excess pore pressures (-1 kPa). Subsequent thermal loading with 6 short period cycles indicated no additional detrimental effects associated with load reversals in soft soils. The maximum recorded excess pore pressures were respectively 2.5 kPa and -1 kPa for the nearest instrument to the thermal pile.

The change in pore pressures is strongly linked to the measured change in temperature, which peaked at approximately 5°C above the average soil temperature during the thermal response test, and 3 °C during the cyclic program for the nearest instrument for pile wall temperatures of 25–27°C. Given the asymmetry in the amount of energy injected and extracted during the extended thermal response test, the average soil temperature during the cyclic tests was approxiamtely 0.4°C higher than at the start of the test series.

The thermal loading program did not lead to significant pile head displacements, which were < 2 mm. Furthermore vertical deformations in the soil fall below the measurement accuracy of the bellow-hoses i.e. < 5 mm. No additional surface displacements were recorded.

Pile head loads, applied as dead-weight loading, varied by an inconsequential 0.5 kN for both the thermal and reference pile. This is associated to the dimensional stability of the steel cantilever rig used to apply the load and the accuracy of the load cell in the system.

In order to compare the effect of the thermal loading on the pile bearing capacity, both the thermal and reference pile were brought to failure in a static load test. The failure load proved to be similar for both piles corresponding to 0.65 times the undrained shear strength s_u of the clay.

The result from the TRT tend to overestimate the thermal conductivity of the clay in relation to the laboratory measurements with about 10% to 25%. The TRT test duration and evaluation method used matters, specially for the concrete pile, having large thermal resistance. The difference in the evaluated thermal conductivity between a basic line source approximation and more advanced methods is up to 20-25%. For the steel pile there is just a marginal difference, <5%

Geotechnical implications for floating thermal displacement piles

The soil conditions at the depths were the pile resistance, hence pile settlements, are originating (i.e. below the neutral plane) are favorable for the change arising in effective stress from the thermal consolidation effect during monotonic and cyclic heating and cooling. This is validated by the monitored absence of pile head displacements during this heating/cooling periods as well as the undetectable small vertical soil deformations. Furthermore, all changes in excess pore pressures were activated by a temperature change. No additional generation of excess pore water pressures or soil deformations, associated

with collapse of the micro structure in the clay adjacent to the pile could be detected during the tests and in the month after finishing the thermal loading program.

A tentative interpretation for these findings is that in the current tests with 50 W/m power injection/extraction, the zone where the largest changes in pore pressures and temperatures are measured the clay is (partly) remoulded, whereas the zone with intact clay still does not experience significant changes in temperature and effective stress. This is motivated by the fact that the pile installation has distorted the clay to a large degree within a distance from the pile equal to 2-5 pile diameters as well as that remoulded clays are less sensitive to temperature change as no appreciable fabric is left (Olsson 2013).

Additional thermal response tests on an unloaded pre-cast concrete pile with 275 mm square cross section installed at the same test site indicates that the thermal boundary conditions applied in the executed field test, 115 mm circular section steel pile, provides a conservative scenario for the soil response, as the thermal capacity of the concrete reduces the heating/cooling rate compared to the steel pile. It is expected that this will lead to smaller thermal effects compared to the steel test pile in terms of excess pore pressure generation in the soil surrounding the pile.

In conclusion, in the 3 month period considered, and the energies injected and extracted, 50 W per meter pile length, there is no appreciable difference between the geotechnical response (according to the measured strain and maintained loading test result) of floating thermal and ordinary displacement piles.

6.2 Recommendations

The results presented in this Thesis are limited to single floating displacement piles in soft sensitive clay. Furthermore, the total testing period is small compared to the total life time of such a foundation. In order to generalise these results, it is recommended to complement these experimental findings with advanced numerical modelling that incorporates both the thermo-hydro-mechanical coupling, an adequate constitutive model for soft soils and pile installation effects. The following aspects should be considered in these numerical analyses after satisfactory calibration against the presented experimental results:

- Study the long-term serviceability limite state (SLS) response in scenarios with longer piles loaded with more long duration thermal load cycles that reflect the use of thermal piles over the life time of a structure.

- Investigate pile group effects (spacing and configuration) on permanent heating of the subsoil

This recommended numerical work in turn would benefit greatly from further experimental studies on pile group effects. An instrumented installation in a real building would be an attractive approach for further collection of data for research as well as practical experiences. This would also give an opportunity to bring competences on a complete building installation together.

Future field tests on piles would benefit from extraction of soil samples close to the pile at different times. This will enable studies of the interface pile-soil and changes

in soil properties during the pile test, as those are not captured with traditional field instrumentation. This would help to assess adequate design loads for thermal piles as well as the extent of the disturbed zone resulting from pile installation.

References

Abdelaziz, S.L.A.M. (2013). "Deep energy foundations: geotechnical challenges and design considerations". Doctoral thesis. Virginia Tech.

Adolfsson, K. and G. Sällfors (1987). *Energilagring i lera*. Tech. rep. R23:1987. Swedish Council for Building Research (BFR).

— (1990). *Energilagring i lera med sanddränering*. Tech. rep. R92:1990. Swedish Council for Building Research (BFR).

Akrouch, G.A., M. Sanches, and J-L. Briaud (2014). Thermo-mechanical behaviour of energy piles in high plasticity clays. *Acta Geotechnica* **9**.3, pp. 399–412.

Alberdi-Pagola, M., S.E. Poulsen, R.L. Jensen, and S. Madsen (2016). Thermal response testing of precast pile heat exchangers: fieldwork report. *Energy and Buildings*.

Alén, C. (2012). *Pile foundations - Short handbook*. Chalmers University of Technology.

Alheid, P., G. Axelsson, B. Berggren, B. Berglars, I. Hermansson, and F. Sarvell (2014). *Verifiering av geoteknisk bärförmåga för pålar enligt Eurokod*. Tech. rep. Swedish Pile Commission, Report 106.

Amatya, B. L., K. Soga, Bourne-Webb P. J., Amis T., and Laloui L. (2012). Thermo-mechanical behaviour of energy piles. *Geotechnique* **62**.6, pp. 503–519.

Andersen, K.H. (2009). Bearing capacity under cyclic loading - offshore, along the coast, and on land. The 21st Bjerrum Lecture. *Canadian Geotechnical Journal* 46, pp. 513–535.

ASHRAE (2007). *HVAC Applications*. Tech. rep. American Society of Heating, Refridgerating and Air-Conditioning Engineers, Atlanda, USA.

BAT (2015). *BAT Groundwater Monitoring System*. www.bat-gms.com.

Bear, J. and A. Verruijt (2012). *Modeling Groundwater Flow and Pollution*. Vol. 2. Springer Science & Business Media.

Bengtsson, P-E. and G. Sällfors (1983). Floating piles in soft, highly plastic clays. *Canadian Geotechnical Journal* **20**, pp. 159–168.

Bjerrum, L. (1967). Engineering geology of Norwegian normally-consolidated marine clays as related to settlements of buildings. *Norwegian Geotechnical Institute* 71, pp. 8–38.

Bourne-Webb, P. (2013). "An overview of observed thermal and thermo-mechanical response of piled energy foundations". *European Geothermal Congress, Pisa, Italy, EGC 2013*.

Bourne-Webb, P., B. Amatya, K. Soga, T. Amis, C. Davidson, and P. Payne (2009). Energy pile test at Lambeth College, London: geotechnical and thermodynamic aspects of pile response to heat cycles. *Geotechnique* **59**.3, pp. 237–248.

Bourne-Webb, P., S. Burlon, S. Javed, S. Kurten, and F. Loveridge (2016). Analysis and design methods for energy geostructures. *Renewable and Sustainable Energy Reviews* **65**, pp. 402–419.

Boverket (2015). BFS 2015 6 EKS 10, Boverkets föreskrifter och allmänna råd om tillämpning av europeiska konstruktionsstandarder.

Brandl, H. (2006). Energy foundations and other thermo-active ground structures. *Geotechnique* **56**.2, pp. 81–122.

Campanella, R.G. and J.K. Mitchell (1968). Influence of temperature variations on soil behavior. *Soil Mechanics and Foundation division. Proceedings of the American Society of Civil Engineers*, pp. 709–734.

Carlsson, S. (2015). *Energipålar - Termiskt responstest på prefabricerad energipåle i betong*. Lund University. Student Paper.

Chen, W.Z., Y.S. Ma, H.D. Yu, F.F. Li, X.L. Li, and X. Sillen (2017). Effects of temperature and thermally-induced microstructure change on hydraulic conductivity of Boom Clay. *Journal of Rock Mechanics and Geotechnical Engineering* **9**.3, pp. 383–395.

Claesson, J., B. Eftring, P. Eskilson, and G. Hellström (1985). *Markvärme, En handbok om termiska analyser*. swe. Tech. rep. T16:1985. Swedish Council for Building Research (BFR).

Claesson, P. (2003). "Long term settlements in soft clay". Doctoral thesis. Chalmers University of Technology.

Claesson, P., G. Holmberg, and J. Romell (2007). *Höghus Lilla bommen Göteborg, Uppföljning av kohesionspålning i mäktiga lerlager*. swe. Tech. rep. SBUF, Svenska Byggbranschens Utvecklingsfond.

Dijkstra, J. (2015). "On displacement pile installation in sand and clay". *Grundläggningsdagen 2015*.

Engdahl, M. and T. Påsse (2014). *Geologisk beskrivning av Säveåns dalgång*. swe. Tech. rep. Sveriges geologiska undersökning.

Eriksson, L.G. (1989). "Importance of strain rate and temperature effects in geotechnical engineering". *Proc. 12th ICSMFE, Rio de Janeiro*.

Eriksson, P., L. Jendeby, T. Olsson, and T. Svensson (2004). *Kohesionspålar*. Tech. rep. Swedish Pile Commission, Report 100.

Fellenius, B.H. (1972). Down-drag on Piles in Clay due to Negative Skin Friction. *Canadian Geotechnical Journal* **9**.4, pp. 323–337.

— (1984). "Negative skin friction and settlement of piles". *Proceedings of the Second International Seminar, Pile Foundations*, pp. 1–12.

— (2014). *Basics of foundation design, a text book. Revised Electronic Edition*.

Gabrielsson, A., M. Lehtmets, L. Moritz, and U. Bergdahl (1997). *Heat storage in soft clay. Field tests with heating (70° C) and freezing of the soil*. Tech. rep. Swedish Geotechnical Institute.

GSHPA et al. (2012). *Thermal Pile Design, Installation and Materials Standards*. Ground Source Heat Pump Association, National Energy Centre, Davy Avenue, Knowlhill, Milton Keynes, MK5 8NG.

Hemmingway, P. and M. Long (2013). "Energy piles: site investigation and analysis". *Proc. of the ICE-Geotechnical Engineering*, pp. 561–575.

Hintze, S., S. Liedberg, R. Massarsch, M. Hanson, H. Elvhammar, B. Lundahl, and S-E. Rehnman (1997). *Omgivningspåverkan vid pål- och spontslagning*. Tech. rep. Swedish Pile Commission, Report 95.

Hu, P., J. Zha, F. Lei, N. Zhu, and T. Wu (2014). A composite cylindrical model and its application in analysis of thermal response and performance for energy pile. *Energy and Buildings* **84**, pp. 324–332.

ISO (2016). *prEN ISO 22477-1, Geotechnical investigation and testing — Testing of geotechnical structures — Part 1: Pile load test by static axially loaded compression.* Tech. rep.

Javed, S. (2010). "Design of ground source heat pump systems. Thermal modelling and evaluation of boreholes". Licentate thesis. Chalmers University of Technology.

— (2012). "Thermal modelling and evaluation of borehole heat transfer." Doctoral thesis. Chalmers University of Technology.

— (2013). "Thermal Response Testing: Results and Experiences from a Ground Source Heat Pump Test Facility with Multiple Boreholes". *Proceedings of 11th REHVA World Congress (Clima 2013), June 16–19, Prague, Czech Republic.*

Javed, S. and J. Spitler (2017). Accuracy of borehole thermal resistance calculation methods for grouted single U-tube ground heat exchangers. *Applied Energy* **187**, pp. 790–806.

Jordvärmegruppen/CTH (1979). *Nordic Symposium on Earth Heat Pump Systems. Chalmers University of Technology.*

Karlsrud, K., B. Kalsnes, and F. Nowacki (1993). Response of piles in soft clay and silt deposits to static and cyclic axial loading based on recent instrumented pile load tests. *Offshore Site Investigation and Foundation Behaviour* **28**, pp. 549–583.

Karlsson, M., A. Emdal, and J. Dijkstra (2016). Consequences of sample disturbance when predicting long-term settlements in soft clay. *Canadian Geotechnical Journal* **53**.12, pp. 1965–1977.

Kesti, J. (2015). "Energy-efficient solutions for steel structures- case study of nearly zero-building". *Nordic Steel Construction Conference 2015*, pp. 61–69.

Laloui, L., M. Nuth, and L. Vulliet (2006). Experimental and numerical investigations of the behaviour of a heat exchanger pile. *International Journal for Numerical and Analytical Methods in Geomechanics* **30**.8, pp. 763–781.

Larsson, R. (2008). *Jords egenskaper.* Tech. rep. Swedish Geotechnical Institute (SGI).

— (2015). *CPT-sondering utrustning, utförande, utvärdering. En in-situ metod för bestämning av jordlagerföljd och egenskaper i jord.* Tech. rep. Swedish Geotechnical Institute (SGI).

Lehane, B.M., F.C. Chow, McCabe B.A., and Jardine R.J. (2000). Relationships between shaft capacity of driven piles and CPT end resistance. *Geotechnical Engineering* No 143, pp. 93–101.

Lehane, B.M. and R.J. Jardine (1994). Displacement pile behaviour in a soft marine clay. *Canadian Geotechnical Journal* No 31, pp. 181–191.

Lennon, D.J., E. Watt, and T.P. Suckling (2008). "Energy piles in Scotland". *Fifth International Symposium on Deep Foundations on Bored and Auger Piles*, pp. 349–355.

Leroueil, S. and M.E.S. Marques (1996). Importance of strain rate and temperature effects in geotechnical engineering. *Measuring and Modelling Time Dependent Soil Behaviour, Geotechnical Special Publications ASCE,* No 61, pp. 1–60.

Loveridge, F. (2012). "The Thermal Performance of Foundation Piles used as Heat Exchangers in Ground Energy Systems". Doctoral thesis. University of Southampton.

Loveridge, F., W. Powrie, and D. Nicholson (2014). Comparison of two different models for pile thermal response test interpretation. *Acta Geotechnica* **9**.3, pp. 367–384.

Lunne, T., P.K. Robertson, and J.J.M. Powell (2009). Cone-penetration testing in geotechnical practice. *Soil Mechanics and Foundation Engineering* **46**.6, pp. 237–237.

Marques, M.E.S., S. Leroueil, and M.S.S. de Almeida (2004). Visqous behaviour of St-Roch-de-l'Achigan clay, Quibec. *Canadian Geotechnical Journal* **41**, pp. 25–38.

McCartney, J.S. and K.D. Murphy (2012). Strain Distributions in Full-Scale Energy Foundations. *DFI Journal: The Journal of the Deep Foundations Institute* **6**.2, pp. 26–38.

Meijer, G. and J. Dijkstra (2013). A novel methodology to regain sensitivity of quick clay in a geotechnical centrifuge. *Canadian Geotechnical Journal* **50**.9, pp. 995–1000.

Mitchell, J.K. and K. Soga (2005). *Fundamentals of Soil Behavior*. John Wiley & Sons Hoboken, NJ.

Moritz, L. (1995). *Geotechnical Properties of Clay at Elevated Temperatures*. Tech. rep. 47. Swedish Geotechnical Institute (SGI).

Muir Wood, D. (2009). *Soil Mechanics*. Cambridge University Press.

Murphy, K.D., J.S. McCartney, and K.S. Henry (2015). Evaluation of thermo-mechanical and thermal behaviour of full-scale energy foundations. *Acta Geotechnica* **10**.2, pp. 179–195.

Ng, C.W.W., C. Shi, A. Gunawan, and L. Laloui (2014). Centrifuge modelling of energy piles subjected to heating and cooling cycles in clay. *Geotechnique letters* **4**.4, pp. 310–315.

Nguyen, V.T., A.M. Tang, and J-M Pereira (2017). Long-term thermo-mechanical behavior of energy pile in dry sand. *Acta Geotechnica*, pp. 1–9.

Olsson, C. and G. Holm (1993). *Pålgrundläggning*. Tech. rep.

Olsson, M. (2010). "Calculating long term settlement in soft clay, with special focus on the gothenburg region". Licentiate thesis. Chalmers University of Technology.

— (2013). "On Rate-Dependency of Gothenburg clay". Doctoral thesis. Chalmers University of Technology.

Pålkommissionen (2016). *Pålstatistik för Sverige 2015 (Piling statistics for Sweden 2015)*. Tech. rep. Swedish Pile Commission, Information 2016:1.

Park, H., S. Lee, S. Yoon, and J. Choi (2013). Evaluation of thermal response and performance of PHC energy pile: Field experiments and numerical simulation. *Applied Energy* **103**, pp. 12–24.

Pasten, C. and J.C. Santamarina (2014). Thermally induced long-term displacement of thermoactive piles. *Journal of Geotechnical and Geoenvironmental Engineering* **140**.5, pp. 06014003 1-5.

Poulos, H.G. (1989). *The mechanics of calcareous sediments*. University of Sydney, School of Civil and Mining Engineering.

Randolph, M. F. (2003). Science and empiricism in pile foundation design. *Geotechnique* **53**.10, pp. 847–875.

Rankka, K., Y. Andersson-Sköld, C. Hulten, R. Larsson, V. Leroux, and T. Dahlin (2004). *Quick clay i Sweden*. Tech. rep. Swedish Geotechnical Institute, Report 65.

Rhen, I. (1988). *Sunclay-anläggningen i Kungsbacka*. Tech. rep. Chalmers University of Technology.

Ronchi, F., D. Salciarini, N. Cavalagli, and C. Tamagnini (2016). Numerical Model of Energy Foundation Behavior: The Prototype of a Geothermal Micro-pile. *Procedia Engineering* **158**, pp. 326–331.

Sandegren, E., U. Bergdahl, B. Fellenius, L. Hellman, G. Hult, S.-E. Rehnman, Sahlström, J. Wennerstrand, and L. Bjerin (1980). *Recommendations for Pile Driving Test with Subsequent Load Testing.* Tech. rep. Swedish Pile Commission, Report 59.

SGF (1993). *Recommended standard for field vane shear test.* Tech. rep. Swedish Geotechnical Society, Report 2:93E.

Singh, R.M., A. Bouazza, B. Wang, C.H. Haberfield, S. Baycan, and Y. Carden (2015). "Thermal and Thermo-Mechanical Response of a Geothermal Energy Pile".

Sivasithamparam, Nallathamby, Minna Karstunen, and Paul Bonnier (2015). Modelling creep behaviour of anisotropic soft soils. *Computers and Geotechnics* **69**, pp. 46–57.

Stewart, M.A. and J.S. McCartney (2013). Centrifuge modeling of soil-structure interaction in energy foundations. *Journal of Geotechnical and Geoenvironmental Engineering* **140**.4.

Sundberg, J. (1991). *Termiska egenskaper i jord och berg.* Tech. rep. Swedish Geotechnical Institute (SGI).

Sutman, M., C. G. Olgun, and T. Brettmann (2015). "Full-scale field testing of energy piles". *IFCEE 2015*, pp. 1638–1647.

Taylor, RN ed (2003). *Geotechnical centrifuge technology.* CRC Press.

Tidfors, M. (1987). "Temperaturens påverkan på leras deformationsegenskaper - en laboratoriestudie". Licentiate thesis. Chalmers University of Technology.

Tomlinson, M.R. (1994). *Pile Design and Construction Practice.* Longman Singapore Publishers (Pte) Ltd.

Torstensson, B-A (1973). *Kohesionspålar i lös lera. En fältstudie.* Tech. rep. R38:1973. Swedish Council for Building Research (BFR).

Vieira, A., M. Alberdi-Pagola, P. Christodoulides, S. Javed, F. Loveridge, F. Nguyen, F. Cecinato, J. Maranha, G. Florides, Prodan I., G. Van Lysebetten, E. Ramalho, D. Salciarini, A. Georgiev, S. Rosin-Paumier, R. Popov, S. Lenart, S. Erbs Poulsen, and G. Radioti (2017). Characterisation of Ground Thermal and Thermo-Mechanical Behaviour for Shallow Geothermal Energy Applications. *Energies (Accepted for publication).*

Wichtmann, T., K.H. Andersen, M.A. Sjursen, and T. Berre (2013). Cyclic tests on high-quality undisturbed block samples pf soft marine Norwegian clay. *Canadian Geotechnical Journal* **50**.

Wrana, B. (2015). Pile load capacity, calculation methods. *Studia Geotechnica et Mechanica* **37**.4.

Yannie, J. (2016). "On the long-term behaviour of tension loaded piles in natural soft soils, A field study and numerical modelling". Doctoral thesis. Chalmers University of Technology.

Yin, Zhen-Yu, Minna Karstunen, Ching S Chang, Mirva Koskinen, and Matti Lojander (2011). Modeling time-dependent behavior of soft sensitive clay. *Journal of Geotechnical and Geoenvironmental Engineering* **137**.11, pp. 1103–1113.

You, S., X. Cheng, H. Guo, and Z. Yao (2016). Experimental study on structural response of CFG energy piles. *Applied Thermal Engineering* **96**, pp. 640–651.

Yu, K.L., R.M. Singh, A. Bouazza, and H.H. Bui (2015). Determining soil thermal conductivity through numerical simulation of a heating test on a heat exchanger pile. *Geotechnical and Geological Engineering* **33**.2, pp. 239–252.

Zarrella, A., G. Emmi, R. Zecchin, and M. De Carli (2017). An appropriate use of the thermal response test for the design of energy foundation piles with U-tube circuits. *Energy and Buildings* **134**.Supplement C, pp. 259–270.

A Appendicies

A.1 Utby Test Field

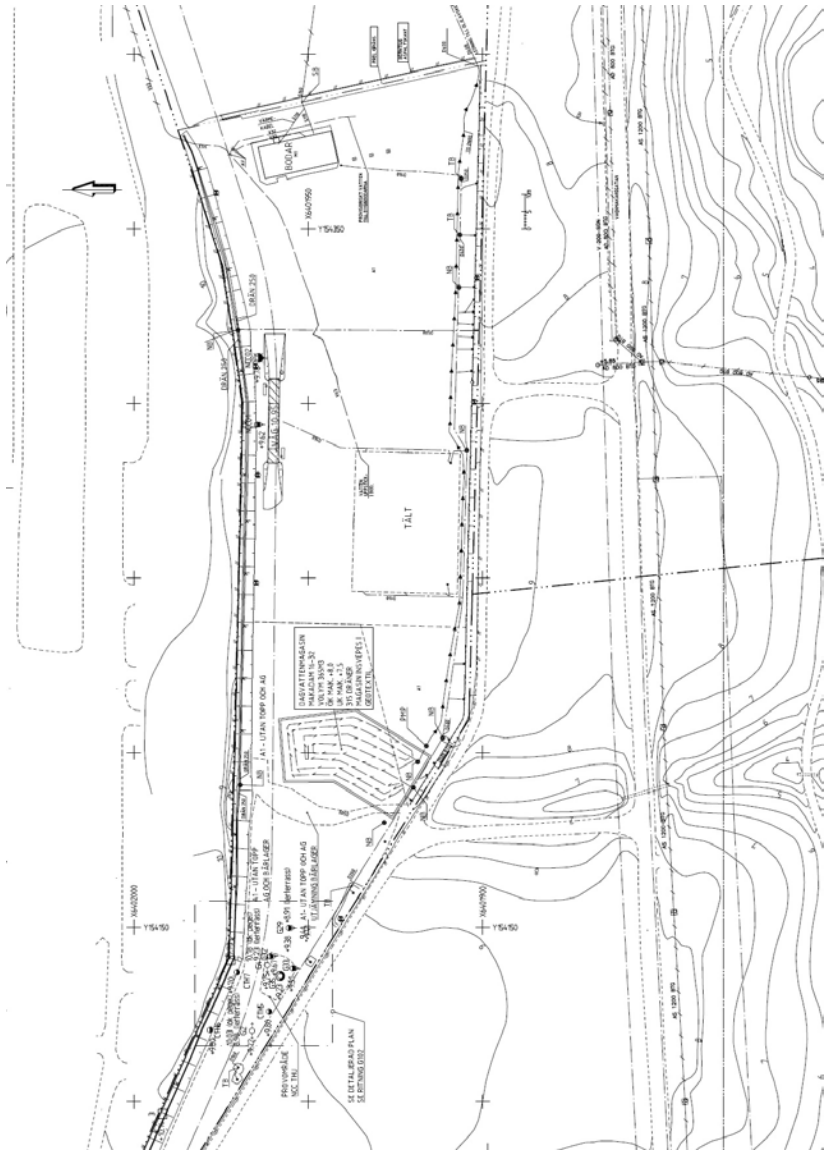

Figure A.1: *Utby estate 192:5. The test field is located in the west end of the plan. Detailed plan in Figures A.2 and 4.1.*

Figure A.2: *Plan test field. Geotechnical investigation ID:s. The 4 black circles are steel piles, including the test piles and the supporting piles for the loading rig. Note the external reference point to the west including bellowhose (B6), piezometer pipe (GW6) and levelling plate.*

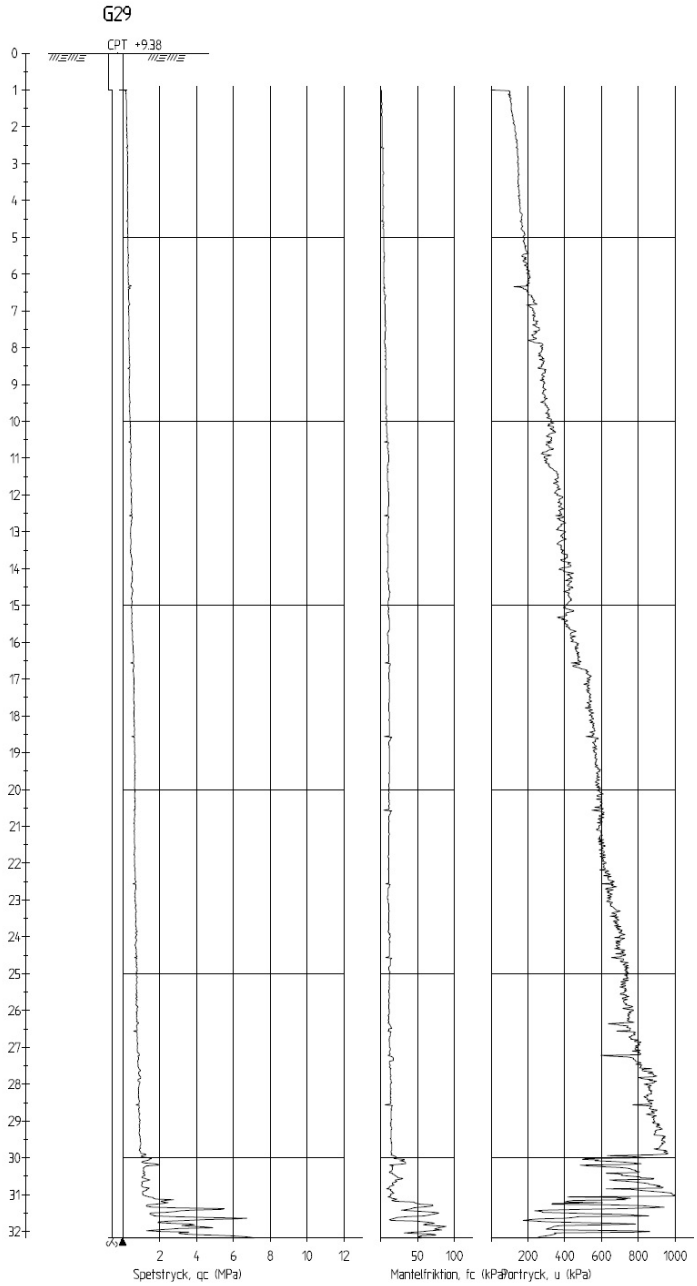

Figure A.3: *CPT from the same position as the north concrete test pile, G29 in Figure A.1.*

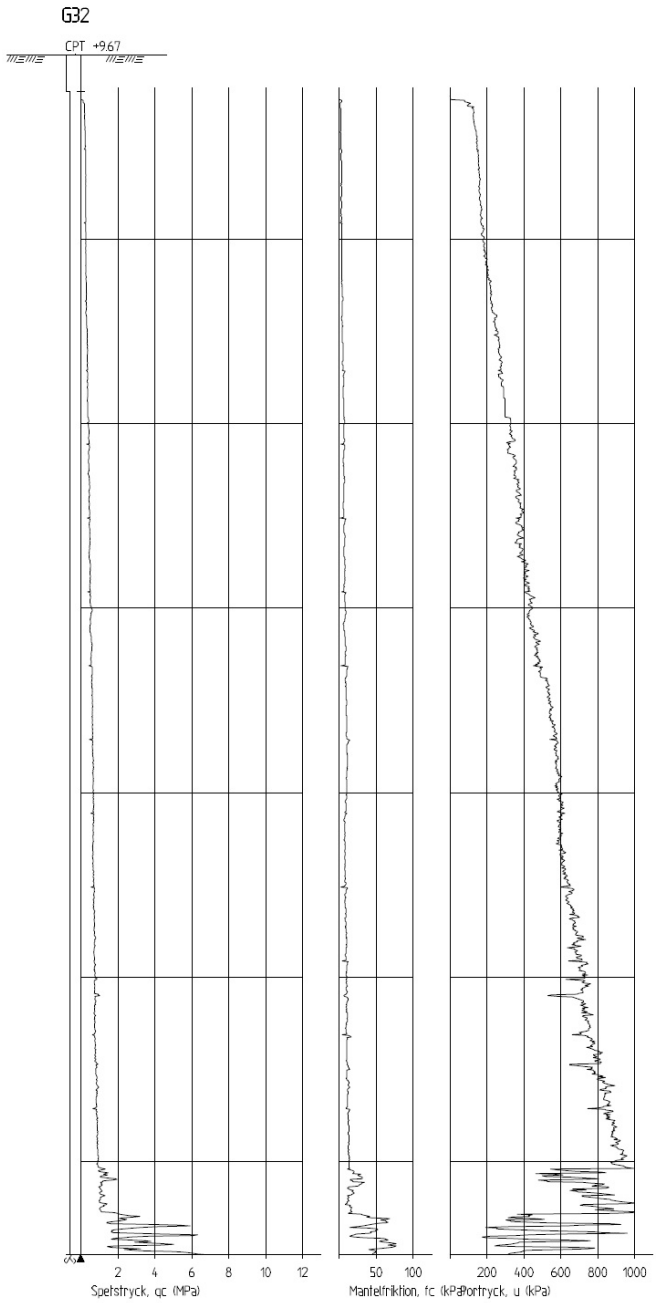

Figure A.4: *CPT from the same position as the thermal test pile, G32 in Figure A.1.*

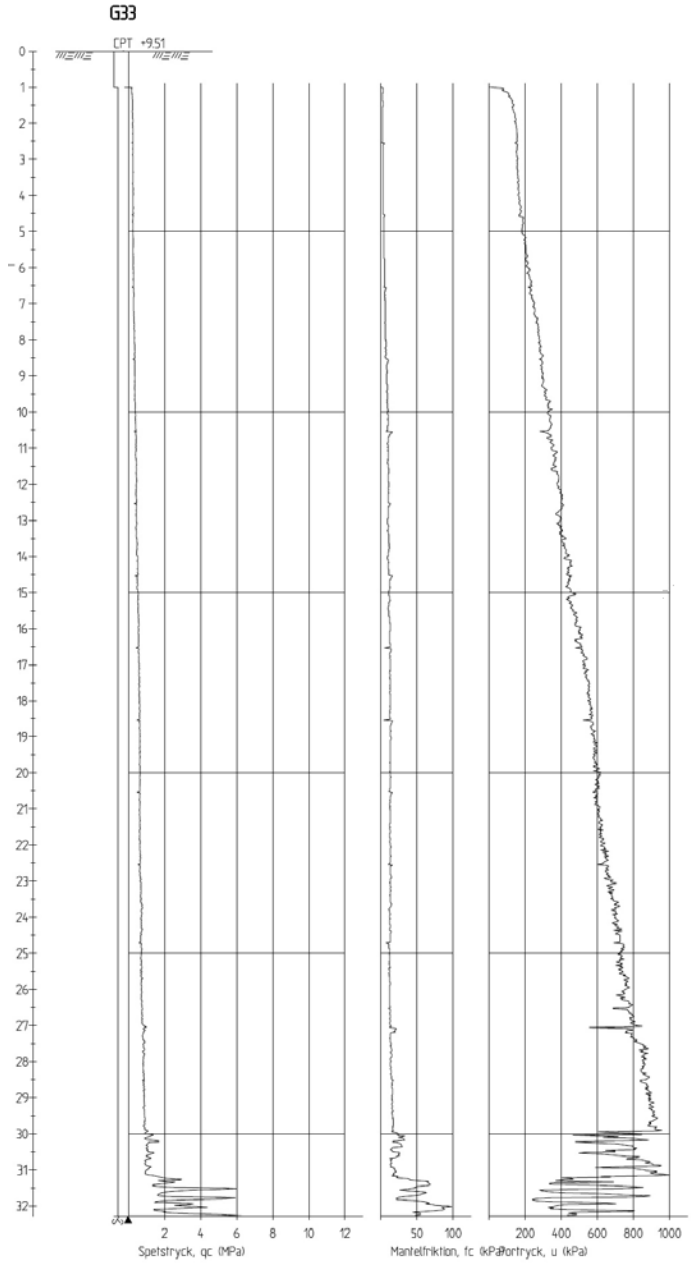

Figure A.5: *CPT from the same position as the thermal/or reference pile, G33 in Figure A.1.*

A.2 Calibration of thermal sensors

The thermal sensor calibration is presented in Section 4.5.

Table A.1: Calibration of the thermal sensors installed in the in soil. Utby test site.

Installation depth (m)	Distance from the thermal pile (m)	Sensor ID	Temperature in field sensor (°C)	Temperature in calibration thermometer (°C)	dT (°C)
7	0.5	3912	7.8	7.6	0.2
			18.8	18.6	0.2
	1.5	3879	7.8	7.4	0.2
			19.0	18.9	0.1
			42.9	42.8	0.1
	3.5	3917	7.5	7.4	0.1
			18.7	18.6	0.1
	6.5	3915	7.7	7.4	0.3
			18.8	18.6	0.2
13	0.5	3916	7.5	7.4	0.1
			18.7	18.6	0.1
	1.5	3913	7.6	7.4	0.2
			18.7	18.6	0.1
	3.5	3914	7.4	7.3	0.1
			18.6	18.5	0.1
	6.5	3927	7.5	7.4	0.1
			18.7	18.6	0.1
19	0.5	3923	7.5	7.4	0.1
			18.7	7.6	0.1
	1.5	3918	7.5	7.4	0.1
			18.7	18.5	0.2
	3.5	3926	7.5	7.4	0.1
			18.5	18.4	0.1
	6.5	3919	7.7	7.5	0.2
			18.8	18.6	0.2
20.9	5.5	3924	7.5	7.4	0.1
			18.6	18.5	0.1

Table A.2: Calibration of the thermal sensors installed in the soil. Utby test site.

Installation depth (m)	Distance from the thermal pile (m)	Sensor ID	Temperature in field sensor (°C)	Temperature in calibration thermometer (°C)	dT (°C)
27	0.5	3922	7.6	7.4	0.2
			18.8	18.6	0.2
	1.5	3921	7.7	7.4	0.3
			18.8	18.6	0.2
	3.5	3925	7.4	7.3	0.1
			18.6	18.5	0.1
	6.5	3920	7.7	7.5	0.2
			18.8	18.6	0.2

A.3 Calibration of pore water pressure sensors

The sensor calibration is presented i Section 4.5. The calibration of the BAT pore water pressure sensors is performed in a specially designed cell equipped for adjustable pressure. The BAT sensor body together with a plastic pipe section is mounted in the cell, Figure A.6. The pressure in the cell is controlled against a calibrated pressure indicator DPI800P. The accuracy of the indicator is $\pm 0.01\%$. The correlation between the measured pressure in the calibration pressure indicator and the field test BAT sensors is presented in Table A.3.

Figure A.6: *Test cell for calibration of pore pressure sensors.*

In Figure A.7 is presented the correlation data from the calibration test of BAT-sensor 3879. In Table A.3 the correlation for all the BAT-sensors used in the field test i presented.

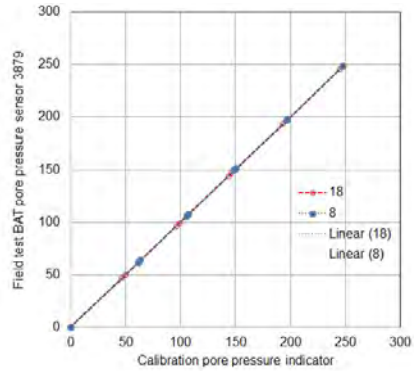

Figure A.7: *Field test BAT-sensor 3879 calibration data. Pore pressure (kPa) from the BAT-sensor in relation to the linear corresponding data from the pore pressure calibration pressure indicator DPI800P.*

Table A.3: Correlation between the measured pressure in the calibration pressure indicator and the field test BAT sensors. The BAT-sensor response (y) as a function of pressure indicator PDI800P (x).

Installation depth (m)	Distance from the thermal pile (m)	Sensor ID	Correlation at 8 °C	Correlation at 18 °C
7	0.5	3912	y=0.9999x+0.2387	y=0.9999x+0.2949
	1.5	3879	y=1.0000x+0.2509	y=1.0002x+0.2148
	3.5	3917	y=0.9998x+0.2633	y=0.9998x+0.2923
	6.5	3915	y=1.0000x+0.1617	y=0.9997x+0.2178
13	0.5	3916	y=0.9998x+0.1867	y=0.9999x+0.2480
	1.5	3913	y=1.0001x+0.1369	y=1.0000x+0.2329
	3.5	3914	y=0.9999x+0.1937	y=0.9996x+0.3156
	6.5	3927	y=1.0002x+0.1616	y=0.9997x+0.2828
19	0.5	3923	y=0.9998x+0.2387	y=0.9995x+0.3076
	1.5	3918	y=1.0001x+0.1635	y=1.0000x+0.2163
	3.5	3926	y=0.9999x+0.2515	y=1.0000x+0.3240
	6.5	3919	y=0.9998x+0.1969	y=0.9995x+0.3062
20.9	0.5	3924	y=1.9996x+0.2562	y=0.9995x+0.2947
27	0.5	3922	y=0.9998x+0.2060	y=0.9997x+0.2412
	1.5	3921	y=0.9999x+0.2244	y=0.9999x+0.2184
	3.5	3925	y=0.9994x+0.2194	y=0.9998x+0.2190
	6.5	3920	y=0.9997x+0.2553	y=0.9996x+0.2268

A.4 Calibration of strain gages response in test pile segments

For strain measuring in the steel piles, strain gages are installed at the inside of the pile shafts as described in Section 4.3.5. To enable calibration in the laboratory, the strain gage installation is made in shorter pile sections, small enough to be handled manually and to fit in the testing rig. As segment and strain gages arre calibrated as one unit they become a measuring unit of strain response in itself. The strain response is then translatable to a corresponding axial loading, presented in Table A.4, if the measured strains assumed fully symmetrically distributed over the pile cross section. Least square method is used to provide the correlation from the measured data scatter.

Table A.4: Correlation between the applied axial load in compression and the strain gage response in the pile segment. The temperature during the calibration tests was 20-22 °C.

Position, depth (PT=thermal pile, PR=referense pile	Loading interval (kN)	Measured strain gage response (mV/V)	Evaluated correlation (y=N, x=mV/V)
PT 1 m	0–300	-0.367–0.504	y=344050x+126490
PT 7 m	0–200	-0.141–0.429	y=350298x+49385
PT 14 m	0–250	0.463–1.171	y= 353086x-163551
PT 21 m	0–230	-0.210–0.399	y=379582x+79388
PR 1 m	0–300	0.042–0.652	y= 377386x-15968
PR 7 m	0–250	-0.209–0.505	y= 349977x+73157
PR 14 m	0–200	0.152–0.710	y=358742x-54697
PR 21 m	0–230	0.049–0.705	y=350469x-17167

Figure A.8: *One of the pile segments under controlled axial compression loading in the laboratory test rig. The pile segment is positioned upside down in the test rig together with the pile hat and load cell, later installed at the pile head in the test field.*

A.5 Calibration of inclinometer sensors for the mechanical loading rig

The inclinometer sensors are presented in Section 4.3.4. The calibration is performed using an adjustable (1/100° accuracy) rig, Figure A.9. The two sensors installed at the loading rig in the field is calibrated in the range of ± 20°inclination and show equivalent linear response:

y=36.707-14.599x (sensor positioned above the thermal pile)
y=36.687-14.556x (sensor positioned above the reference pile)

where y is the inclination (°) and x is the sensor voltage response (V).

Figure A.9: *The rig used for calibration. The inclinometer is fixed at the right side of the rotatable floor.*